Charles University
Faculty of Pharmacy in Hradec Králové
Department of Pharmaceutical Chemistry and Pharmaceutical Analysis

Sapienza University of Rome
Faculty of Pharmacy
Department of Drug Chemistry and Technologies

Design and synthesis of novel 3-aroyl-1-arylpyrrole derivatives as potential tubulin polymerization inhibitors

Diploma Thesis

Katharina Zenkerová

Supervisors: Assoc. Prof. PharmD. Jan Zitko, Ph.D.; Prof. Romano Silvestri

Rome, Italy 2020

Author’s Declaration: „I declare that this thesis is my original author's work, which has been composed solely by myself (under the guidance of my consultant). All the literature and other resources from which I drew information are cited in the list of used literature and are quoted in the paper. The work has not been used to get another or the same title.“

Place, date: Hradec Králové, 31/08/2020

……

Katharina Zenkerová

ACKNOWLEDGMENT

I would like to express my very deep gratitude to Domiziana Masci, Ph.D. for her valuable and constructive suggestions during the planning and development of this research work. Her support, patience and willingness to give her time generously had been very much appreciated.

I am particularly grateful for the help provided by Mrs. Michella Puxxedu and Prof. Romano Silvestri, for their patient guidance and useful critiques of this research work.

My great appreciation belongs to Prof. Jan Zitko, for kindly becoming my mentor and helping me working out this thesis to my satisfaction.

Special thanks should also be given to Erasmus+ program, for making this great experience happen.

Last, but not least, I would like to thank my loving parents and boyfriend, for all the unconditional support, for always believing in me, boosting my confidence and encouraging me to always do my best.

This work was supported by the Ministry of Education, Youth and Sports of the Czech Republic (SVV 260 547), and by Italian Ministry of Education, University and Research, title “Design and synthesis of new anticancer agents to treat the Glioblastoma”.

TABLE OF CONTENTS

1. LIST OF ABBREVIATIONS

ADCC	Antibody dependent cellular cytotoxicity
ALK	Anaplastic lymphoma kinase
ALL	Acute lymphocytic leukemia
AML	Acute myeloid leukemia
APML	Acute promyelocytic leukemia
ARAP	3-aroyl-1-arylpyrrole
ASR	Age Standardized Rate
ATCC	American Type Culture Collection
BCRP	Breast cancer resistance protein
bFGF	Basic fibroblast growth factor
BSS	Balanced Salt Solution
CA-1	Combretastatin A-1
CA-4	Combretastatin A-4
CBS	Colchicine binding site
CBSI	Colchicine binding site inhibitor
CHex	Cyclohexane
CML	Chronic myelogenous leukemia
CTLA-4	Cytotoxic T-lymphocyte-associated antigen 4
DCM	Dichloromethane
DDR	DNA damage response
DMEM	Dulbecco's modified Eagle's medium
DMSO	Dimethylsulfoxide

DNA	Deoxyribonucleic acid
EB	End-binding
MAPS	Microtubule-associated proteins
e.g.	exempli gratia (for example)
EGFR	Epidermal growth factor receptor
Equiv	Equivalent
EtOAc	Ethyl Acetate
FBS	Fetal bovine serum
FDA	Food and drug administration
FEN1	Flap endonuclease 1
GDP	Guanosine diphosphate
GnRH	Gonadotropin-releasing hormone
GTP	Guanosine triphosphate
HDAC	Histone deacetylase
HDI	The Human Development Index
HEPES	(4-(2-hydroxyethyl)-1-piperazineethanesulfonic acid)
HER	human epidermal growth factor receptor
HNSCC	Neck squamous cell carcinoma
HPLC	High Pressure Liquid Chromatography
IARC	International Agency for Research on Cancer
IC_{50}	Half maximal inhibitory concentration
IHIS CR	Institute of Health Information and Statistics of the Czech Republic
IM	Imatinib Mesylate
NA	Not Available
MCF-7	Michigan Cancer Foundation-7
MDR1	Multidrug resistance protein 1

MGMT	O6-methylguanine DNA methyltransferase
MNs	Malignant Neoplasms
MRP1	Multidrug resistance-associated protein 1
MT	Microtubule
MTA	Microtubule targeting agent
MW	Microwave
MZCR	Ministerstvo Zdravotnictví České Republiky (Ministry of Health of the Czech Republic)
NA	Not available
NFκB	Nuclear factor kappa B
NMR	Nuclear Magnetic Resonance
NOR	National Oncologic Registry
NSCLC	Non-small-cell lung cancer
PBMC	Peripheral Blood Mononuclear Cell
PBS	Phosphate-Buffered Saline
pH	Potential of hydrogen
rt	Room temperature
SEMCl	2-(Trimethylsilyl)ethoxymethyl chloride
SERM	Selective estrogen receptor modulator
TBAF	Tetrabutylammonium fluoride
TFA	Trifluoroacetic Acid
THF	Tetrahydrofuran
TLC	Thin layer chromatography
UV	Ultraviolet
ÚZIS	Ústav zdravotnických informací a statistiky ČR (Institute of Health Information and Statistics of the Czech Republic)

VEGF	Vascular endothelial growth factor
VEGFR	Vascular endothelial growth factor receptor
WHO	World Health Organization

2. AIM OF WORK

3-Aroyl-1-arylpyrroles (ARAPs)

Chemistry and design

As interfering with tubulin function has been observed in natural compounds such as colchicine **(1)**, combretastatin **(2)**, vincristine and vinblastine, attempts to design and synthesize new potent tubulin targeting agents that show weaker toxicity and improved pharmacokinetic properties have been made. Professor Silvestri et al. have developed arylthioindole **(3)** and aroylindole **(4)** derivatives as potent inhibitors of microtubules assembly and cancer cells growth. The mechanism of action of these derivatives is binding to the colchicine site on β-tubulin and inhibit the binding of [^{3}H]colchicine to tubulin. Several of these compounds showed improved efficacy than above mentioned colchicine, combretastatin, vincristine and vinblastine and have potential as new anticancer agents. [1]

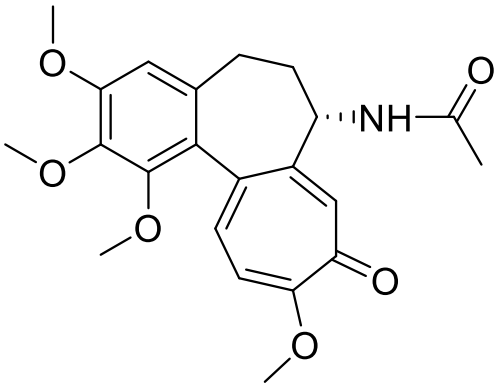

Colchicine **(1)**

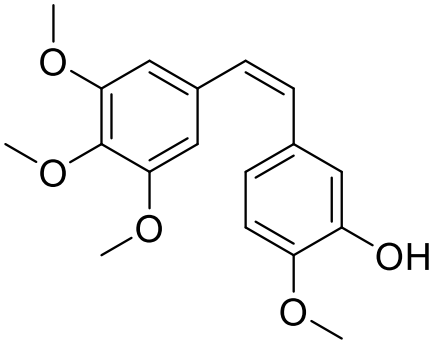

Combretastatin **(2)**

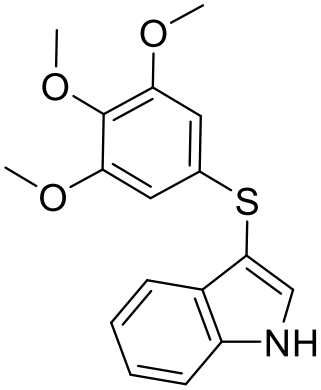

Arylthioindole **(3)**

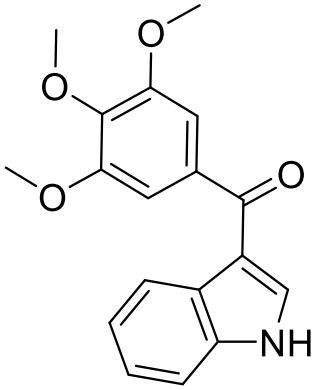

Aroylindole **(4)**

Splitting of fused rings often leads to obtaining new active entities that show the same mechanism of action. Applying this strategy and disjunctioning **(Scheme 1)** of the indole ring of **(3)** into 1-phenylpyrrole led to designing ARAPs **(5)** as the building block for new anticancer class of derivatives. [1]

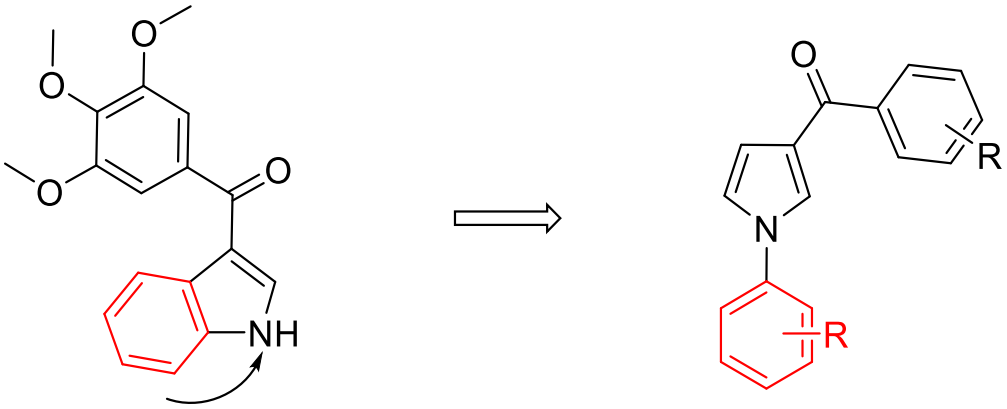

Aroylindole **(4)** ARAP derivative **(5)**

Scheme 1: Disjunction

Professor Silvestri et al. successfully synthesized and evaluated 55 new ARAP derivatives with different substituents on the pendant 1-phenyl ring. Five of the 55 new ARAP derivatives yielded IC_{50} values ≤ 1μM and 12 ARAPs inhibited the growth of human MCF-7 cells with IC_{50} values ≤50 nM. [1]

Following this success, we aim at synthetizing different 3-aroyl-1-arylpyrrole (ARAP) derivatives as potential anticancer agents using different bases as the substituents on the pendant 1-phenyl ring.

3. BACKGROUND

3.1 Cancer

Cancer, also commonly called neoplasm or malignant tumor, is the second leading cause of death globally and a leading cause of suffering and death in the developed world. Cancer is responsible for an estimated 9.6 million deaths in 2018. Generally, about 1 in 6 deaths are due to cancer. [2, 5, 6]

3.1.1 Characterization of cancer

The origin of the word cancer dates back to the 4th century BC when Hippocrates used a Greek word for crab "*karkinoma"* to describe appendage-like projections extending from tumors. This perilous illness is a group of diverse disorders originating within almost any organ and tissue of the body. Caused by a specific and often unique accumulation of genetic and epigenetic alterations, the parent cancer cell starts to grow and divide uncontrollably, forming daughter cancer cells that go beyond their usual boundaries, using oxygen and nutrients meant for other healthy cells, and invade adjoining parts of the body. Eventually, the cancer cells may spread to other organs and tissues. This tendency of spreading and invading surrounding sites is well known as metastasizing and is the major cause of death from cancer. Tumors that tend to invade adjacent tissues are called malignant and are considerably more dangerous than their benign counterparts, where the growth is confined to the original tissue. Certain types of cancer manifest themselves as distinguishable tumors, whereas, others, such as leukemia, do not and thus are harder to recognize in early stages. [5, 6]

There are over 200 types of cancer; lung, prostate, colorectal, stomach and liver cancer being the most common types of cancer in men, while breast, colorectal, lung, cervical and thyroid cancer are the most common among women. [6]

3.1.2 Etiology of cancer

Gender, ethnicity, life-style, infection, inflammation and genetics are factors that greatly affect the incidence of cancer. Furthermore, the risk of developing cancer increases notably with advancing age, as well as being influenced by behavior and environment. While ethnicity, gender and genetics are non-modifiable, life-style choices remain one of the major factors that can help to decrease the risk of developing a cancer. It is unlikely for a single cause to result in cancer. An appropriate accumulation of risk factors, predispositions and environmental triggers is required to develop a tumor. [5, 7]

Genetic factors

Human cells contain around 20 000 genes. Genes are segments of DNA that control cell functions, including how fast it grows, divides and lives. Over time, genes can mutate, and the cell becomes cancerous. Despite the common conviction, that DNA changes are involved in all cancers, “inherited genetic factors make only a minor contribution to susceptibility to most types of neoplasms while environmental factors have the principal role in causing sporadic cancer”. [8] Regardless of huge gaps in the knowledge of genetics in cancer, there is some evidence for genetic links in certain cancers, for instance, Down’s syndrome is often associated with leukemia. Certain tumors tend to cluster in families (e.g. breast, ovary and colon). Female relatives of a breast cancer patient have twice the risk of suffering the same disease. However, evidence indicates that one or more environmental triggers are essential for cancer to develop in a genetically predisposed patient. [7]

Environmental factors

Exposure to mutagens- agents causing mutations- can increase the frequency of genetic alterations, leading to cancer. On the other hand, carcinogens are agents that contribute to developing a cancer without interfering with DNA. Most chemical carcinogens are also mutagens and seem to be the chief contributors, 90% of lung cancers are considered to be associated with carcinogens from tobacco smoking. [7, 9]

Both ionizing and ultraviolet radiation are known for their carcinogenic effect on all tissues. The most relevant is UV radiation in sunlight, which account for most skin and lip cancers. Radiation from nuclear industry, nuclear weapons, and medical diagnostical and therapeutic equipment have been reported to cause malignancies.

The possible effects of microwaves, mobile phones, and over-head cables are so far lacking evidence and they are under investigation. [7, 9]

Some viruses are confirmed carcinogens. AIDS patients' immunity and tumor resistance drop making them susceptible to multiple types of cancer (e.g. Kaposi's sarcoma). There is also a link between cervical cancer and human papilloma virus (HPV), Burkitt's lymphoma and Epstein-Barr virus. Hepatitis B and C increase the risk of liver cancer. [7, 9]

Dietary factors together with obesity play a considerable role in carcinogenesis, with obesity being a well-known cause of colorectal cancer, as well as breast or prostate tumors. Excess fats, red meat, food additives and nitrates (contained in smoked meat) are alleged to be harmful, whereas vitamins A, C and fibre rich foods hold beneficial anticancer effect. [7, 9]

Sex hormones, particularly estrogens in HRT and oral contraceptives, may encourage tumors in sex organs, although this matter is still being investigated. Alcohol consumption contributes heavily, especially if combined with smoking. [7, 9]

Some drugs may be the offenders of causing cancer as well, with the best example being cytotoxics, acting as both immunosuppressors and mutagens. [7, 9]

Trauma and irritation also appear to contribute to some cases of cancer. For instance, vaginal cancer is linked to an early intercourse or poor genital hygiene, and oral cancers to ill-fitting dentures. The reason may be the faster proliferation rate in the repair tissue, which increases the likelihood of a mutation. Similarly, chronic stress is believed to precede the onset of cancer. [7, 9]

The prevention of cancer remains complicated because of the complex causation that still requires greater understanding. [7, 9]

3.1.3 Epidemiology of cancer

3.1.3.1 Epidemiology in Czech Republic

The Czech Republic possesses a unique instrument for registration of oncologic diseases- National Oncologic Registry (NOR). This registry contains data on all patients under consideration, serves as a database and provides information for both national and international statistics. NOR is being regulated by current

legislation, particularly by:

- Act No. 372/2011 Coll. on health services and conditions of their provision [12],
- Regulation (EC) No 373/2016 on the transferring of data to Institute of Health Information and Statistics of the Czech Republic [13],
- Act No. 110/2019 Coll. On personal data processing [14],
- Regulation (EU) 2016/679 of the European Parliament and of the council of 27 April 2016 on the protection of natural persons with regard to the processing of personal data and on the free movement of such data, and repealing Directive 95/46/EC (General Data Protection Regulation) [15].

NOR has been run by Institute of Health Information and Statistics of the Czech Republic (IHIS CR) since 1976 and the acquired data have been essential in predicting the needs of oncological care, observing the incidence of cancer, risk factors and outcomes of treatment including survival rate. [10-11]

The burden of cancer in Czech population ranges among the highest globally. [11] It is the second leading cause of death in the Czech Republic, following cardiovascular diseases. In 2016, 96 500 newly diagnosed cancers were registered in NOR, including 49 302 cases in men and 47 198 in women **(table 1)**. [18]

Table 1: Incidence and Mortality for MNs in Males and Females in 2015 and 2016. Taken from [18]

Incidence of MNs and Carcinoma in situ ICD-10, dx. C00–C97 and D00–D09	**2015**			**2016**		
	Males	**Females**	**Total**	**Males**	**Females**	**Total**
Number	49,152	46,192	95,344	49,302	47,198	96,500
Incidence per 100 000	948.8	861.4	904.3	949.4	878.5	913.4
Standardised incidence per 100 000 (European standard)	738.7	587.4	640.7	727.3	593.3	638.7
Mortality from MNs ICD-10, dx. C00–C97	**2015**			**2016**		
	Males	**Females**	**Total**	**Males**	**Females**	**Total**
Number of deaths	14,826	12,026	26,852	15,095	12,166	27,261
Mortality per 100 000	286.2	224.3	254.7	290.7	226.5	258.0
Standardised mortality per 100 000 (European standard)	221.7	133.1	170.0	220.5	132.7	169.4

Although the incidence of many cancers in the Czech Republic have been growing steadily, a number have either stagnated or even decreased in incidence (colorectal, lung) **(figure 3, figure 6)**. The trend of increasing incidence of neoplasms may be connected with aging of population. Age is inevitably one of the main risk factors of developing cancer, as a shift in the distribution of country population towards older ages results in accumulation of additional mutagens effects and the depletion of natural defense effects in elderly. Moreover increasing environmental pollution relates to higher occurrence of physical and chemical carcinogens. Improving medical

healthcare and diagnostics contribute to increased age of population and may also be a cause of higher cancer reports. Preventive screenings enhance the detection of cancer in its early stages which increases the survival rate and quality of life in cancer patients. Preventive mammography screening in the Czech Republic was officially started in 2002, cervical screening in 2008, and colorectal screening in 2009. From a legislative point of view, the preventive examinations are covered under regulation No. 70/2012 Coll. on preventative check-ups of MZCR, determining the content and intervals of preventive examinations. [17-18]

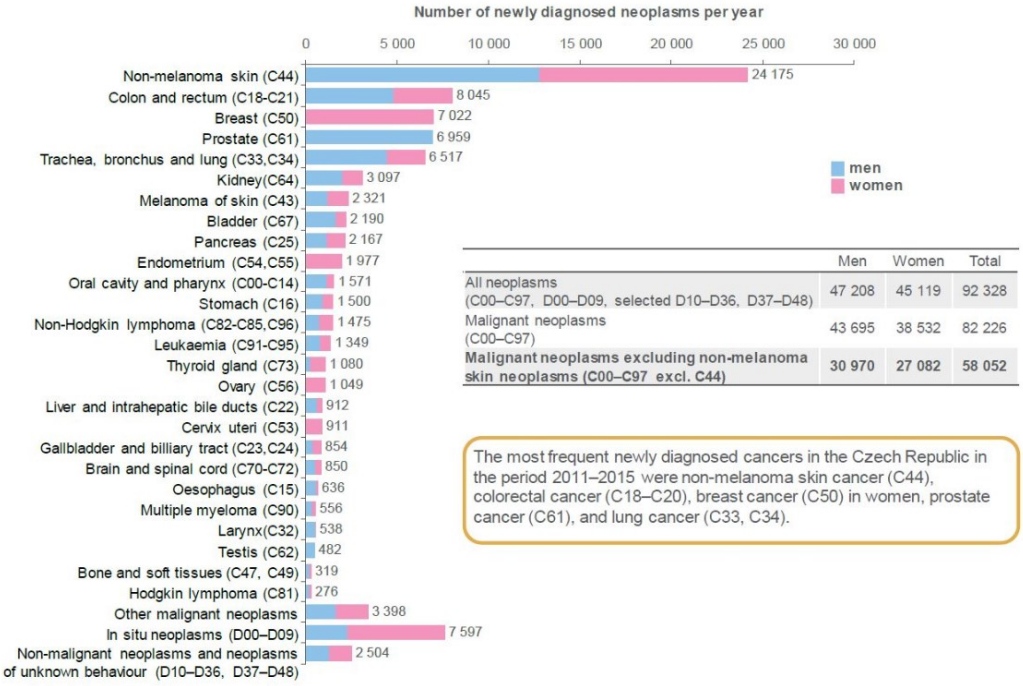

Figure 1: Incidence of individual cancer diagnoses in Czech Republic in the period 2011–2015. Taken from [11]

From Figure 1, it is evident that the most frequent newly diagnosed type of cancer in the period 2011—2015 was non-melanoma skin cancer (C44), followed by colon and colorectal cancer (C18-C21), breast cancer in women (C50), prostate cancer in men (C61) and lung cancer (C33, C34) **(figure 1-6)**. According to ÚZIS, 28 251 new non-melanoma tumors were reported in 2016, representing almost one third of all cancers diagnosed that year. Incidence has been higher for men than women, although the mortality stays low for both **(figure 2)**, owing to early diagnoses and general favorable prognosis associated with this disease. [18]

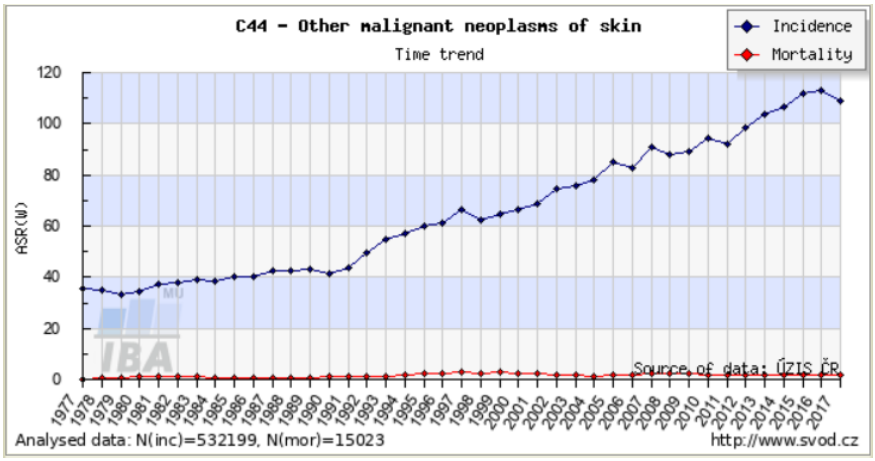

Figure 2: Non-melanoma skin cancer incidence and mortality in the Czech Republic (both sexes), per 100 000 persons (ASR). Taken from [16]

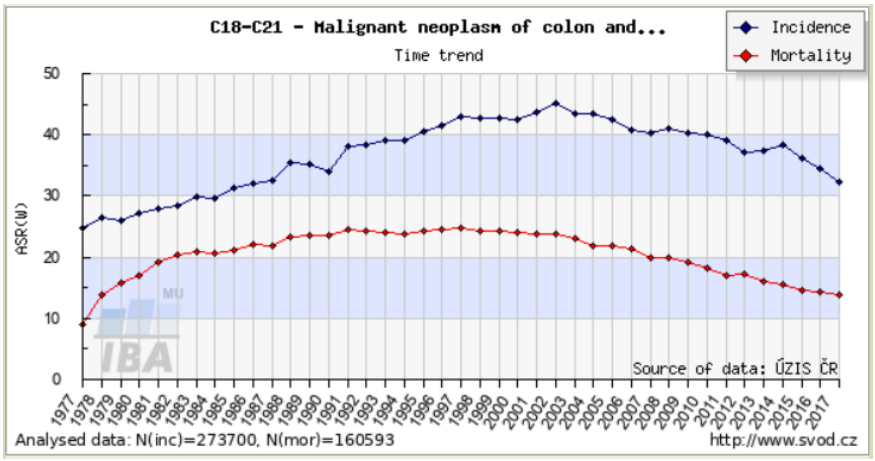

Figure 3: Colon and rectal cancer incidence and mortality in the Czech Republic (both sexes), per 100 000 (ASR). Taken from [16]

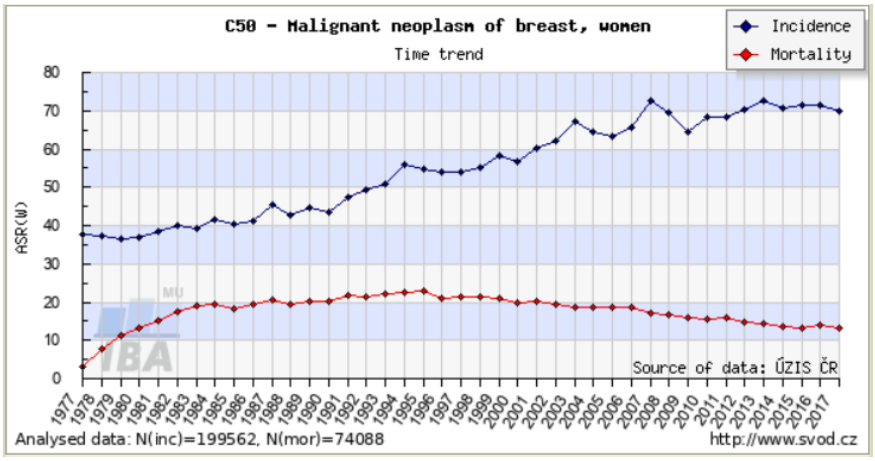

Figure 4: Breast cancer incidence and mortality in the Czech Republic (women), per 100 000 persons (ASR). Taken from [16]

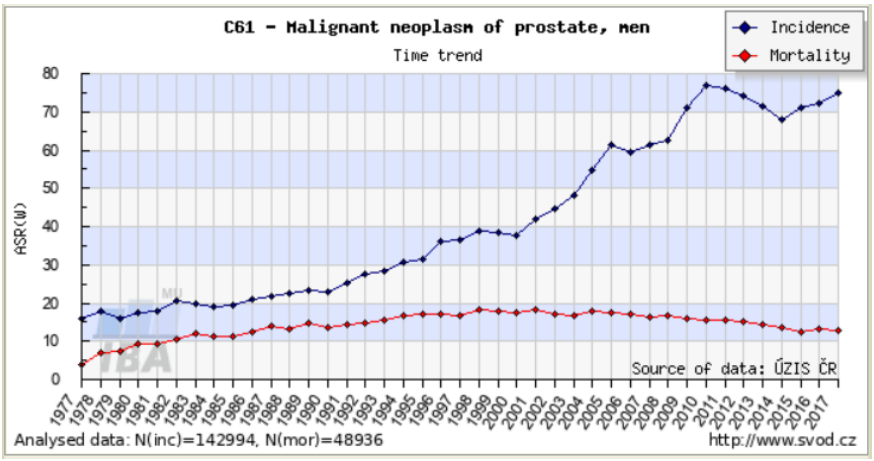

Figure 5: Prostate cancer incidence (blue) and mortality (red) in the Czech Republic (men), per 100 000 persons (ASR). Taken from [16]

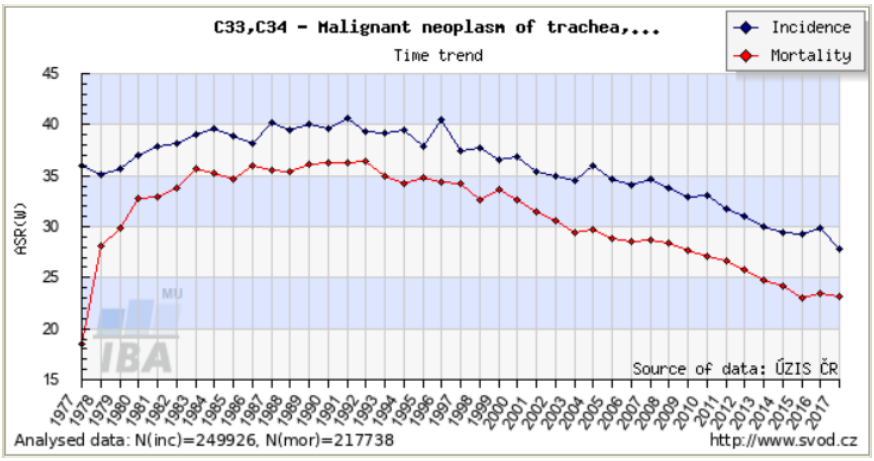

Figure 6: Trachea, bronchus and lung cancer incidence and mortality in the Czech Republic (both sexes), per 100 000 persons (Age standardized rate). Taken from [16]

The current priority is to continue the effort to diagnose and treat cancer at the earliest stages possible to improve prognosis of cancer patients which could also lead to lowering of treatment expenses.

3.1.3.2 Epidemiology Worldwide

Cancer is the second leading cause of death globally. In 2018, 18.1 million new cases of cancer and 9.6 million deaths were estimated to occur. Statistically, 1 in 5 men and 1 in 6 women develop cancer during their lifetime, and 1 in 8 men and 1 in 11 women die from the illness. Global cancer statistics are provided by GLOBOCAN, an interactive database ran by IARC Global Cancer Observatory which comes under WHO. [2]

Over the years, the burden of cancer has been increasing, owing to population growth and aging, as well as increasing prevalence of risk factors linked to social and economic development. There is a significant difference between high HDI (The Human Development Index) and lower-HDI countries. High and very high HDI countries tend to ranks highest in cancer incidence, though the mortality remains low due to easily accessible medical care and timely detection of the disease. On the other hand, medium and low HDI countries have lower cancer incidence, yet mortality nearly equals that of high HDI countries. The reasons for this phenomenon are higher frequencies of cancer types characteristic for poorer survival (cervical cancer) and deficient healthcare service quality. Despite the developmental differences between countries, lung cancer has been number one globally in term of incidence and mortality. 2.1 million diagnoses of lung cancer were estimated in 2018, representing approximately 11.6 % of the total cancer incidence. Breast cancer approaches a similar incidence level, and remains the most common cancer in women. The survival of lung cancer patients is poor (1.8 million deaths in 2018), compared to breast cancer which has a more favorable prognosis (0.6 million in 2018). The third leading cancer in terms of incidence is colorectal cancer (1.8 million), and is responsible for more deaths than breast cancer (0.9 million). Common cancer in men is prostate cancer, with incidence estimated around 1.3 million in 2018. Cervical cancer, typical for developing countries totalled 0.6 million cases in 2018. Although very severe with a poor prognosis, cancers of the stomach and liver are less widespread **(figures 7 and 8)**. [19]

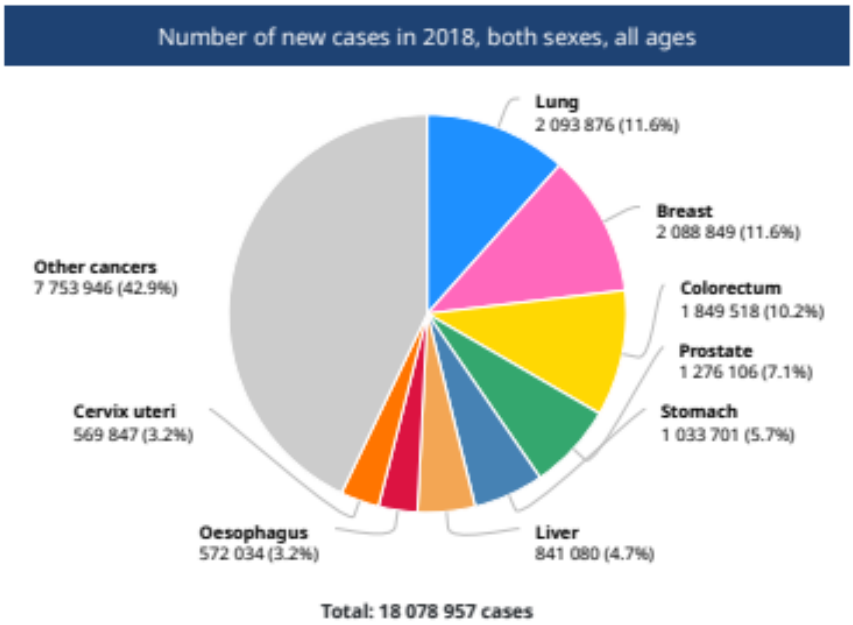

Figure 7: Incidence of new cases of cancer in 2018, both sexes, all ages. Taken from [20]

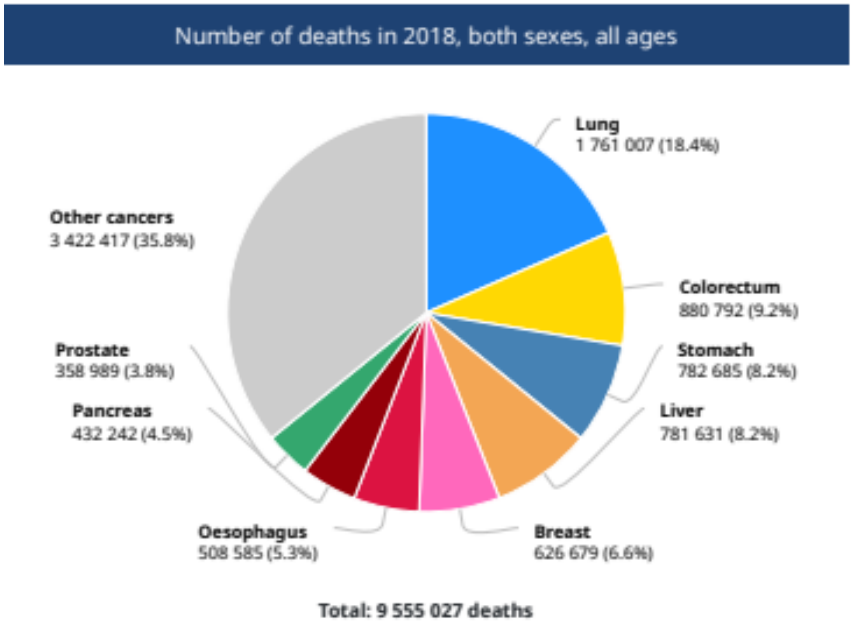

Figure 8: Cancer mortality in 2018, both sexes, all ages. Taken from [20]

According to available data, 48.4% of new cases and 57.3% of deaths of cancer are estimated to occur in Asia, primarily because the continent is inhabited by nearly 60% of global population. Although Europe has only 9% of the world's population, it accounts for 23.4% of the global incidence and 20.3% of cancer deaths. The Americas have 13.3% of the global population and account for 21.0% of new cancer cases and 14.4% mortality. Africa accounts for only 5.8% incidence worldwide, but mortality ranks 7.3%. The higher proportions of mortality compared to incidence in Asia and Africa are caused by previously mentioned higher frequencies of cancer types linked to poorer survival and limited access to early diagnoses and treatment. Prevention efforts may be the reason of decreasing incidence of some cancer types, including lung cancer in developed countries and cervical cancer in Africa. Nevertheless, global patterns show that the absolute number of new cases requiring treatment and care has been increasing in most countries. "These new figures highlight that much remains to be done to address the alarming rise in the cancer burden globally and that prevention has a key role to play," says IARC Director Dr. Christopher Wild. "Efficient prevention and early detection policies must be implemented urgently to complement treatments in order to control this devastating disease across the world." [19] **(figures 9 and 10)**

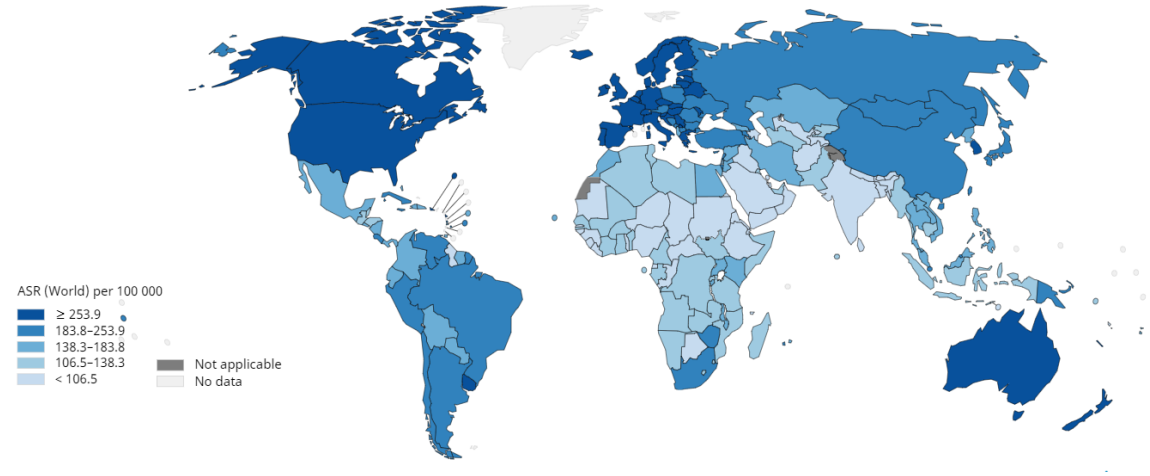

Figure 9: Estimated age-standardized incidence rates (World) in 2018, all cancers, both sexes, all ages. Taken from [21]

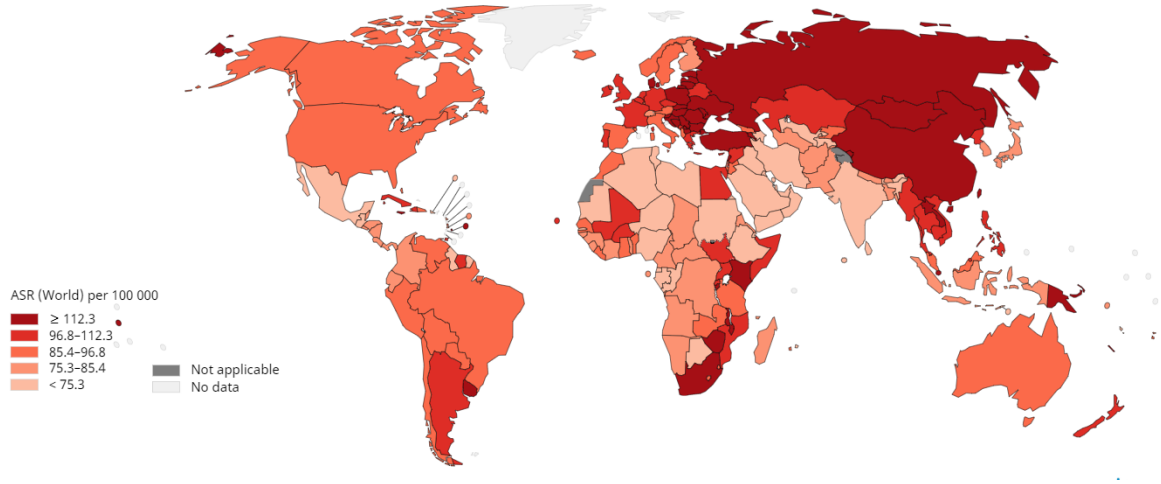

Figure 10: Estimated age-standardized mortality rates (World) in 2018, all cancers, both sexes, all ages. Taken from [22]

3.1.4 Diagnosis and clinical manifestation of cancer

Symptoms of cancer can vary as much as cancer itself. Not only it causes problems in the site of a growing tumor, but it can also reach distant tissues by affecting nerves or secreting bioactive molecules. Cancer is often detected during preventive screening tests, routine exams, or after specific symptoms observation. It is always crucial to confirm the diagnosis and determine the type of cancer by biopsy. Methods used to classify the malignant disease include immunohistochemical stains, flow cytometry, electron microscopy, chromosome and nucleic acid based studies. Lastly, it is essential to assess the stage of cancer using the WHO TNM classification, where T stands for tumor spread, N for node involvement and M for metastasis. With

increasing tumor size, lymph nodes involvement, and metastasis the prognosis worsens and more aggressive treatment is required. [5]

Paraneoplastic syndromes

One of the earliest manifestations of cancer may be paraneoplastic syndrome. Paraneoplastic syndromes are symptom complexes induced by cancer, though not by the local impact of the tumor spread. The most frequent source of paraneoplastic syndromes are substances released from a tumor. For instance, some tumors may release hormones, including serotonin that may lead to flushing, diarrhea, wheezing, and rapid heartbeat. Another common cause of paraneoplastic syndrome is an immune reaction to a tumor. Tumors can stimulate antibody activity, causing them to attack nervous system cells, manifesting as neurologic disorders. These symptoms, although rare, are often irreversible, sometimes even life-threatening, and can precede other cancer symptoms by months. [5]

Pain

Although there is usually a little or no pain during the early stages of cancer, pain is one of the most feared complications of advanced cancer. Cancer induced pain can result from both direct and indirect mechanisms. Direct mechanisms include direct pressure, obstruction, invasion of sensitive adjacent tissues, stretching of visceral surfaces, tissue destruction, infection, and inflammation. Pain can also manifest in distant sites of the primary tumor owing to metastasis. Furthermore, pain may also be affected by fear, anxiety, sleep loss, fatigue, and overall physical deterioration. Certain cancer types are more frequently connected with pain, e.g. bone, pancreas, stomach, or esophagus tumors. [23] Subjective perception of pain varies among individuals and, hence, makes it harder to diagnose and treat. [5]

Fatigue

Despite being the most frequently reported symptom of cancer and its treatment, the mechanism of developing fatigue is still not fully understood and needs further investigation. Some of the anticipated causes include lack of sleep, biochemical changes linked to cancer and its treatment, psychosocial factors, level of activity, nutritional status, and other physical and environmental factors. Studies of muscle function indicate decreased muscle contractility and function in cancer patients. Other research implies that metabolic products of cancer treatment cause muscle loss due to circulating cytokines (e.g. TNF-α, IL-1). Similar to pain, fatigue is a subjective

symptom that patients often describe as tiredness, weakness, lack of energy, exhaustion, incapability to concentrate, depression, boredom or lack of motivation. [5]

Cachexia

Cachexia represents a collection of symptoms comprising of anorexia, early satiety, weight loss, anemia, asthenia, taste alterations and altered protein, lipid and carbohydrate metabolism. Even cancer patients with sufficient caloric intake can suffer from cachexia, because of metabolic disorders, including insulin resistance and hyperglycemia, hypertriglyceridemia, muscle wasting and general malfunction of metabolism. Taste alterations, lack of appetite, early satiety and anorexia contribute significantly to weight loss. Pain, depression, chemotherapy/radiotherapy can often lead to anorexia. Specific tumor metabolites may also accelerate the onset of cachexia, e.g. a factor called proteolysis-inducing factor often found in urine cause muscle catabolism. [5]

Anemia

Another symptom commonly associated with cancer is anemia. Chronic bleeding, malnutrition, cytotoxic chemotherapy, and malignancy of blood forming organs can all cause anemia. Colorectal and genitourinary tumors are generally linked to blood losses and iron deficiencies. Malabsorption of iron and folate deficiency is observed in gastrointestinal cancers, such as tumors of pancreas, stomach, or upper intestines. Methotrexate treatment is known for causing megaloblastic anemia as a side effect. Other phenomena, such as defects in erythropoietin production reduction and drop of red cells survival rate, have been observed in malignant diseases. Administering erythropoietin in persons with cancer has been proven to be effective in preventing anemia. On the other hand, recent studies warn that erythropoietin treatment results in blood clot forming and lower cancer survival. [5]

3.2 Therapy of cancer

Many health systems in low- and middle-income countries are least prepared to manage cancer burden, and large numbers of patients globally do not have access to timely quality diagnosis and treatment. In countries where health systems are strong, survival rates of many types of cancers are improving thanks to accessible early detection, quality treatment, and survivorship care. [6]

3.2.1 Current therapy approaches

The rapid division of cancer cells has been the main target of cancer treatment. Hence, anticancer drugs can be classified according to their interference with cell reproduction. Some drugs aim for DNA replication, while other target protein synthesis or impede the signal pathways from promoting cell division. Inhibition of RNA synthesis has been under thorough investigation. Another common way to categorize anticancer drugs is their mechanism of action. The 4 major groups are cytotoxic drugs (e.g. alkylating agents, mitosis inhibitors), hormonal therapies (e.g. steroids, antihormonal treatments), immunotherapy (e.g. interferon), and the remaining are classified as 'miscellaneous' drugs.

3.2.1.1 Chemotherapy targeted at the tumor DNA

Alkylating agents

Alkylating agents attack rapidly dividing cells, bind to their DNA, resulting in death of the cells. The most common alkylation target of the DNA strand is 7-nitrogen or oxygen at C-6 of a guanine nucleobase, where an alkylating agent forms a carbonium ion. Though this DNA disruption can occur in any state of cell cycle, the most efficient impact is during the synthesis (S) phase. Cells in the resting (G_0) phase often manage to repair DNA breakage by replacing the targeted guanine with a new one and continue its cycle. Alkylating agents are most potent against granulocytes and thrombocytes and thus are known for their bone marrow toxicity. Nitrogen mustards are alkylating agents derived from a toxic mustard gas used and studied during World War II. These molecules contain 2 chlorethyl groups and side chain of a general formula Cl-CH_2-CH_2-R-CH_2-CH_2-Cl, where the R group varies among different agents. Cyclophosphamide **(6)** is one of the most frequently used alkylating agents and is less toxic to the bone marrow, liver and gastrointestinal tract than others. Ifosfamide, is structurally similar to cyclophosphamide. Both drugs cause a rare toxicity of urinary bladder called haemorrhagic cystitis which can be prevented by administering mesna. Other less effective alkylating agents include chlorambucil and melphalan, which have mostly been replaced by newer drugs in several indications.

Nitrosoureas are molecules named after their distinctive structure containing urea and a nitroso group. Carmustine **(7)** and lomustine are nitrosourea agents well soluble in lipid tissues, giving them the ability to cross the blood brain barrier into the central nervous system, and be utilized in the treating of brain tumors.

Busulfan **(8)** and treosulfan belongs to a group of alkyl sulphonates. Owing to its selective effect on the bone marrow, busulfan is used to treat myeloid leukemia, myelofibrosis and polycethaemia vera. Treosulfan is indicated for ovarian cancer. ThioTEPA is the major member of aziridines currently used for bladder, ovarian and breast cancers. [28-29]

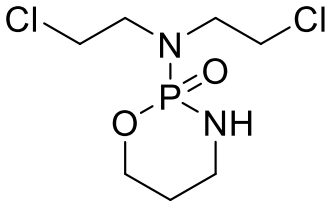

Cyclophosphamide **(6)**

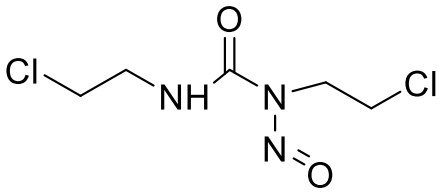

Carmustine **(7)**

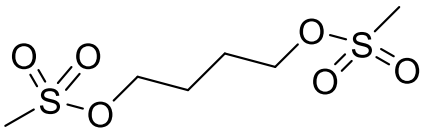

Busulfan **(8)**

Antimetabolites

Antimetabolites are derived from endogenic molecules involved in DNA/RNA synthesis. Due to slight modifications in their structure, they act as antagonists with affinity to target structures of their analogues.

Methotrexate **(9)** is the most commonly used folate **(10)** antimetabolite. Methotrexate inhibits the key enzyme dihydrofolate reductase, essential for DNA, RNA, and protein synthesis. Besides treating solid tumors, leukemias, and lymphomas, it is used to treat psoriasis, rheumatic arthritis, and Crohn disease due to its anti-inflammatory and immunosuppressive effects. One of methotrexate drawbacks is its nephrotoxicity, though the general toxicity is fairly low compared to other anticancer drugs. Purine analogues imitate the structure of guanine and adenine nucleobases, stopping DNA and RNA synthesis by acting as false substrates. 6-Mercaptopurine **(11)** and tioguanine are derived from guanine, while fludarabin and cladribine are adenine analogues. 6-Mercaptopurine is an active metabolite of azathioprine and is used in the treatment of acute and chronic leukemias. The same indication applies to tioguanine. Both 6-mercaptopurine and tioguanine share the same side effects, namely bone marrow inhibition, mucositis, and liver dysfunction.

Pyrimidine analogues act as false substrates for DNA and RNA synthesis, resembling cytosine or uracil. One of the oldest pyrimidine analogues 5-Fluorouracil **(12)**, and its

prodrug capecitabine, mimic uracil and incorporate into RNA, causing its breakage. Both drugs are used for solid tumors, including colon and breast cancer. Cytosine related drugs include cytarabine and gemcitabine. Gemcitabine is one of the newer antimetabolites, cytotoxic to breast, lung, pancreas, and ovary tumors. [28-29]

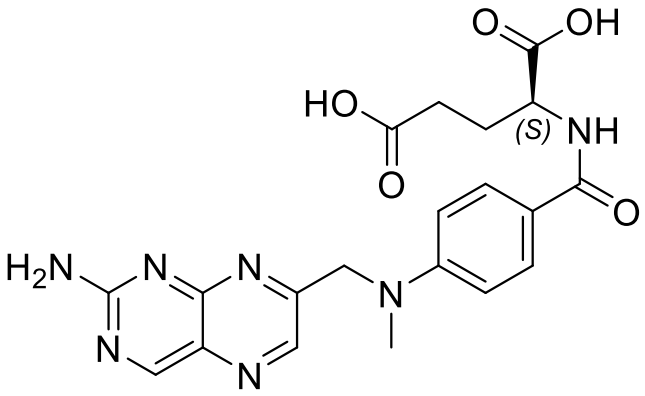

Methotrexate **(9)**

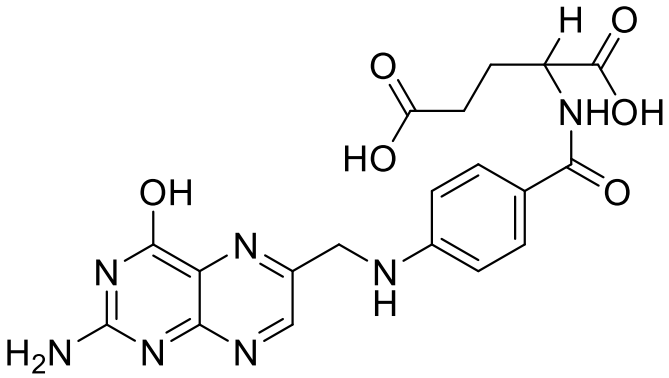

Folate **(10)**

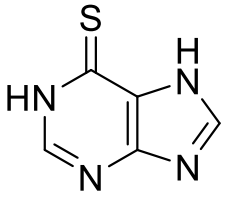

6-Mercaptopurine **(11)**

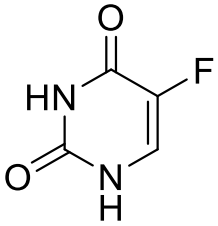

5-Fluorouracil **(12)**

Topoisomerase I inhibitors

Currently used topoisomerase I inhibitors include irinotecan **(13)** and topotecan. Both were derived from one of the original topoisomerase I inhibitor, camptothecin, acquired from the bark of *Camptotheca acuminate*, and both are administered intravenously. Irinotecan is a prodrug with cholinergic activity, often resulting in diarrhea as a side effect that can be treated with loperamide. In vivo, irinotecan is converted to a highly potent metabolite, SN-38, by carboxylesterases. Irinotecan is

aimed against lung and colorectal carcinomas. Topotecan has a more favorable gastrointestinal side effect profile than irinotecan and treats colorectal, cervical, lung and gastric cancers. [28-29]

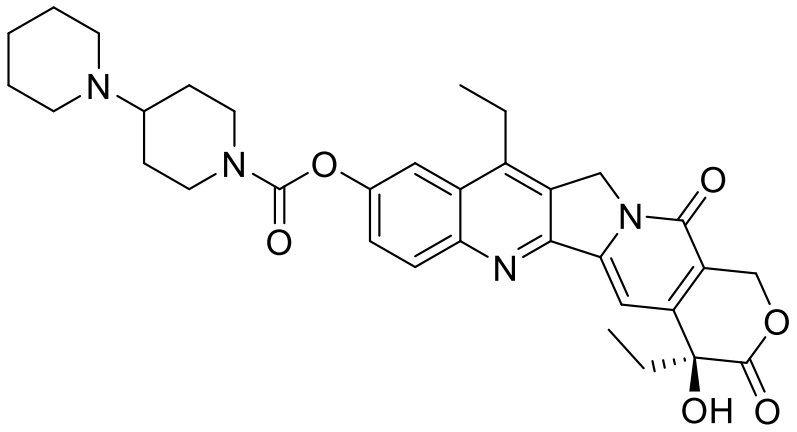

Irinotecan **(13)**

Hormone and anti-hormonal therapy

Sex hormones work by binding to cell receptors of sensitive tissues (e.g. breast, prostate, testes), form a complex, enter the nucleus and stimulate genes transcription. Gene transcription then culminates in protein synthesis or inhibition/enhancement of corresponding tissue's growth. Examples of hormone cancer therapy are diethylstilbestrol and ethinylestradiol used to treat prostatic tumors. Nevertheless, due to being poorly tolerated, they are not in first-line treatment. Estramustine is a more recent combination of an oestrogen molecule and a nitrogen mustard, again potent against prostate cancer, however loaded with side effects of both alkylating agents and oestrogens (e.g. cardiovascular disorders, gynaecomastia).

Another approach is to block the effect of sex hormone on the tissue by hormone antagonists. Tamoxifen **(14)** is the best known oestrogen receptor antagonist used in treating breast cancer. It is a first generation selective estrogen receptor modulator (SERM). Due to its partial oestrogen agonist effect, it increases the bone density and lowers blood levels of cholesterol. However, reports show that its agonist effect on the ovaries, it increases the risk of developing an ovarian cancer. Fulvestrant is another SERM example. Unlike tamoxifen, fulvestrant has no oestrogenic effect on the endometrium and bones and therefore may inhibit endometrial cancer. Anti-androgens are indicated for prostate cancer treatment and can be divided into steroidal (e.g. cyproteron acetate) and non-steroidal (e.g. flutamide, bicalutamide, nilutamide) groups. Besides blocking androgen receptors, cyproteron acetate **(15)**

also inhibits oestrogen, progestin, mineralocorticoid and lucocorticoid receptors, leading to unpleasant side effects such as decreased libido, hot flushes, or insomnia. Non-steroidal bicalutamide **(16)** and nilutamide have replaced the now obsolete flutamide, because of their better side-effect profile.

Reduction or blocking the production of sex hormones is the last approach to the hormonal therapy of cancer. Aromatase is an enzyme, essential for biosynthesis of oestrogens. This makes aromatase a convenient target of anastrozole and letrozole. The drop of oestrogens as a consequence of aromatase inhibition is followed by side effects such as reduced bone mineral density, hot flushes, vaginal dryness, or headache. Exemestane **(17)** binds covalently to the enzyme, causing its irreversible blockage. It is given orally to post-menopausal women to treat breast cancer. To decrease the production of testosterone in prostate cancer patients, GnRH agonists are used. Some GnRH agonists are goserelin, leuprorelin, triptorelin, buserelin. Goserelin was one of the first GnRH analogues to be discovered and is indicated for the treatment of prostate cancer and estrogen-positive breast cancers. Side effects of GnRH agonists resemble menopausal symptoms (e.g. hot flushes, sexual dysfunction). [28-29]

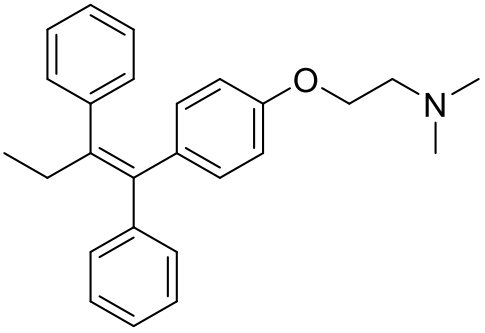

Tamoxifen **(14)**

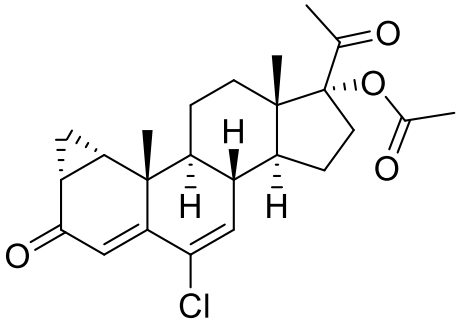

Cyproteron acetate **(15)**

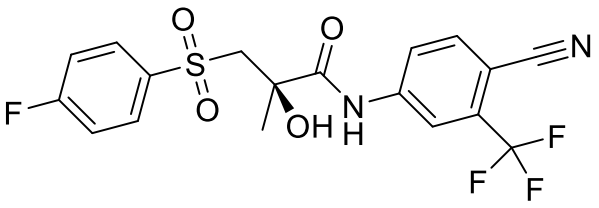

Bicalutamide **(16)**

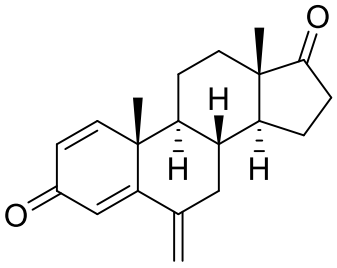

Exemestane **(17)**

Cytotoxic antibiotics

Antibiotics that can fight cancer can be divided into 2 main groups: anthracyclines

and drugs derived from *Streptomyces* species.

Anthracyclines are attributed several mechanisms of actions. Their capability of intercalation into the DNA double helix causes disruption of DNA function. Furthermore, they are believed to inhibit topoisomerase II, resulting in DNA breakage. A third mechanism is the activity of oxygen radicals that are produced in the presence of anthracyclines, utilizing iron from hemoglobin and myoglobin molecules. Radicals cause further damage to DNA, however they are also responsible for anthracyclines' cardiotoxicity. Doxorubicin **(18)** is the most significant cytotoxic anthracycline and is used to treat a wide range of malignancies, for instance breast, lung and bladder cancer, lymphomas, sarcoma, leukemia and multiple myeloma. Daunorubicin, idarubicin and epirubicin are examples of other anthracyclines indicated for cancer therapy.

Streptomyces derived antibiotics are drugs with natural origin that differ from anthracyclines in their structure and mechanism of action. Bleomycin is a glycopeptide antibiotic, capable of binding metal ions, forming a hyperoxide that causes oxidation and DNA breakage. Bleomycin is given for the treatment of many solid tumors, including carcinoma of testes, non-Hodgkin lymphoma, and squamous cell carcinomas. Mitomycin is derived from *Streptomyces lavendulae* and is administered to treat gastrointestinal or bladder cancers. [28-29]

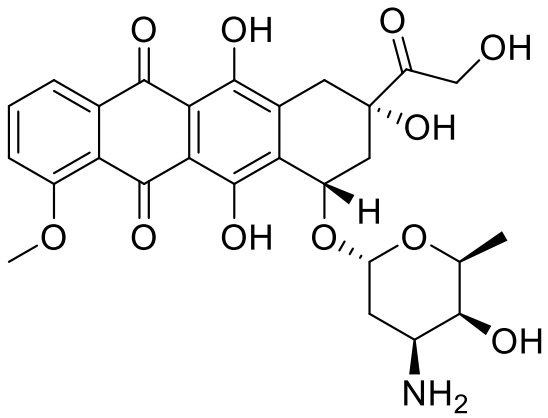

Doxorubicin **(18)**

Podophyllotoxins

Podophyllotoxins are toxins extracted from the roots of *Podophyllum peltatum*. Similar to anthracyclines, podophyllotoxins inhibit topoisomerase II, though they cannot intercalate DNA as anthracyclines do. Etoposide **(19)** is 10 times more potent than teniposide. Both are used for variety of cancers; teniposide is mainly given to

paediatric patients, while etoposide is used to treat lymphoma, lung and testicular cancers. The main side effect is bone marrow suppression. [28-29]

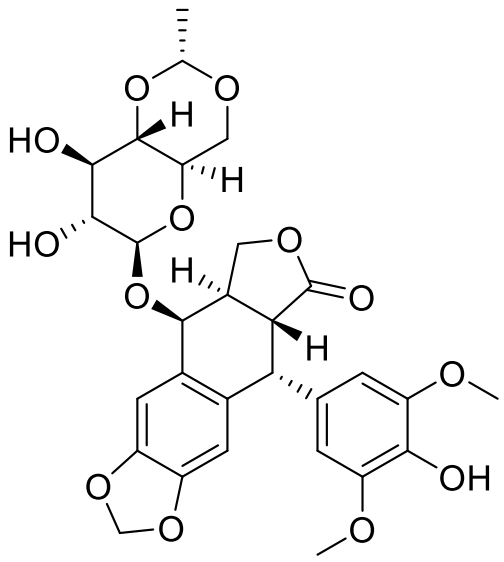

Etoposide **(19)**

Platinum compounds

Platinum compounds work by the similar mechanism as alkylating agents. They are all given intravenously and apart from treating urogenital cancer, they are indicated for head and neck cancers and brain and lung tumors. Cisplatin is the oldest, first generation platinum compound with a strong emetogenic effect and nephrotoxicity. Lower toxicity and better side effect profiles are attributed to the second generation, carboplatin, and the third generation, oxaliplatin **(20)**. Oxaliplatin is used to treat advanced colorectal cancer in combination with folinic acid and fluorouracil. [28]

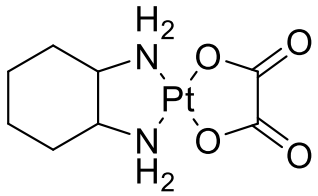

Oxaliplatin **(20)**

Interferons

Interferons are signaling proteins of the immune system that affect cellular proliferation through JAK/STAT signaling pathway. STAT dimers enter the nucleus, bind to DNA, and stimulate gene transcription. The impact on the cancer cells is

believed to be inhibition of cellular growth and differentiation, along with induction of apoptosis. Interferon α is the only interferon currently used in cancer treatment, primarily leukemias, solid tumors and Kaposi sarcoma in AIDS patients. Flu like syndrome often manifests as a side effect. [28]

Retinoids

Bexarotene **(21)** is an analogue of vitamin A and is thought to promote gene transcription through stimulation of retinoid X receptors. Gene transcription leads to protein synthesis that affects cellular growth and differentiation. Bexarotene is used as a second-line agent to treat cutaneous T-cell lymphoma. [28]

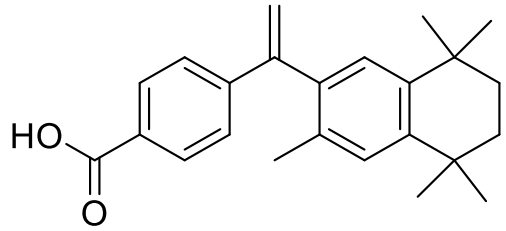

Bexarotene **(21)**

3.2.1.2 Chemotherapy targeted at the tumor proteins

Monoclonal antibodies

Monoclonal antibodies are drugs targeting tumor membrane receptors. Rituximab was one of the first monoclonal antibodies designated for cancer treatment, targeting CD20 receptors, located in the membrane of B-lymphocytes, leading to cell death. Another mechanism of action is activation of immune cells that attack antibody marked cells. This phenomenon is called antibody dependent cellular cytotoxicity (ADCC). Rituximab is given intravenously to treat lymphocytic leukemia and non-Hodgkin lymphoma, and causes depletion of both healthy and cancer B-lymphocytes that takes around 6 months to recover. Alemtuzumab, which is used for treatment of chronic lymphocytic leukemia, binds to the CD52 antigen displayed on the top of lymphocytes and other blood cells. It is linked to neutrophils depletion that may escalate to immunosuppression. Cetuximab and panitumumab target epidermal growth factor receptor (EGFR), also known as human epidermal growth factor receptor 1 (HER1). They work by binding to its extracellular compartment, preventing its activation that would normally lead to cell proliferation and survival, using anti-apoptosis signals. Both are used for metastatic colon cancer, cetuximab is additionally used for advanced squamous cell cancer of the head and neck. Skin

reactions appear in about 90% of patients treated with cetuximab or panitumumab. Trastuzumab and pertuzumab target HER2 receptors and also work through ADCC. They are administered intravenously to treat local or metastatic HER2 positive breast cancer. HER2 receptors are overexpressed in 20-30% of breast cancers cases. Both drugs are associated with infusion-related reactions. Trastuzumab is cardiotoxic. [28-29]

Drugs targeting tumor membrane receptors: tyrosine kinase inhibitors Lapatinib **(22)**, gefitinib and erlotinib are tyrosine kinase inhibitors that bind to ATP binding site on HER1 (lapatinib also binds to HER2), preventing activation of intracellular pathways. Erlotinib treats pancreatic cancer and HER2 positive breast cancer, whereas gefitinib and erlotinib are indicated for lung cancer. Crizotinib is a first in class inhibitor of anaplastic lymphoma kinase (ALK), part of the tyrosine kinase family, which promotes cell proliferation and survival when activated. It is given orally to advanced ALK-positive non-small-cell lung cancer (NSCLC). Possible side effects include higher susceptibility to infections and prolonged QT interval. [28]

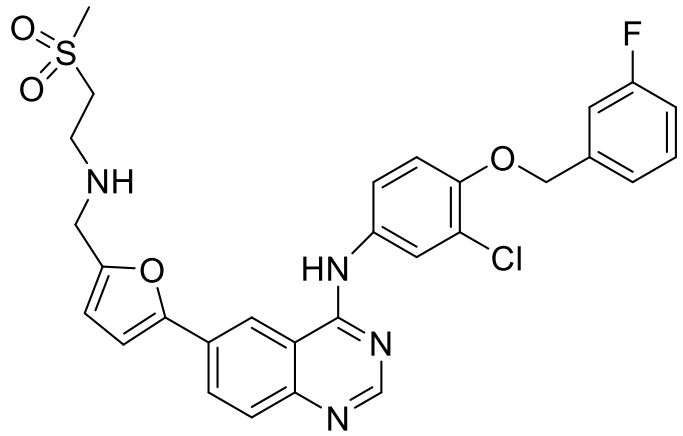

Lapatinib **(22)**

Drugs targeting tumor intracellular pathways: tyrosine kinase inhibitors Imatinib **(23)**, dasatinib and nilotinib target intracellular tyrosine kinases. They are given orally to treat leukemias. Imatinib is also used for stromal tumors of the gastrointestinal tract. Myelosuppression and gastrointestinal discomfort are the main side effects. [28]

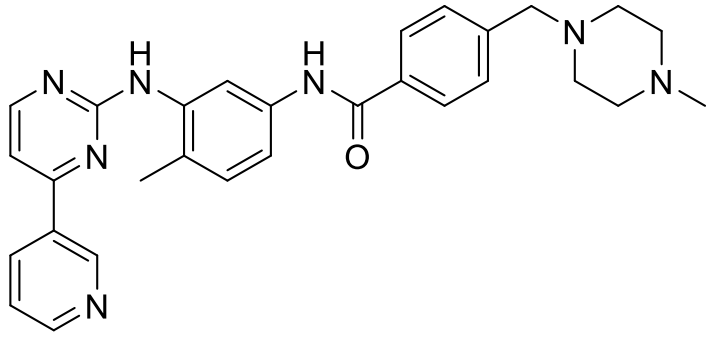

Imatinib **(23)**

Tubulin inhibitors

Tubulin is a globular protein that participates in cell division. Tubulin consists of α- and β-tubulin subunits that bind together and polymerize to form a microtubule. The production of microtubules is initiated during G_2 phase of the cell cycle, preparing for its essential role in the M phase. During mitosis, microtubules attach to the duplicated chromosomes through kinetochore proteins and separate them into the different poles of the cell. The cell than splits into two new daughter cells, each with its own set of chromosomes. The two main groups targeting tubulin are vinca alkaloids and taxanes.

The first Vinca alkaloids were acquired from the Madagascan plant *Catharantus roseus*, though nowadays they are synthetically manufactured. They work by binding to tubulin, preventing its polymerization and hence inducing cell cycle arrest. Vincristine, vinblastine **(24)**, vindesine and vinorelbine are given intravenously to treat range of haemetological and solid tumors including leukemia, sarcomas, lung and breast cancer. Vinblastine is also recommended for testicular cancer and Hodgkin lymphoma. Myelosuppression is the main side effect of vinblastine, vindesine and vinorelbin, while vincristine's shortcoming is neurotoxicity. Extravasation of any vinca alkaloid leads to necrosis.

Taxanes were derived from the bark of yew tree *Taxus brevifolia*, and are one of the strongest cytostatics. They bind to β-tubulin subunits and stabilize them, preventing microtubules from both polymerizing and depolymerizing. The loss of microtubules function induces apoptosis. Paclitaxel **(25)** and docetaxel are given in an intravenous injection to treat ovarian, breast and testicular cancer. Their toxic effects cause alopecia, peripheral neuropathy, mucositis and fluid retention. A recent study indicates that exercise reduces the symptoms of chemotherapy induced peripheral neuropathy. [28-29, 57]

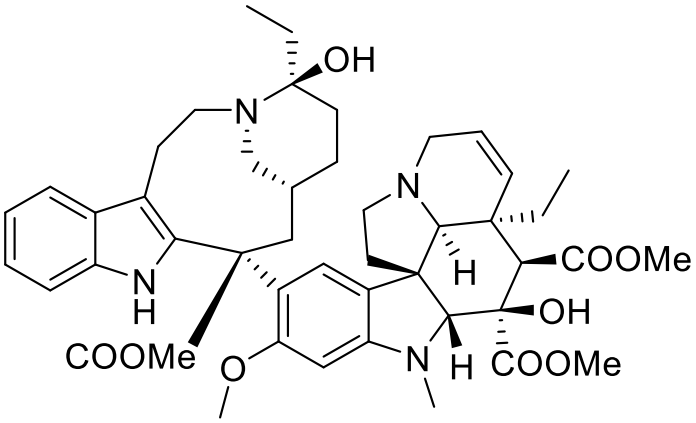

Vinblastine **(24)**

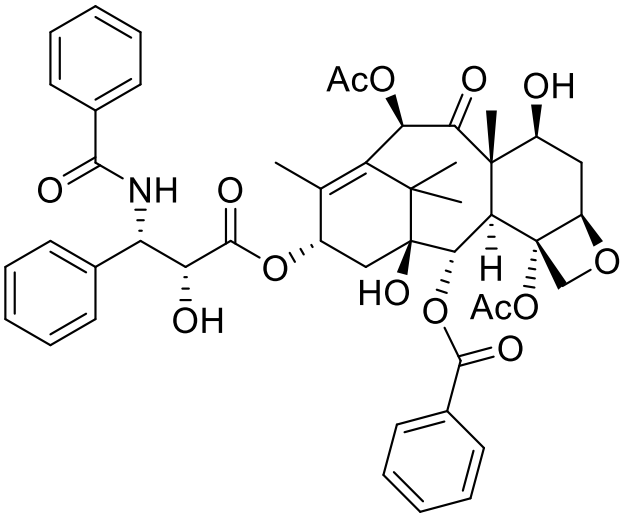

Paclitaxel **(25)**

S26 proteasome inhibitors

Proteasomes are proteases responsible for degradation of intracellular proteins. When inhibited, proteins start to accumulate inside the cell and signaling pathways are inactivated which result in apoptosis. Bortezomib, the first (original) proteasome inhibitor is still in use. Better efficacy, side effects profile and resistance suppression are provided by the second generation, carfilzomib and ixazomib **(26)**. The main indications of proteasome inhibitors are multiple myeloma, lymphocytic leukemia, prostate cancer, colon cancer and pancreatic cancer. Side effects of concern are increased risk of infections, thrombocytopenia, and peripheral neuropathy. [28]

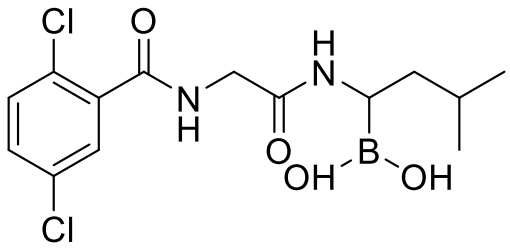

Ixazomib **(26)**

3.2.1.3 Chemotherapy targeted at endothelium

As solid tumors grow, angiogenesis is needed to provide sufficient oxygen and nutrients for newly produced cells. Vascular endothelial growth factor (VEGF) and its receptors (VEGFR) are attractive targets for anticancer drugs preventing angiogenesis. VEGFs induce proliferation of endothelial cells by binding to their membrane-bound VEGFRs. By inhibiting or disabling any of them, new vessels cannot be created, which disables metastasis and 'starves' the tumor. [28]

Monoclonal antibodies against VEGF

Bevacizumab is a monoclonal antibody that binds to VEGF and prevents its interaction with VEGFR. It is administered intravenously and is mostly used for lung, breast and colon cancers. Toxicity may manifest as hypertension, thromboembolic disorders, and vessel damage linked with haemorrhage. [28]

Tyrosine kinase inhibitors against VEGFRs

VEGFR are receptors associated with intracellular tyrosine kinase. Sorafenib, axitinib **(27)**, pazopanib, vandetanib, and sunitinib inhibit tyrosine kinase through VEGFRs, preventing angiogenesis. They are all given orally and treat a wide range of malignancies. All except for vandetanib are used for renal cancers. Sorafenib is also used for hepatocellular and thyroid carcinoma, vandetanib is used for thyroid cancer, and sunitinib is also used to treat gastrointestinal stromal tumors and pancreatic neuroendocrine tumors. They have been associated with hypertension, thromboembolic disorders, fatigue, hypofunction of thyroid gland, bone marrow suppression and less common cardiac toxicity. [28]

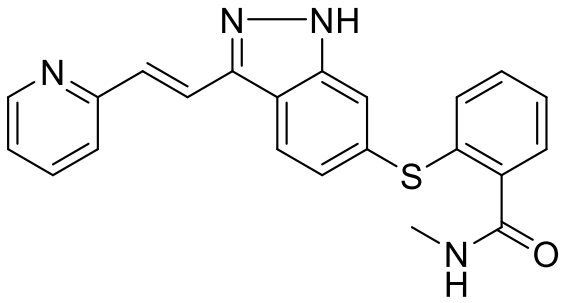

Axitinib **(27)**

Thalidomide and lenalidomide

Thalidomide **(28)** is a drug, originally used as a sedative and antiemetic in pregnant woman. After its teratogenic effects were revealed, usage in pregnant women was banned. Nowadays, thalidomide and lenalidomide are both given orally to treat multiple myeloma. They reduce the production of TNF-α, expression of VEGF and bFGF and suppress interleukin-6, which all contribute to angiogenesis. Thalidomide's side effects include drowsiness and peripheral neuropathy and lenalidomide can cause thromboembolism and neutropenia. [28]

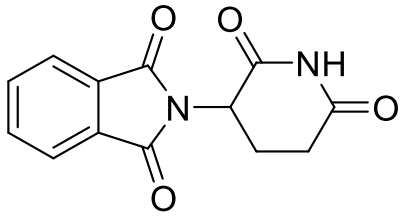

Thalidomide **(28)**

3.2.1.4 Miscellaneous cancer chemotherapies

L-asparaginase

L-asparginase is an enzyme, predominantly derived from *Escherichia coli* bacterium that catalyzes the conversion of a non-essential amino acid asparagine to aspartic acid. Tumor cells in acute lymphocytic leukemia are not capable of synthesizing their own asparagine and need to obtain it from the circulation. However, L-aspariganes cause depletion of asparagine, resulting in tumor cells deterioration. It is given intravenously to treat ALL. Side effects of concern include allergic reactions, liver damage or clotting disorders. [28]

Tretinoin

Treinoin **(29)** is a vitamin A derivative used to treat acute promyelocytic leukemia (APML). In APML, leukocytes are unable to mature and function as normal cells due to a gene translocation of chromosomes 15 and 17. Tretinoin modulates the expression of target genes and promotes differentiation of blood cells in APML patients. [24] It is given orally and may cause retinoic acid syndrome, a severe side effect presenting as fever, dyspnea and respiratory distress that can be treated with corticosteroids. [28]

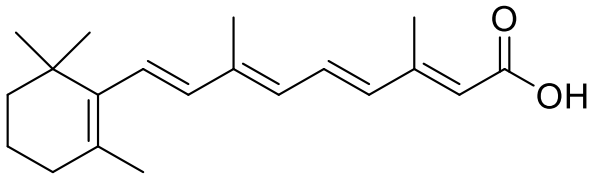

Tretinoin **(29)**

Histone deacetylase inhibitors

Histone deacetylase (HDAC) is a complex of enzymes that maintains balance between acetylated and deacetylated histones. Histones influence the expression of genes and signaling pathways. When acetylated, histones promote gene transcription, while deacetylated histones cause inhibition of gene expression. HDAC inhibitors vary in their mechanism of action, nevertheless they all induce cell cycle arrest, differentiation, and cell death, reduce angiogenesis and modulate immune response. [25] Vorinostat **(30)** and romidepsin have been approved for cutaneous T-cell lymphoma. Romidepsin is associated with QT interval prolongation and vorinostat may cause thromboembolism. [28]

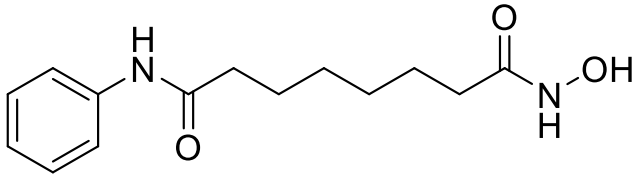

Vorinostat **(30)**

Immune checkpoint blockers

Ipilimumab is a first in class monoclonal antibody drug that binds to the cytotoxic T-lymphocyte-associated antigen 4 (CTLA-4). CTLA-4 antigen expression is increased when cytotoxic T-lymphocytes are activated. Sufficient levels of CD28:B7

are necessary for T-cells proliferation. [27] CTLA-4 competes with CD28 for binding to B7 on the T-cell surface and lowers its response to cancer cells. CTLA-4 inhibitors prevent this competition and restart an effective antitumor response by enabling T-lymphocytes to proliferate. Ipilimumab has been approved by FDA and increases overall survival of patients with metastatic melanoma. [26, 28]

3.2.2 Resistance to cancer chemotherapy

Just like microorganisms, cancer cells have the ability to develop resistance to traditional therapies. Currently, 90% of failures in the chemotherapy are during the invasion and metastasis of cancers related to drug resistance. [31] The prevalence of cancer drug resistance has been increasing and calls for further research and treatment development. [30]

3.2.2.1 Inactivation of the anticancer drugs

Many anticancer drugs undergo complex mechanisms *in vivo* to become activated. They interact with certain proteins in order to alter their structure and gain their efficiency. Cancer cells may benefit from this step and reduce the activation of drugs which leads to their resistance. Cytarabine is a drug used to treat acute myeloid leukemia that needs to be phosphorylated to its lethal form by an enzyme, deoxycytidine kinase. [32] Downregulation or mutation of the enzyme or other proteins involved in phosphorylation reduces cytarabine activity and cancer cells become resistant to its therapeutic effects. [30-31]

3.2.2.2 Drug efflux

Efflux is a physiological process that protects cell from toxin accumulation. Transcellular proteins that work as transporters, react to certain substrates by changing their conformation and forcing the substrate out of the cell. Efflux also participates greatly in cancer drug resistance and is one of the most studied mechanisms. The three chief pumps implicated in drug resistance are multidrug resistance protein 1 (MDR1), multidrug resistance-associated protein 1 (MRP1), and breast cancer resistance protein (BCRP), also generally called the ABC receptors. MDR1 gene is normally expressed in liver, kidneys and colon, and an overexpression of MDR1 has been observed when these tissues become cancerous. Related transporters MRP1 and BCRP are commonly the culprits of drug resistance in tissues

where MDR1 is not expressed. Potent efflux pump inhibitors have been studied, though their application is still restricted due to their adverse effects and obscure clinical efficacy. [30, 33]

3.2.2.3 Cell death inhibition

Cancer cells often acquire the ability to resist programmed cell death or apoptosis, leading to drug resistance. Apoptosis is mediated by many extrinsic and intrinsic pathways including many pre-apoptotic (e.g. Bax, Bclxl, p53) and anti-apoptotic factors (e.g. Bcl2, AKT). Downregulation of genes coding pre-apoptic factors and upregulation of anti-apoptic genes is associated with chemotherapy resistance. Another process causing cell death is autophagy. In this catabolic process, an organelle called a vesicle is formed around the cell and delivers it to lysosomes where the cell is decomposed and dies. Though enhancing autophagy is believed to stop cancer from developing in early stages, advanced cancers profit from autophagy flux. Thus, the question if autophagy inhibitors are beneficial or not is being reconsidered. [31, 34]

3.2.2.4 Changing drug metabolism

Enzymes play key roles in drug metabolism, activating them to carry out their effect on target cells or degrading them into their inert form. In this case, resistance arises from either reducing the activation of pro-drugs or increasing the drug inactivation. Increased P450 enzyme expression has been observed in breast cancer patients resistant to docetaxel. Another example of this type of resistance is increased detoxification of alkylating agents (chlorambucil, melphalan) and platinum compounds (cisplatin) by glutathione-transferase. [31, 35]

3.2.2.5 Alteration of drug targets

A drug's efficacy is dependent on its target and its alteration, including mutations and expression changes. In cancers, these changes eventually lead to drug resistance. For instance, topoisomerase II is a target of doxorubicin, which stabilizes topoisomerase II bond with DNA, causing its breakage and a mitotic arrest. Another common target for certain chemotherapy drugs are kinases, which promote uncontrolled cell growth if over-activated in tumor tissues. For example, HER2 tyrosine kinase which is a target of trastuzumab is overexpressed in approximately 20% of breast cancers. [30-31, 36]

3.2.2.6 DNA damage repair

Certain anticancer drugs' mechanisms include a direct or indirect DNA disruption which leads to apoptosis. Tumor cells can over-activate DNA repair systems to avoid apoptosis and resist those DNA damaging drugs. DNA damage response (DDR) mechanisms include nucleotide excision repair activated by overexpressed flap endonuclease 1 (FEN1) that reverses cisplatin effects in lung cancer cells. [37] Hematopoietic cells were shown to be protected by O6-methylguanine DNA methyltransferase (MGMT) repair system that converts O6 alkylated guanine back to guanine. Increased MGMT expression remains a major known mechanism of resistance of temozolomide, used for the treatment of glioblastoma. [30, 38]

3.2.2.7 Gene amplification

Gene amplification is the culprit of 10% of cancer resistance, mainly in leukemias. Gene amplification provides hundreds of copies of oncogenes which start producing high amounts of oncoproteins. The first demonstrated gene amplification in cultured mammalian cells was the amplification of dihydrofolate reductase gene that confers resistance to methotrexate. [31, 39]

3.2.2.8 Epigenetic altering

Epigenetic altering is one the most important mechanisms of tumor drug resistance and includes methylation of DNA and histone alterations. DNA methylation occurs on cytosine and is catalyzed by methyltransferase, influencing the expression of genes. Tumor suppressor genes can be silenced by methylation whereas oncogenes hypo-methylation leads to their over-expression, both contributing to cancer drugs resistance. According to reports, all colon cancers have aberrantly methylated genes. [40] On the other hand, histones may be altered by acetylation or deacetylation that affect stability and conformation of chromatins and regulate gene expression within the chromosome. Activation of nuclear factor kappa B (NFκB) in head and neck squamous cell carcinoma (HNSCC) induces deacetylation of tumor histones resulting in cisplatin chemoresistance. [30-31, 41]

3.3 Tubulin

3.3.1 Role of tubulin and microtubules in cell life

Microtubules (MTs) are key cytoskeletal elements and have essential roles in cell division, cell motility, intracellular transport, and cell shape maintenance. [43] MTs are composed of α and β tubulins, protein heterodimers that bind together to form chains (protofilaments). There are 13 protofilaments forming one hollow microtubule with a diameter of 25 nm. [42] Both α and β tubulin can accommodate one molecule of guanosine-5′-triphosphate (GTP). Before joining the end of a MT, GTP-tubulin dimers naturally have a 12-degree kink. Once fused with a MT, they become straight and introduce strain energy to the lattice. This energy is released when GTP is hydrolyzed to guanosine diphosphate (GDP) and another conformational change follows. **(Figure 11)**

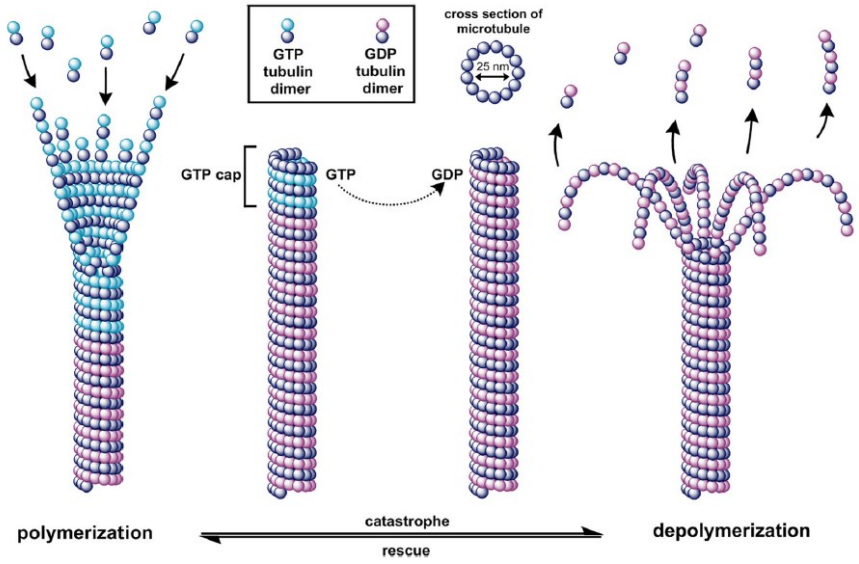

Figure 11: MTs dynamic instability. Conformation changes during polymerization and depolymerization phases. Taken from [3]

MTs are highly dynamic and perform a phenomenon termed ‘dynamic instability’. Dynamic instability includes polymerization and depolymerization of the MTs. During the polymerization phase, MTs grow by the addition of GTP-tubulin dimers, the end being stabilized by a GTP rich cap that prevents instant GTP hydrolyzation and switching to the depolymerization phase. End-binding” (EB) proteins and plenty of other microtubule-associated proteins (MAPs), including microtubule polymerases, depolymerases, and kinesins can attach to the GTP enriched cap and affect the fate of a MT. [44] The structure of MTs in polymerization state is straight owing to lateral interactions. However, as GTP is hydrolyzed and converts to GDP, conformational

changes cause chains of GDP-tubulin dimers to bow outwards from the protofilament and depolymerization begins. **(Figure 11)** Switching between polymerization and depolymerization is responsible for many cell's processes; growth of a MT produces a pushing forces that can center MT asters, mitotic spindles and nuclei, while shrinkage of a MT generates a pulling force if attached to an object. [44]

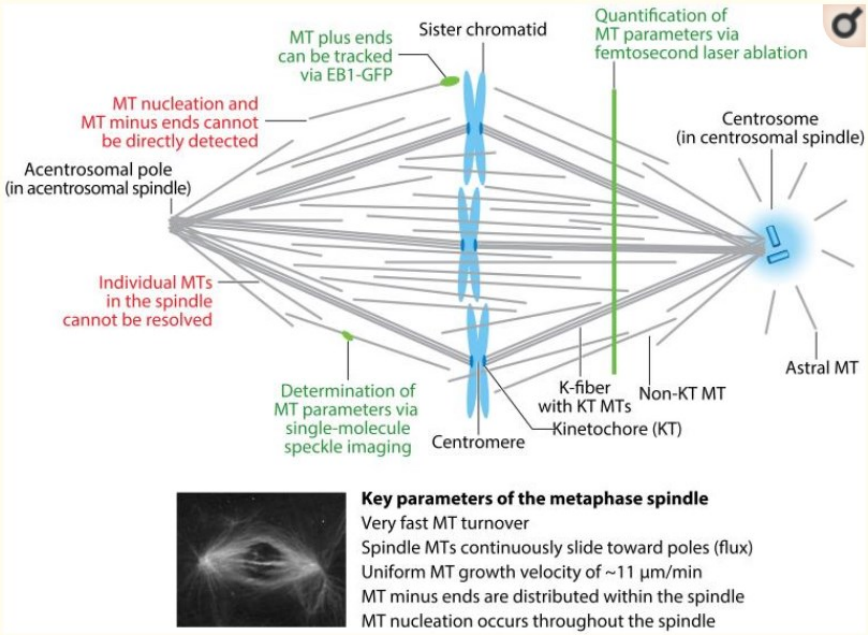

Figure 12: Segregation of sister chromatids by a mitotic spindle during metaphasis. Taken from [45]

Mitotic events are essential for life and they are governed by mitotic spindle and mitotic organizing centers. After breakage of the nuclear envelope around chromosomes, mitotic spindles approach sister chromatids and align at their center. Subsequently, sister chromatids are separated and pulled towards the opposite poles of the cell. Finally, cytokinesis occurs, yielding in two new daughter cells with identical set of chromatids, ready for replication during interphase. **(Figure 12)** [45] In case the mitotic spindle fails to attach the chromosomes, the cell cycle comes to arrests in metaphase, eventually leading to cell death, by both apoptosis and necrosis [3]

3.3.2 Role of tubulin in treating cancer

The vital role of tubulin in cell division makes it an attractive target for anticancer therapy, and many FDA approved drugs disrupting tubulin/MTs dynamics are effective in a wide range of malignancies. Examples of cancers treated with tubulin inhibitors include breast, lung, ovarian, and pancreatic carcinomas. Interfering with MTs leads to abnormal mitotic spindle production and cell cycle arrest in the G2/M phase. To achieve that, the MTs targeting drugs bind to different sites on tubulin, the most frequent being the vinca alkaloid, taxane, laulimalide, and colchicine binding

sites (CBS) [3]. The mechanism of action of colchicine was discovered in 1967 [46], and drugs interacting with CBS have been studied ever since. Generally, tubulin inhibitors can be categorized into two groups: stabilizing agents (e.g. taxanes, laulimalide, epothilones binding site agents), which promote tubulin polymerization and thus stabilize MTs, and destabilizing agents (e.g. vinca alkaloid and colchicine binding site agents), which inhibit tubulin polymerization. Furthermore, both stabilizing and destabilizing agents interfere with MT dynamics in low concentrations [62]. [3]

Taxanes binding site is located within lumen of the β tubulin subunit of an intact heterodimer. The first taxane and first stabilizing agent to be identified was paclitaxel (Taxol) **(25**, **page 39)** [47], followed by its semisynthetic analog docetaxel (Taxotere). Paclitaxel has been mainly used to treat breast and ovarian cancers, while docetaxel was approved to treat breast, lung, prostate, and head and neck malignancies. Moreover, recent studies have shown benefit of stabilizing agents on neurodegenerative diseases [48]. Downsides of taxanes include resistance development, low solubility, high toxicity, and neuropathy. Application of nanomedicine in cancer chemotherapy has led to the development and approval of an albumin-bound paclitaxel (Abraxane) [49], that partially overcomes some of these complications. Other nanoplatforms for delivering taxanes are being thoroughly investigated. [3, 50]

Epothilones represent a newer class of antineoplastic drugs. Similar to taxanes, epothilones bind to β-tubulin subunits and stabilize MTs, although they are less susceptible to tumor resistance caused by mutations of β-tubulin and overexpression of efflux pumps [51]. Two major compounds, epothilone A and epothilone B, were originally isolated from *Sorangium cellulosum*, and many semisynthetic analogues have been developed to improve their adverse effect profile. Ixabepilone is one of the potent semisynthetic analogues of epothilone B and was one of the FDA approved option for treatment of metastatic breast cancer [52]. Sagopilone **(31)** is the first fully synthetic epothilone B analogue and is currently under clinical evaluation. According to phase I/II studies, sagopilone may be effective in patients with recurrent platinum-resistant ovarian cancer. [53-54]

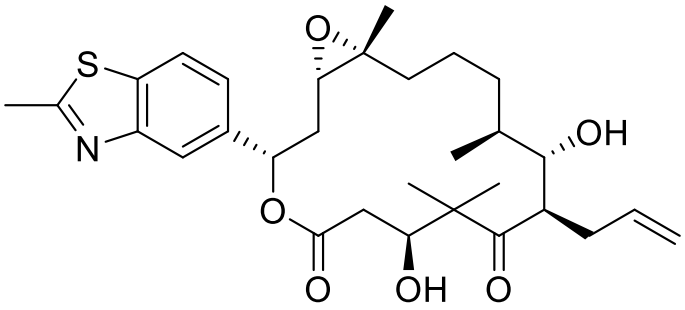

Sagopilone **(31)**

Laulimalide **(32)** is a natural cytotoxic product extracted from a marine sponge, *Cacospongia mycofijiensis*, with a paclitaxel-like MT stabilizing activity. Laulimalide and its analogues bind to their binding site on β-tubulin and show considerable effectiveness against paclitaxel and epothilones resistant cells [55]. In addition, laulimalide binding agents are poor substrates of P-glycoprotein efflux pump, unlike taxanes, who often succumb to this kind of resistance [56-57]. Despite promising results in cell-based and pharmacokinetic studies, laulilamide demonstrated only limited tumor growth inhibition *in vivo* and severe toxicity and mortality have been observed. [56]

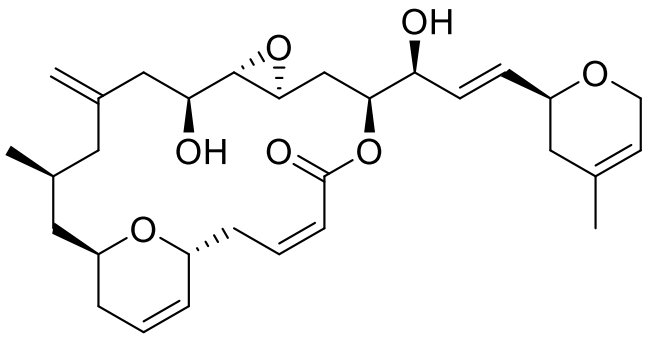

Laulimalide **(32)**

Vinca alkaloids are destabilizing agents, originally extracted from the periwinkle plant, *Catharanthus roseus*. Despite their susceptibility to developing resistance and severe side effects, vinca alkaloids belong to the most commonly used MTAs. The vinca domain is located near the exchangeable GTP site in β-tubulin [62], where vinca alkaloids inhibit GTP hydrolysis to GDP. Vinca alkaloids increase the levels of oxidized glutathione, influence lipid metabolism and membrane lipid content, elevate cAMP and inhibit cAMP phosphodiesterase [58]. Current vinca alkaloids in use include vinblastine **(24, page 10)**, vincristine, vinorelbine, vindesine, and vinflunine, with the latter three being semisynthetic derivatives of vinblastine. The common type of administration is intravenous; intrathecal administration is not recommended since

deaths and neurological devastations have been reported [59]. The most frequent cancers that might by treated with vinca alkaloids involve Hodgkin's lymphoma, leukemias, and breast and lung malignancies. Certain derivatives have been used for treatment of cerebrovascular disorders (e.g. vinpocetine) [60]. New derivatives of natural vinca alkaloids are being synthetized and investigated in order to improve their effect or reduce toxicity. For instance, vindoline has no antitumor effect on its own, however, when coupled with suitable amino acids and certain synthetic pharmacophores, compounds with promising anti cervical cancer results were obtained [61]. [3, 58]

The last major group of tubulin inhibitors are colchicine binding site agents. Colchicine **(1**, **page 10)** is an alkaloid that was extracted from the meadow saffron *Colchicum autumnale*. Colchicine pocket is situated at the interface between α and β-tubulin dimer [62]. When colchicine binds to its binding site, the colchicine-tubulin complex is incorporated in MTs structure and disrupts its lateral interactions, eventually leading to the MT disassemble. [3]. Despite colchicine binding site agents' cytotoxic properties, none has been approved for anticancer therapy. A narrow therapeutic window, poor solubility and harsh side effects including neutropenia, gastrointestinal upset, bone marrow damage and anaemia are the major shortcomings of these tubulin inhibitors [63]. Nevertheless, colchicine binding site inhibitors possess certain qualities that others may lack, such as the ability to prevent the formation of new tumor blood vessels and disrupting the existing ones [64] or limiting mitochondrial metabolism by modifying voltage-dependent channels of mitochondrial membrane [65]. These advantages make a colchicine scaffold an attractive target for further development. Though colchicine did not find its employment in chemotherapy, it has been used for the treatment of gout, gouty arthritis, familial Mediterranean fever, Bechet's disease, and recurring pericarditis with effusion [63].

Combretastatins are a group of diaryl stilbenoids isolated from *Combretum Caffrum*. The most potent colchicine site inhibitors of the natural occurring combretastatins are combretastatin A-4 (CA-4) and combretastatin A-1 (CA-1) [63]. Their efficacy can be elevated by forming phosphate prodrugs with increased solubility and optimized vascular disrupting potential [3]. Combretastatin **(2, page 10)** is structurally related to colchicine and binds to CBS in a similar orientation as colchicine. *Cis* configuration was established to be essential for the interaction with CBS, whereas *trans* isomers demonstrated little or no effect [66]. Many analogues of CA-4 with nanomolar or

picomolar antiproliferative IC50 values have been synthesized. ABI 231 is a highly potent analogue of CA-4 that is currently undergoing clinical trials for prostate cancer, with average IC_{50} values of 5.2 nM. Encouraged by this success, Wang et al. synthesized and evaluated AB 231 analogues, observing promising results in both *in vitro* and *in vivo* studies, with the most potent analogue reaching the IC_{50} value of average IC50 ~ 1.8 nM across a panel of different cell lines [67, 68]. Another successful group of CA-4 derivatives are 3-aroyl-1-arylpyrroles (ARAPs) **(5**, **page 11)**, synthesized and evaluated by La Regina et al. in Italy. ARAPs proved to be potent inhibitors of tubulin polymerization and Hh signaling pathway, with five compounds yielding IC50 values ≤1.0 μM [1].

At present, certain combretastatin analogues are being evaluated in clinical trials. Fosbretabulin (CA-4P) **(33)** is a CA-4 phosphate salt derivative that failed to show satisfying results in monotherapy trials [69]. Combination regimens with fosbretabulin are being explored [70]. Oxi4503 is a diphosphate derivative of AC-1, that demonstrated modest anti-leukemic activity in patients with AML [71]. The combination of Oxi4503 and cytarabine is being studied for the same indication [72].

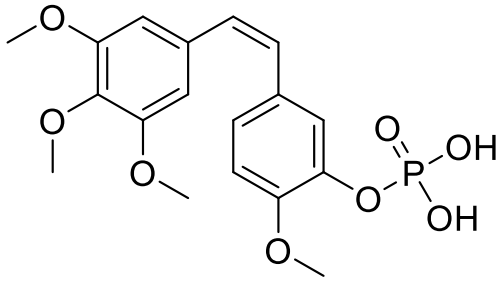

Fosbretabulin **(33)**

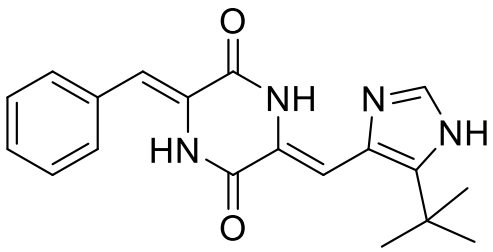

Plinabulin **(34)**

Moreover, there are several potent CBSIs derived from sources other than combretastatins that are currently undergoing clinical trials and may dictate the future of anticancer therapy, e. g. plinabulin **(34)**, lisavanbulin, crolibulin [63].

4. EXPERIMENTAL PART

4.1 Laboratory equipment and instruments

Regular laboratory glassware was used during my whole project (e.g. beakers, one neck- or two-necks-round-bottom flasks, stirring rods, test tubes, funnels, separating funnels, condensers, vials) and most of the reactions were carried out at room temperature.

Metal laboratory tools such as spoons, spatulas and tweezers were utilized for handling the intermediates, weighing the reagents and for other applicable situations.

All reagents and solvents were handled according to the material safety data sheet of the supplier and were used as purchased from Sigma-Aldrich (St. Louis, Missouri, USA) without further purification.

Most of reactions were conducted under argon atmosphere in oven-dried glassware unless stated otherwise.

In order to increase the yield of some reactions, microwave (MW)-assisted reactions were performed on Discover S-Class (CEM, Matthews, North Carolina) single mode microwave reactor, equipped with an Explorer 72 autosampler, controlling the instrument settings with PC-running Synergy 1.6 software (CEM, Matthews, North Carolina). All experiments were carried out in closed vessel mode using capped MW-dedicated vials (1 mL or 35 mL) with a cylindrical stirring bar (length 8 mm, diameter 3 mm). Stirring, temperature, irradiation power, PowerMAX (*in situ* cooling during the microwave irradiation), ramp and hold times were set as indicated in the following procedures. Reaction temperature was monitored by an external CEM fiber optic temperature sensor. After completion of the reaction, the mixture was cooled to 25 °C via air-jet cooling.

In contrast the reactions which required high temperature conditions, DrySyn heating blocks (Asynt, Isleham, UK) were used.

Organic solutions were dried over anhydrous sodium sulfate. Evaporation of solvents was carried out on a Rotavapor R-210 equipped with a V-850 vacuum controller and a V-700 vacuum pump (Büchi, Flawil, Switzerland)

The progress of the reactions was checked and confirmed by TLC. Silica gel thin layer chromatography (TLC) cards (silica gel precoated aluminum cards with fluorescent indicator visualizable at 254 nm) (Macherey-Nagel, Düren, Germany) were used for TLC. Developed plates were visualized with a ENF 260C/FE UV apparatus (Spectroline, Westbury, NY, USA).

Considering the purification process, column chromatography was performed using columns packed with silica gel from Macherey-Nagel (70-230 mesh). Proton nuclear magnetic resonance (^{1}H NMR) spectra were recorded with a Varian Mercury (300 MHz) or a Bruker Avance (400 MHz) spectrometer at room temperature (rt) operating in both solvent and frequencies indicated. The corresponding fid files were processed by MestreReNova 6.2.1-769 software (MestreLab Research SL, Santiago de Compostela, Spain).

Mass spectra were recorded on a MicroTOF LC/MS mass spectrometer (Bruker Daltonics, Massachusetts, USA) equipped with a positive ion ESI source. Compound purity was checked by high pressure liquid chromatography (HPLC). Purity of tested compounds was found to be >95%.

The HPLC system used - Dionex UltiMate 3000 (Thermo Fisher Scientific Inc., Massachusetts, USA) consisted of an SR-3000 solvent rack, a LPG-3400SD quaternary analytical pump, a TCC-3000SD column compartment, a DAD-3000 diode array detector, and an analytical manual injection valve with a 20 mL loop. Samples were dissolved in acetonitrile (1 mg/mL). HPLC analysis was performed by using a Thermo Fisher Scientific Inc. Acclaim 120C18 column (5 mm, 4.6mm_ 250 mm) at 25 ± 1 ˚C with an appropriate solvent gradient (acetonitrile/water), flow rate of 1.0 mL/min and signal detector at 206, 230, 254 and 365 nm. Chromatographic data were acquired and processed by Chromeleon 6.80 SR15 Build 4656 software (Thermo Fisher Scientific Inc., Massachusetts, USA).

Melting points (mp) were determined on a Stuart Scientific SMP1 apparatus (Stuart Equipment, Stone, UK) and are uncorrected.

Software CS ChemDraw professional 19.0 (PerkinElmer, Massachusetts, USA) was used to generate all the molecule's structures and to determine molecular weight and lipophilicity parameter logP.

4.2 General procedure

The synthesis of my compounds composed of 5 steps; 1. acylation of the pyrrole intermediate at position C_3 (Friedel-Crafts reaction), 2. hydrolysis of the pyrrole intermediate, 3. protection of the base using a silyl group, 4. coupling reaction between the hydrolyzed pyrrole intermediate and the protected base, 5. cleavage of the silyl group

1. The first step of the preparation of new ARAP compounds was the Friedel-Crafts reaction **(Scheme 2)**. This reaction was necessary to carry out under argon stream in a previously oven-dried two-necks round-bottom flask. First, the 1-(p-tolylsulfonyl)pyrrole (200 mg; 0.9 mmol; 1 equiv) was weighed and added to the flask, dissolved in dry dichloromethane (DCM) (3 mL) and stirred vigorously on a magnetic plate. Next, the aluminium trichloride (146.7 mg; 1.1 mmol; 1.2 equiv) was weighed and added, a respiratory protection was mandatory to wear during the handling, due to aluminium trichloride's harmful effects to lungs. Aluminium trichloride works as a catalyst in Friedel-Crafts reaction. Finally, 2-fluorobenzoylchloride (119.4 µl; 1 mmol; 1.1 equiv) was dissolved in dry DCM (2 mL) in a dropping funnel and added dropwise over a 5 min period to the solution in the flask. The argon stream was replaced with a balloon which had been filled with argon to keep an inert atmosphere. After 20 min the TLC (8:2 CHex/EtOAc) was checked, to find out if the reaction was complete and if there was any starting material left. When there was a significant spot representing the product, the reaction was terminated adding ice and a base- sodium hydrogen carbonate (saturated solution). The reaction mixture was transferred to a separating funnel. In case it formed an emulsion, hydrochloric acid (2 M) was added, to neutralize the pH. To separate the organic and inorganic compounds of the reaction, extraction was performed, using water as the inorganic phase and DCM as the organic phase. Due to a higher density, the DCM represented the bottom layer. The organic phase was then washed twice with brine. In addition, the water phase was also washed with DCM, to be sure that all the product was dissolved in the organic phase. The organic phases were collected, dried over anhydrous sodium sulphate and filtered with cotton into a clean, dry and pre-weighed round-bottom flask. The flask was then placed on the Rotavapor to evaporate solvents. When the flask content was dry, column chromatography was performed, to get the pure product of the reaction. Suitable eluent system (8:2 CHex/EtOAc) was

prepared according to the retention factors of the previously done TLCs. The size of the column was chosen according to the amount of dry product (20g column, 40g column or combination of both). Because the mixture was not soluble in the eluent system, DCM and methanol were used to dissolve it instead. After obtaining a clear solution, silica powder was added, and the solvents were evaporated on Rotavapor subsequently. Acquired dry powder was then transferred to the column and the chromatography was initiated. The progress was checked again by TLC. The test tubes that contained the pure product of the reaction were collected into a pre-weighed round-bottom flask, they were washed with DCM, and the flask contents were concentrated once again on Rotavapor. A sample from the dry product was taken for identity check using NMR method.

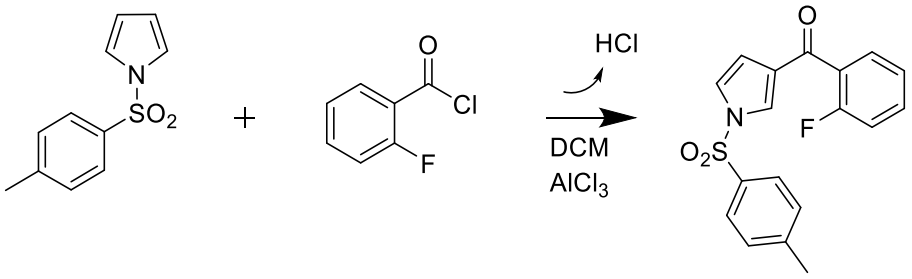

Yield: 85%

Code: RS6350

Scheme 2: Acylation of the pyrrole intermediate at position C3 (Friedel-Crafts reaction)

2. The next reaction was the hydrolysis of the acylated intermediate from previous reaction **(Scheme 3)**. For this reaction a round-bottom flask, an electric magnetic heated plate with a thermometer, a condenser and a magnetic stirrer were used. In a beaker, a solution of sodium hydroxide (6 M in water; 10 mL) was prepared. As the sodium hydroxide was dissolving, the acylated pyrrole (163 mg; 0.5 mmol) was placed in the round-bottom flask and dissolved in sufficient amount of ethanol absolute. Then the prepared sodium hydroxide solution was slowly added, and the temperature was increased to 80 ˚C. The condenser was attached, with cold water stream running through. After 1 hour the TLC (7:3 CHex/EtOAc) was checked and after there was no starting material left, ice and hydrochloric acid solution (2 M) were added to terminate the reaction and to adjust the pH to neutral, using pH paper. The next step was the work-up. In this case, EtOAc was chosen as the

organic phase, while the inorganic phase remained water. This time organic phase was the top layer. The water phase was washed with EtOAc and the organic phase was extracted with brine. As usual, sodium sulphate was added, the organic phase was filtrated into a pre-weighed round-bottom flask and placed on a Rotavapor to evaporate the solvents. TLC was spotted again to find out how pure the product was- provided it was pure enough, there was no need to perform the column chromatography. If other organic compounds were present, column purification was necessary and was carried out using the suitable size of the column and eluent system (7:3 CHex/EtOAc).

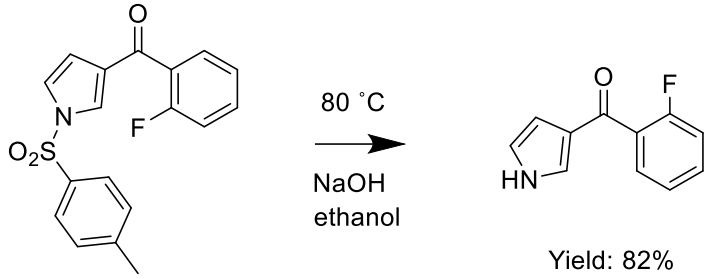

Code: RS6350 Code: RS6351

Scheme 3: Hydrolysis of the pyrrole intermediate

3. The third reaction was protection of the base reagent (**Schemes 4-6)**. The reason of the protection was to prevent bonding in the unwanted position during coupling of the base with the hydrolyzed pyrrole intermediate. This reaction was performed once more under argon stream in an oven-dried two-necks round-bottom flask. Sodium hydride (60% in mineral oil) (176 mg; 4.4 mmol; 1.1 equiv) was dissolved in dry DMF (5 mL) at 0°C. Then the base reagent (853 mg; 4 mmol; 1 equiv) was added, previously dissolved in dry DMF (10 mL) as well. Sodium hydride is a strong base that works as a deprotonation agent. After 15 min the deprotonation was done, 2-(Trimethylsilyl)ethoxymethyl chloride (SEMCl) (849.5 ml; 4.8 mmol; 1.2 equiv) was added to protect the deprotonated nitrogens of the base reagent, and the reaction was continued stirring at about 0°. After 1 hour the progress of the reaction was checked by TLC (7:3 CHex/EtOAc). If needed, the reaction was left overnight. After the reaction was completed, it was terminated with ice and the mixture was transferred to a separating funnel. For the work-up, water and DCM were utilized as the solvents. The water phase was washed again

with DCM, organic phase was washed with brine. Sodium sulphate was added in the collected organic phase, to get rid of any remaining water. After filtrating the organic mixture into a pre-weighed round-bottom flask, the solvents were evaporated on Rotavapor. To obtain the pure product, column chromatography was performed (9:1 CHex/EtOAc). The product was collected in a round-bottom flask and placed on Rotavapor in order to get the dry pure product of the reaction. The purity of this compound was checked through NMR.

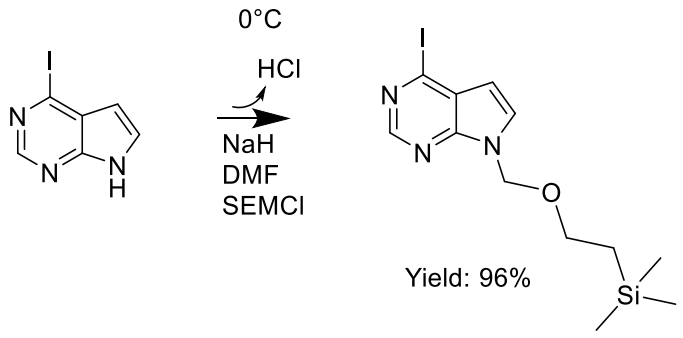

Code: RS6357

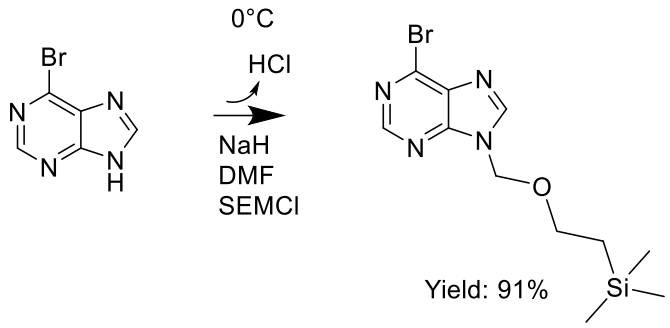

Code: RS6322

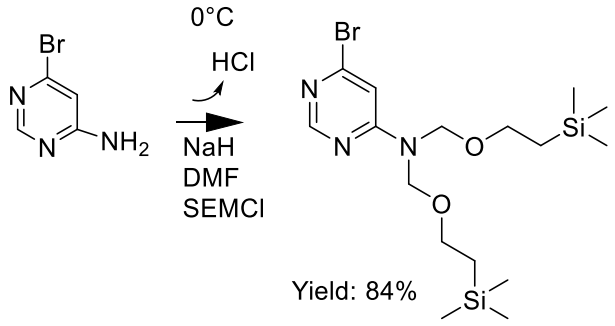

Code: RS6376

Schemes 4-6: Overview of protection of the base using a silyl group

4. The next reaction was the coupling between the products of the second and the third reaction **(Schemes 7-9)**. This step needed to be done under argon stream at increased temperature. A two-necks round-bottom flask, a magnetic stirrer and a condenser were put in the oven for 15 min. Then the reagents were combined, starting with the hydrolyzed pyrrole intermediate (60 mg; 0.3 mmol). The solvent- dioxane (1 mL) was poured in. Cesium carbonate (155 mg; 0.5 mmol; 1.5 equiv), copper iodide (30 mg; 0.2 mmol; 0.5 equiv) and phenanthroline (6 mg; 0.03 mmol; 0.1 equiv) were consecutively added at room temperature. Finally, the protected base (143 mg; 0.38 mmol; 1.2 equiv) was added, the condenser was attached and the temperature increased to 110 ˚C. The reaction was either left reacting overnight, or a microwave assisted reaction, which only takes 25 min, was performed. After the completion of the reaction was checked by TLC (7:3 CHex/EtOAc), the extraction was performed, using water and EtOAc. The water phase was washed with EtOAc and organic phase was washed with brine. To make sure there was no organic compounds left in the water phase, another TLC was carried out. Then, it was time to add some sodium sulphate, filter the organic phase with cotton into a round-bottom flask and evaporate the solvents on Rotavapor. To obtain the pure product column chromatography (8:2 CHex/EtOAc) was performed. The purity of the compound was checked by NMR.

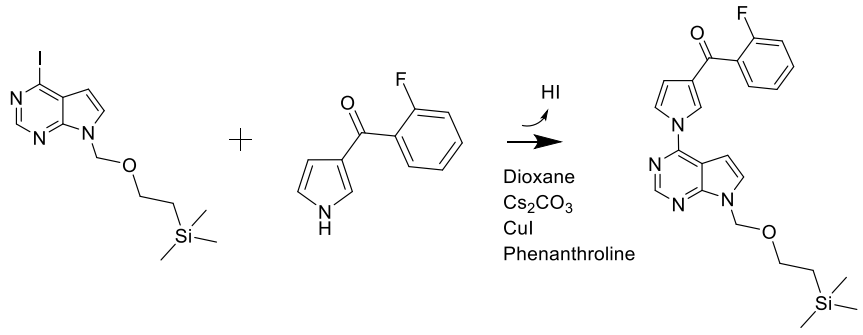

Yield: 83%

Code: RS6357 Code: RS6351 Code: RS6387

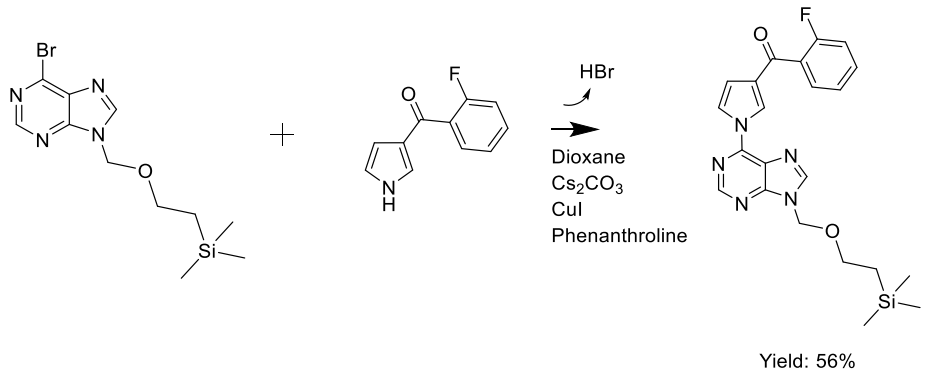

Yield: 56%

Code: RS6322 Code: RS6351 Code: RS6352

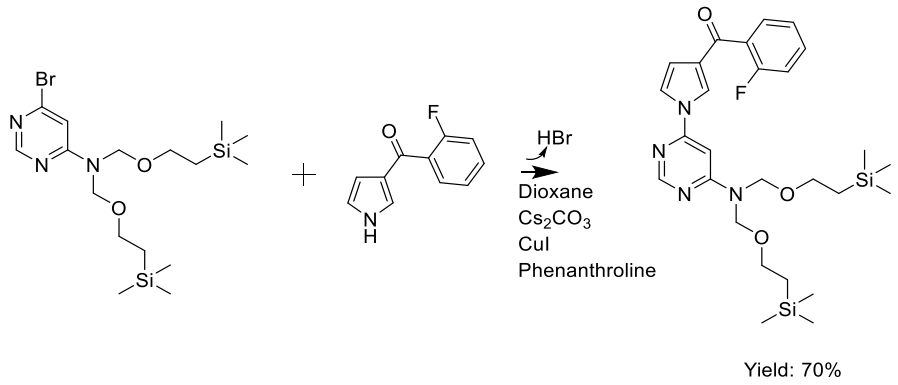

Yield: 70%

Code: RS6376 Code: RS6351 Code: RS6385

Schemes 7-9: Overview of coupling reactions between the hydrolyzed pyrrole intermediate and the protected base

5. The last step of the synthesis was the cleavage of the silyl group (**Schemes 10-12)**. The glassware utilized in this reaction was a round-bottom flask. The flask was placed in an ice bath. The coupled intermediate (78 mg; 0.18 mmol) from the last reaction was put in the flask and dissolved in DCM (4 mL) (codes RS6387, RS6352) or in tetrahydrofuran (THF) (code RS6385). Then trifluoroacetic acid (TFA) (0.4 mL) was added dropwise **(Schemes 10-11)**. Since trifluoroacetic acid is a strong acid, safety gloves were a mandatory protective equipment for handling the reagent. After all the acid was added, the ice bath was removed, the flask was sealed with a tap and the reaction was left reacting at room temperature overnight. In the case of code RS6385, due to effort to increase the yield of the reaction, tetrabutylammonium fluoride (TBAF) (1 M in THF; 1.5 mL) was added **(Scheme 12)**, no ice bath was needed in this case. The mixture was stirred vigorously at 70°C for 5 h. The completion of the reaction was checked yet again by TLC (3:7 CHex/EtOAc)

and the last extraction was performed, using water and DCM (codes RS6387, RS6352) or water and EtOAc (code RS6385). The organic phase was dried over sodium sulphate, filtered, and concentrated. The residue was purified by column chromatography (7:3 CHex/EtOAc) on silica to give the pure final product, that was confirmed by NMR.

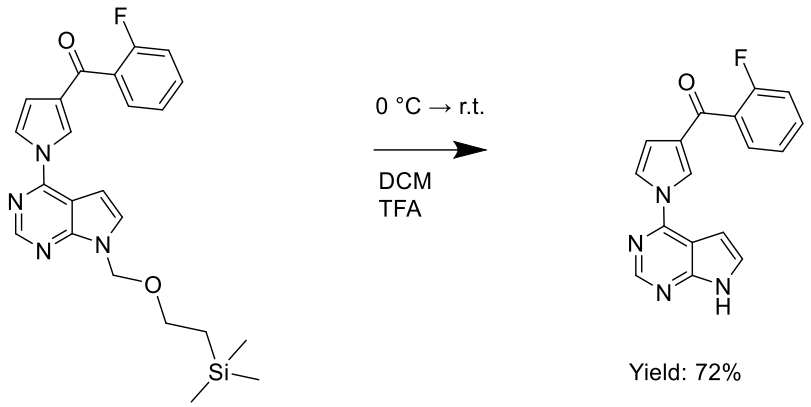

Code: RS6387 Code: RS6362

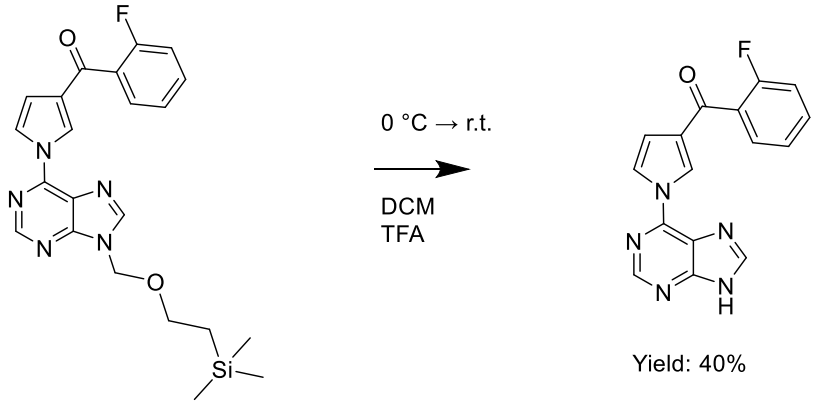

Code: RS6352 Code: RS6355

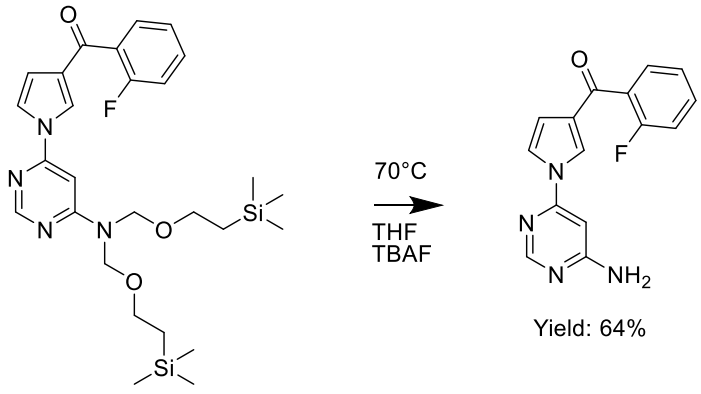

Code: RS6385 Code: RS6386

Schemes 10-12: Overview of cleavage of the silyl group reactions

4.3 Analytical Data of Prepared Compounds

4.3.1 (2-Fluorophenyl)(1-tosyl-1*H*-pyrrol-3-yl)methanone

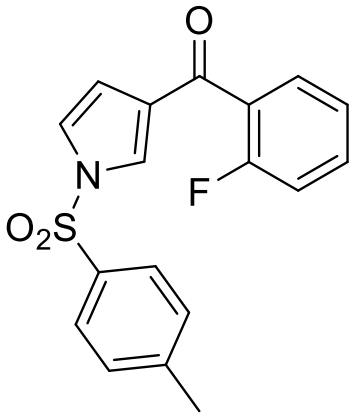

Code: RS6350

Chemical Formula: $C_{15}H_{11}FN_4O$

Molecular weight: 343.37

Appearance: White powder

m.p.: 192 °C

LogP: 3.82

R_f (7:3 CHex/EtOAc): 0.34

^{1}H NMR: (DMSO-d6, 400 MHz): δ 2.37 (s, 3H), 6.73 (dd, *J* = 1.6 and 3.3 Hz, 1H), 7.33-7.39 (m, 2H), 7.45 (d, *J* = 8 Hz, 2H), 7.50 (dd, *J* = 2.2 and 3.3 ,1H), 7.83-7.87 (m, 3H), 7.97-7.99 (m, 2H) ppm

Elemental analysis (calculated): C, 62.96; H, 4.11; F, 5.53; N, 4.08; O, 13.98; S, 9.34

4

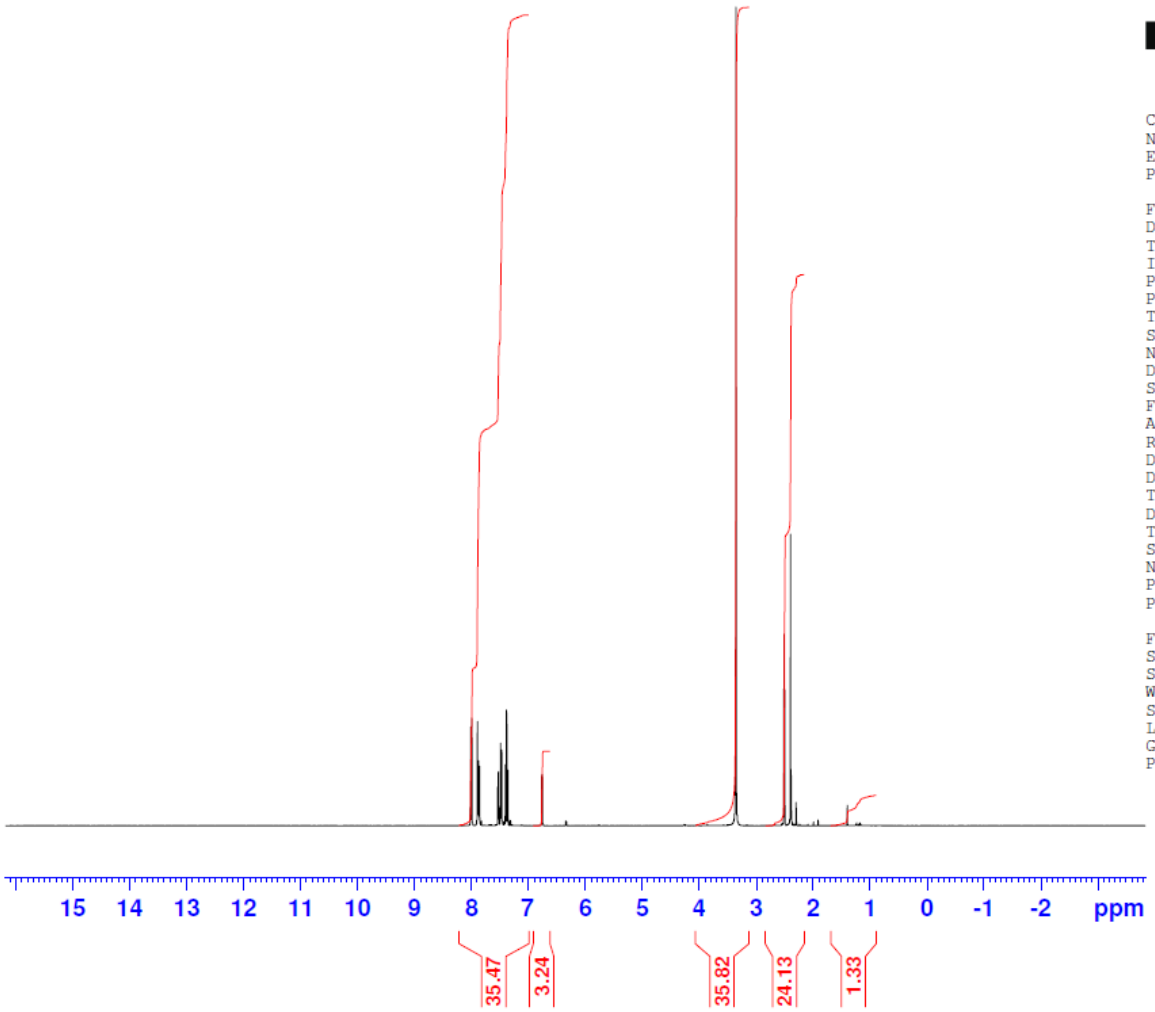

Current Data Parameters
NAME silvestri07112019
EXPNO 5
PROCNO 1

F2 - Acquisition Parameters
Date_ 20191107
Time 10.55 h
INSTRUM spect
PROBHD Z167430_0010 (
PULPROG zg30
TD 65536
SOLVENT DMSO
NS 16
DS 2
SWH 8012.820 Hz
FIDRES 0.122266 Hz
AQ 4.0894465 sec
RG 157.67
DW 62.400 usec
DE 10.00 usec
TE 298.2 K
D1 1.00000000 sec
TD0 1
SFO1 400.1324708 MHz
NUC1 1H
P1 12.00 usec
PLW1 9.00000000 W

F2 - Processing parameters
SI 65536
SF 400.1300000 MHz
WDW EM
SSB 0
LB 0.30 Hz
GB 0
PC 1.00

4.3.2

(2-Fluorophenyl)(1*H*-pyrrol-3-yl)methanone

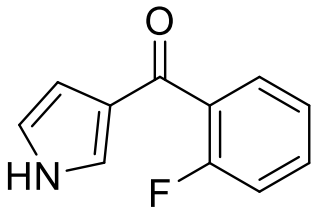

Code: RS6351

Chemical Formula: $C_{11}H_8FNO$

Molecular weight: 189.19

Appearance: White powder

m.p.: 125 °C

LogP: 1.89

R_f (3:2 CHex/EtOAc): 0.28

^{1}H NMR: (DMSO-d6, 400 MHz): δ 6.62-6.64 (m, 1H), 6.73-6.75 (m, 1H), 7.07-7.09 (m, 1H) 7.24 (td, *J* = 1.5 and 7.4 Hz, 1H), 7.28-7.38 (m, 3H), 8.73 (s, broad signal, disappeared after treatment with D2O, 1H) ppm

Elemental analysis (calculated): C, 69.84; H, 4.26; F, 10.04; N, 7.40; O, 8.46

1

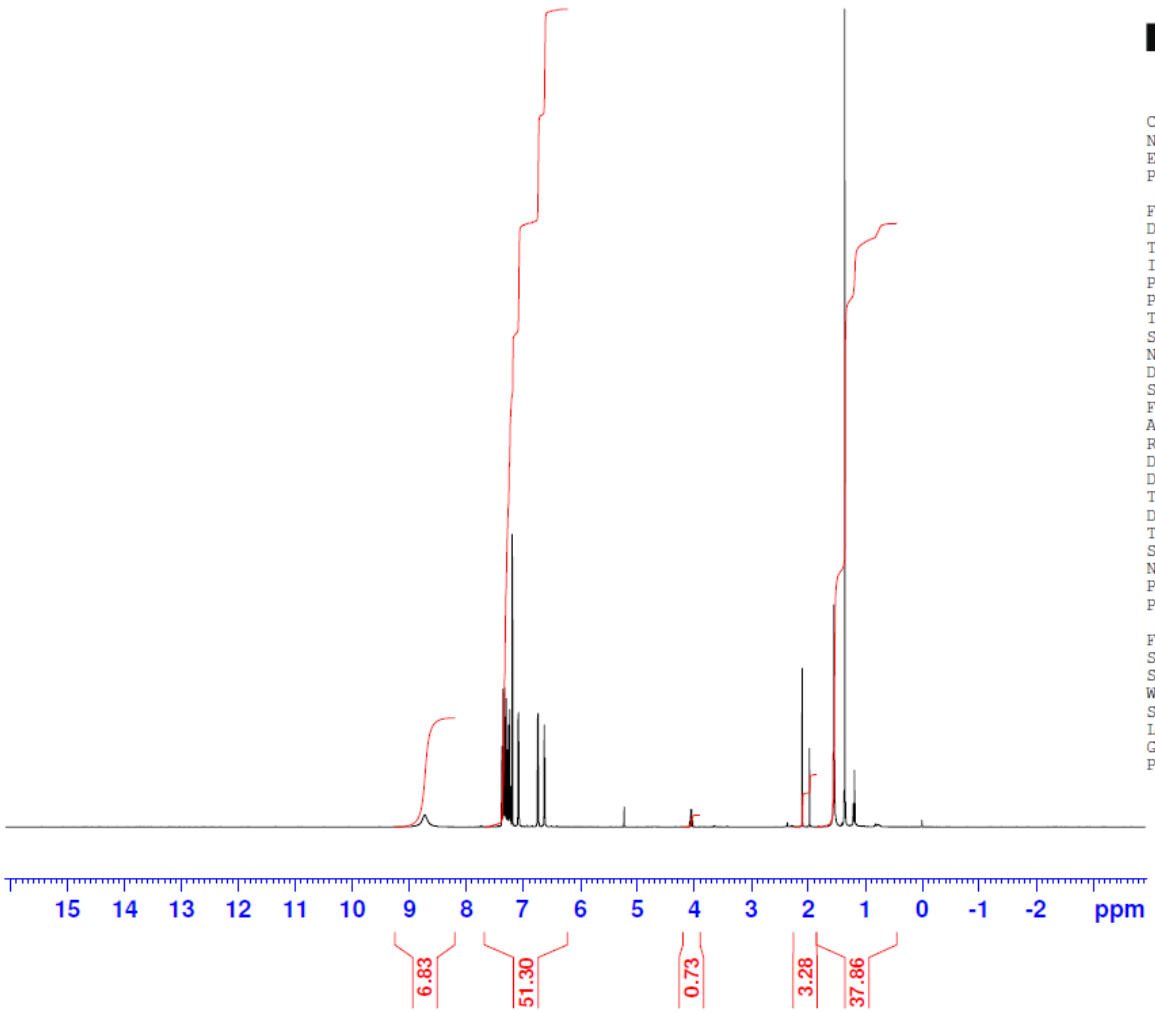

Current Data Parameters
NAME silvestri04112019
EXPNO 1
PROCNO 1

F2 - Acquisition Parameters
Date_ 20191104
Time 12.54 h
INSTRUM spect
PROBHD Z167430_0010 (
PULPROG zg30
TD 65536
SOLVENT CDC13
NS 32
DS 2
SWH 8012.820 Hz
FIDRES 0.122266 Hz
AQ 4.0894465 sec
RG 143
DW 62.400 usec
DE 10.00 usec
TE 298.2 K
D1 1.00000000 sec
TD0 1
SFO1 400.1324708 MHz
NUC1 1H
P1 12.00 usec
PLW1 9.00000000 W

F2 - Processing parameters
SI 65536
SF 400.1300372 MHz
WDW EM
SSB 0
LB 0.30 Hz
GB 0
PC 1.00

4.3.3

4-Iodo-7-((2-(trimethylsilyl)ethoxy)methyl)-7*H*-pyrrolo[2,3-*d*]pyrimidine

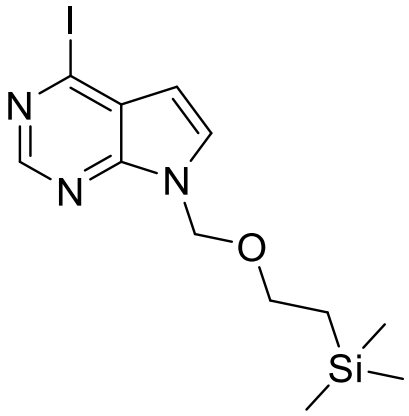

Code: RS6357

Chemical Formula: $C_{12}H_{18}IN_3OSi$

Molecular weight: 375.29

Appearance: Colorless oil

m.p.: NA

LogP: NA

R_f (7:3 CHex/EtOAc): 0.5

^{1}H NMR: (DMSO-d6, 400 MHz): δ 0.00 (s, 9H), 0.92 (t, *J* = 7.9 Hz, 2H), 3.61 (t, *J* = 7.9 Hz, 2H), 5.71 (s, 2H), 6.54 (d, *J* = 3.7 Hz, 1H), 7.94 (d, *J* = 3.7 Hz, 1H), 8.63 (s, 1H) ppm

Elemental analysis (calculated): C, 38.41; H, 4.83; I, 33.82; N, 11.20; O, 4.26; Si, 7.48

1

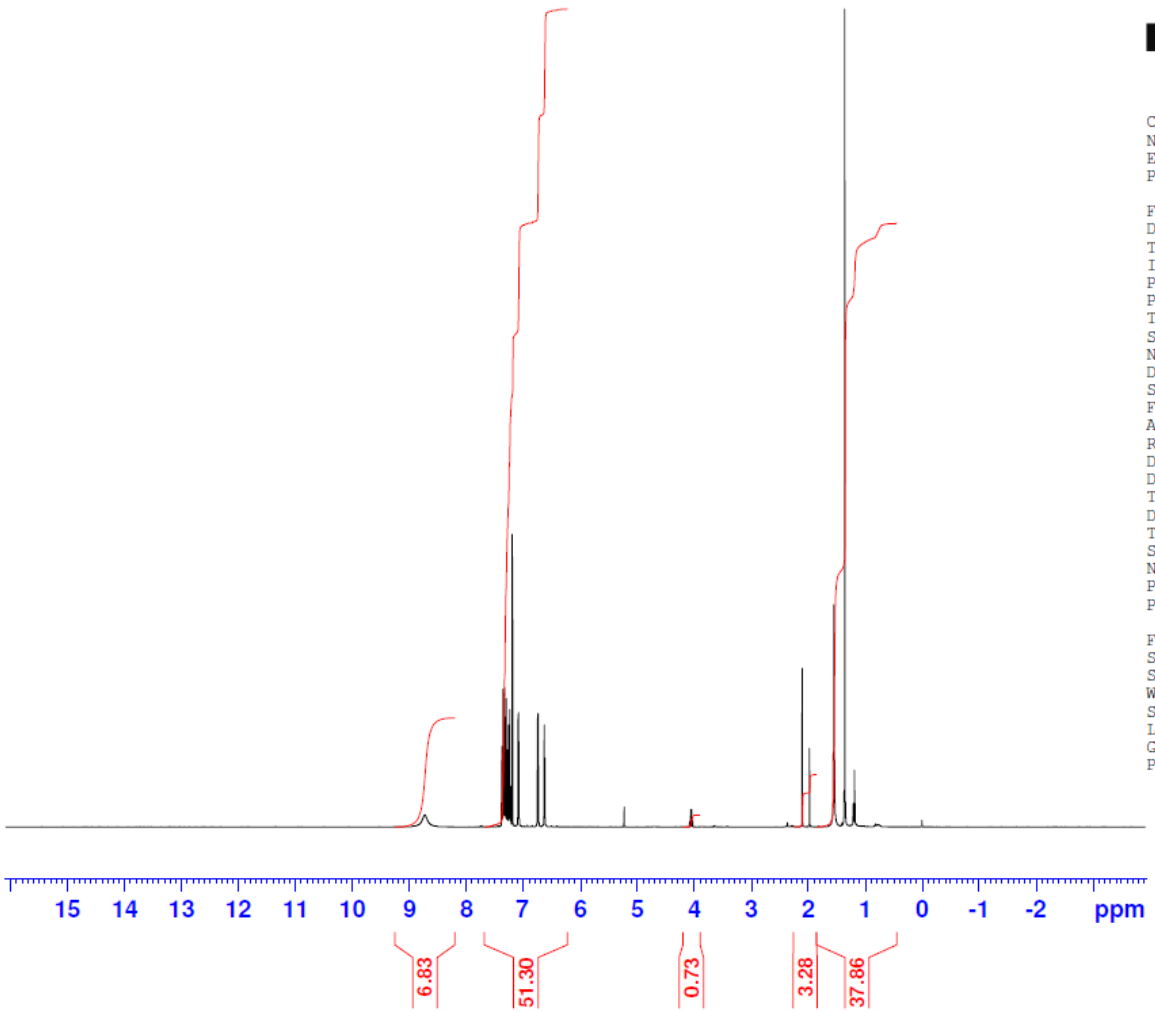

Current Data Parameters
NAME silvestri04112019
EXPNO 1
PROCNO 1

F2 - Acquisition Parameters
Date_ 20191104
Time 12.54 h
INSTRUM spect
PROBHD Z167430_0010 (
PULPROG zg30
TD 65536
SOLVENT CDC13
NS 32
DS 2
SWH 8012.820 Hz
FIDRES 0.122266 Hz
AQ 4.0894465 sec
RG 143
DW 62.400 usec
DE 10.00 usec
TE 298.2 K
D1 1.00000000 sec
TD0 1
SFO1 400.1324708 MHz
NUC1 1H
P1 12.00 usec
PLW1 9.00000000 W

F2 - Processing parameters
SI 65536
SF 400.1300372 MHz
WDW EM
SSB 0
LB 0.30 Hz
GB 0
PC 1.00

4.3.4

6-Bromo-9-((2-(trimethylsilyl)ethoxy)methyl)-9*H*-purine

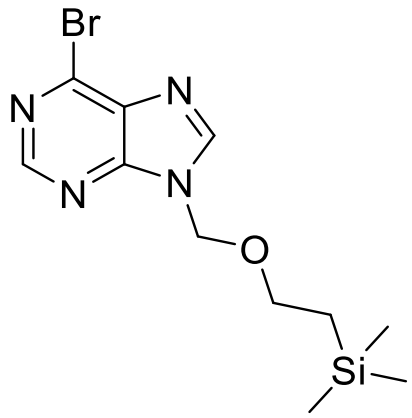

Code: RS6322

Chemical Formula: $C_{11}H_{17}BrN_4OSi$

Molecular weight: 329.27

Appearance: Colorless oil

m.p.: NA

LogP: NA

R_f (7:3 CHex/EtOAc): 0.42

^{1}H NMR: (DMSO-d6, 400 MHz): δ 0.09 (s, 9H), 0.84 (t, *J* = 8.0 Hz, 2H), 3.59 (t, *J* = 8.0 Hz, 2H), 5.66 (s, 2H), 8.77 (s, 1H), 8.86 (s, 1H) ppm

Elemental analysis (calculated): C, 40.13; H, 5.20; Br, 24.27; N, 17.02; O, 4.86; Si, 8.53

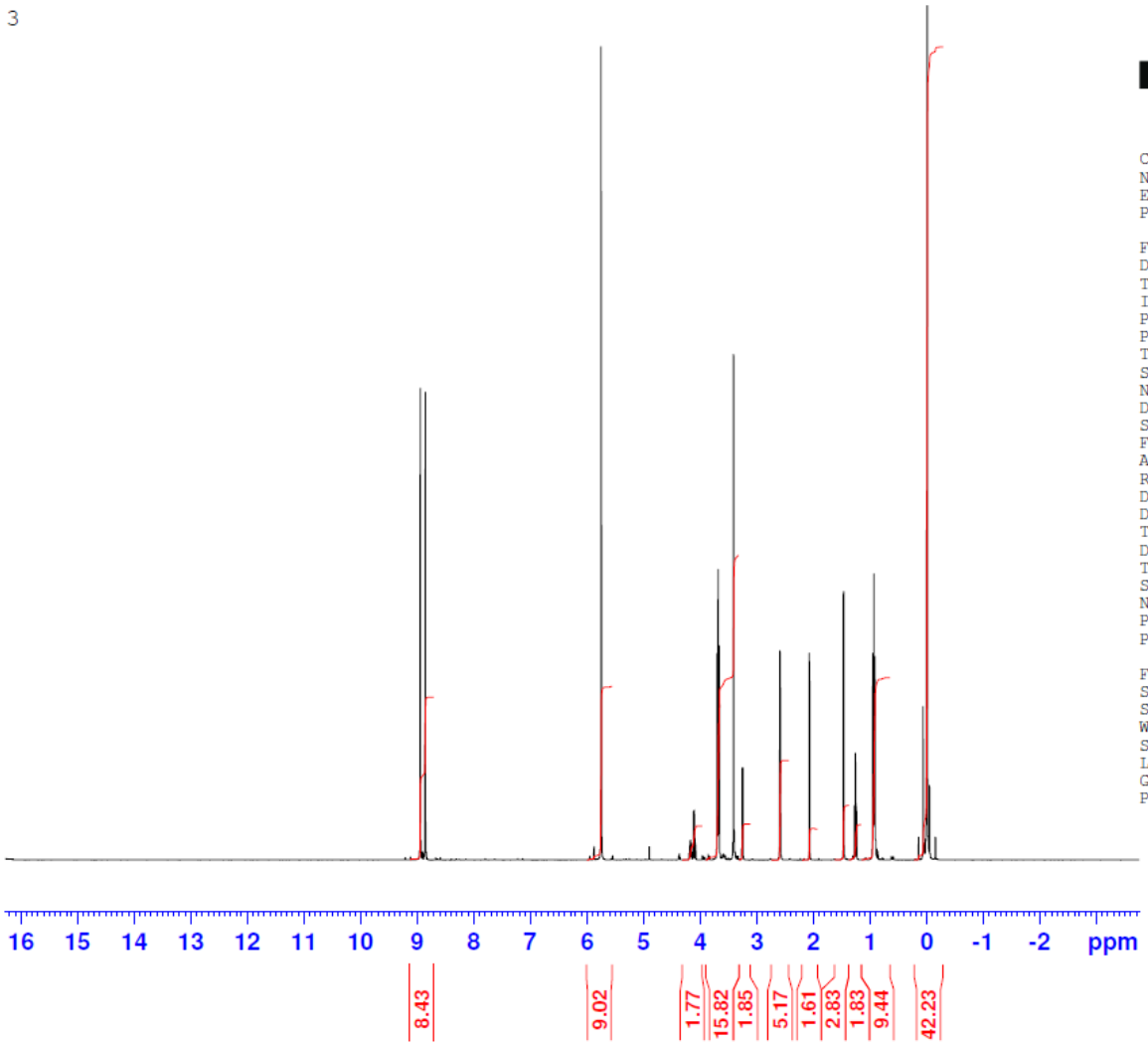

BRUKER

```
Current Data Parameters
NAME      silvestri20062019
EXPNO                     3
PROCNO                    1

F2 - Acquisition Parameters
Date_           20190620
Time                9.29 h
INSTRUM            spect
PROBHD   Z108618_0121 (
PULPROG             zg30
TD                 65536
SOLVENT             DMSO
NS                    16
DS                     2
SWH              8012.820 Hz
FIDRES           0.122266 Hz
AQ               4.0894465 sec
RG                 110.92
DW                 62.400 usec
DE                  6.50 usec
TE                 298.0 K
D1            1.00000000 sec
TD0                    1
SFO1         400.1324708 MHz
NUC1                  1H
P1                 14.70 usec
PLW1         10.18000031 W

F2 - Processing parameters
SI                 65536
SF           400.1299654 MHz
WDW                   EM
SSB       0
LB                 0.30 Hz
GB        0
PC                 1.00
```

4.3.5

6-Bromo-*N*,*N*-bis((2-(trimethylsilyl)ethoxy)methyl)pyrimidin-4-amine

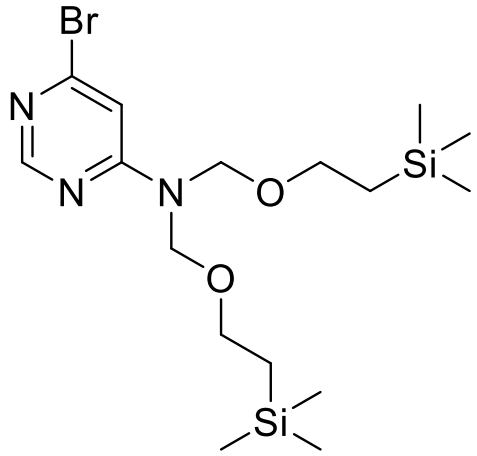

Code: RS6376

Chemical Formula: $C_{16}H_{32}BrN_3O_2Si_2$

Molecular weight: 434.53

Appearance: Pale yellow oil

m.p.: NA

LogP: NA

R_f (7:3 CHex/EtOAc): 0.6

^{1}H NMR: (DMSO-d6, 400 MHz): δ 0.00 (s, 18H), 0.90 (t, *J* = 7.7 Hz, 4H), 3.57 (t, *J* = 7.7 Hz, 4H), 5.03 (s, 4H), 7.10 (s, 1H), 8.47 (s, 1H) ppm

Elemental analysis (calculated): C, 44.23; H, 7.42; Br, 18.39; N, 9.67; O, 7.36; Si, 12.93

4

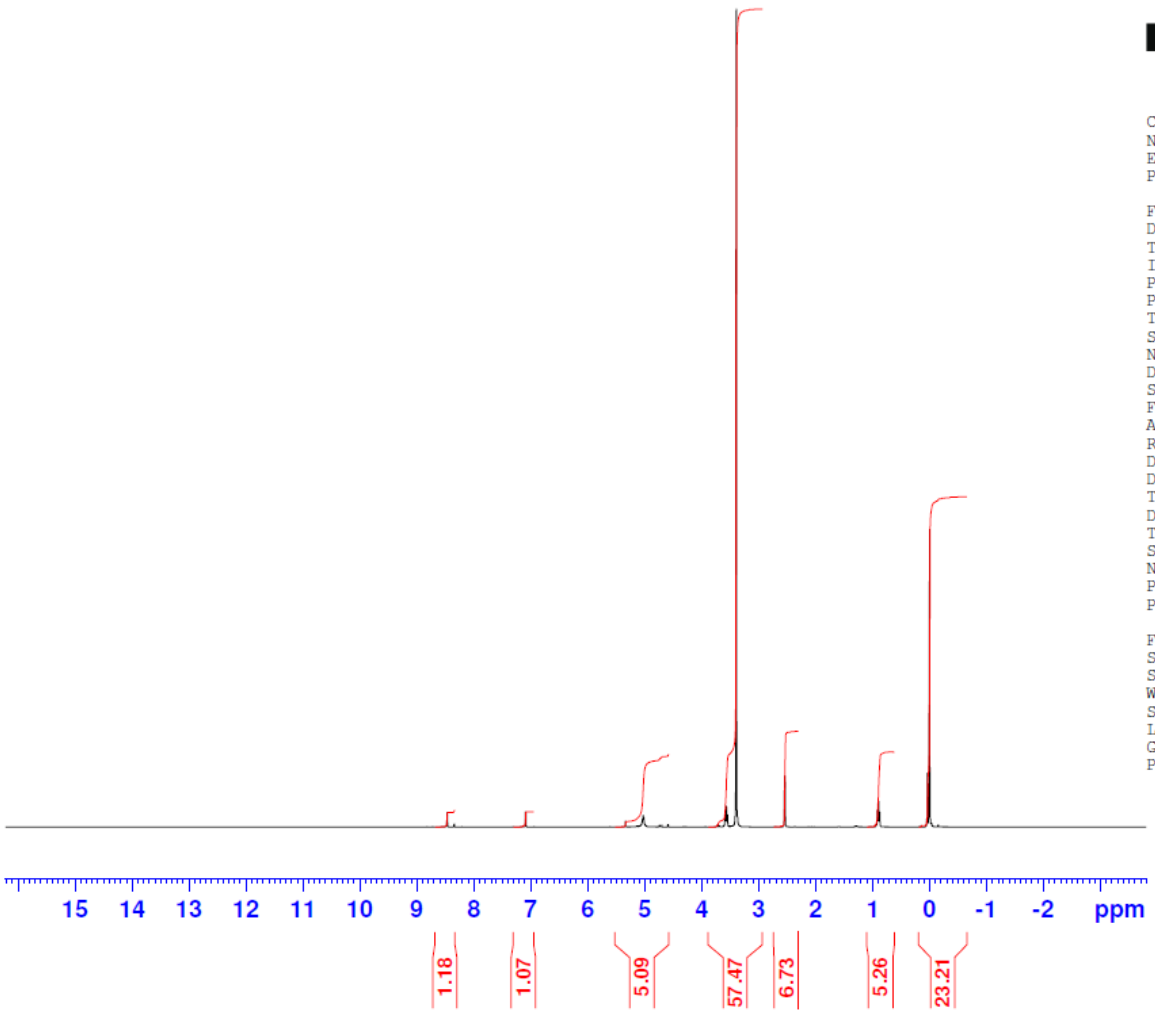


```
Current Data Parameters
NAME      silvestri06122019
EXPNO                    4
PROCNO                   1

F2 - Acquisition Parameters
Date_             20191206
Time                 9.43 h
INSTRUM              spect
PROBHD   Z167430_0010 (
PULPROG              zg30
TD                  65536
SOLVENT              DMSO
NS                     16
DS                      2
SWH               8012.820 Hz
FIDRES               0.122266 Hz
AQ                4.0894465 sec
RG                   110.92
DW                   62.400 usec
DE                   10.00 usec
TE                   290.4 K
D1              1.00000000 sec
TD0                     1
SFO1           400.1324708 MHz
NUC1                   1H
P1                   12.00 usec
PLW1            9.00000000 W

F2 - Processing parameters
SI                   65536
SF             400.1299861 MHz
WDW                    EM
SSB       0
LB                   0.30 Hz
GB        0
PC                   1.00
```

4.3.6

(2-Fluorophenyl)(1-(7-((2-(trimethylsilyl)ethoxy)methyl)-7*H*-pyrrolo[2,3-*d*]pyrimidin-4-yl)-1H-pyrrol-3-yl)methanone

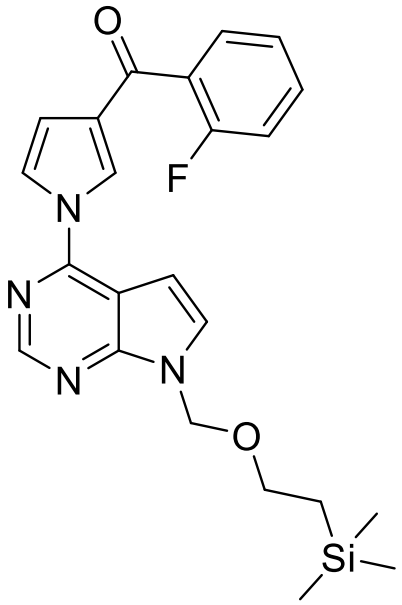

Code: RS6387

Chemical Formula: $C_{23}H_{25}FN_4O_2Si$

Molecular weight: 436.56

Appearance: Colorless oil

m.p.: NA

LogP: NA

R_f (7:3 CHex/EtOAc): 0.42

^{1}H NMR: (DMSO-d6, 400 MHz): δ 0.00 (s, 9H), 0.94 (t, *J* = 7.9 Hz, 2H), 3.69 (t, *J* = 7.9 Hz, 2H), 5.77 (s, 2H), 6.56 (d, *J* = 3.6 Hz, 1H), 6.99-7.00 (m, 1H), 7.61 (td, *J* = 1.5 and 6.6 Hz, 1H), 7.67-7.73 (m, 3H), 7.92 (d, *J* = 3.6 Hz, 1H), 8.46 (dd, *J* = 2.1 and 3.3 ,1H), 8.63 (t, *J* = 1.6, 1H), 8.8 (s, 1H) ppm.

Elemental analysis (calculated): C, 63.28; H, 5.77; F, 4.35; N, 12.83; O, 7.33; Si, 6.43

6

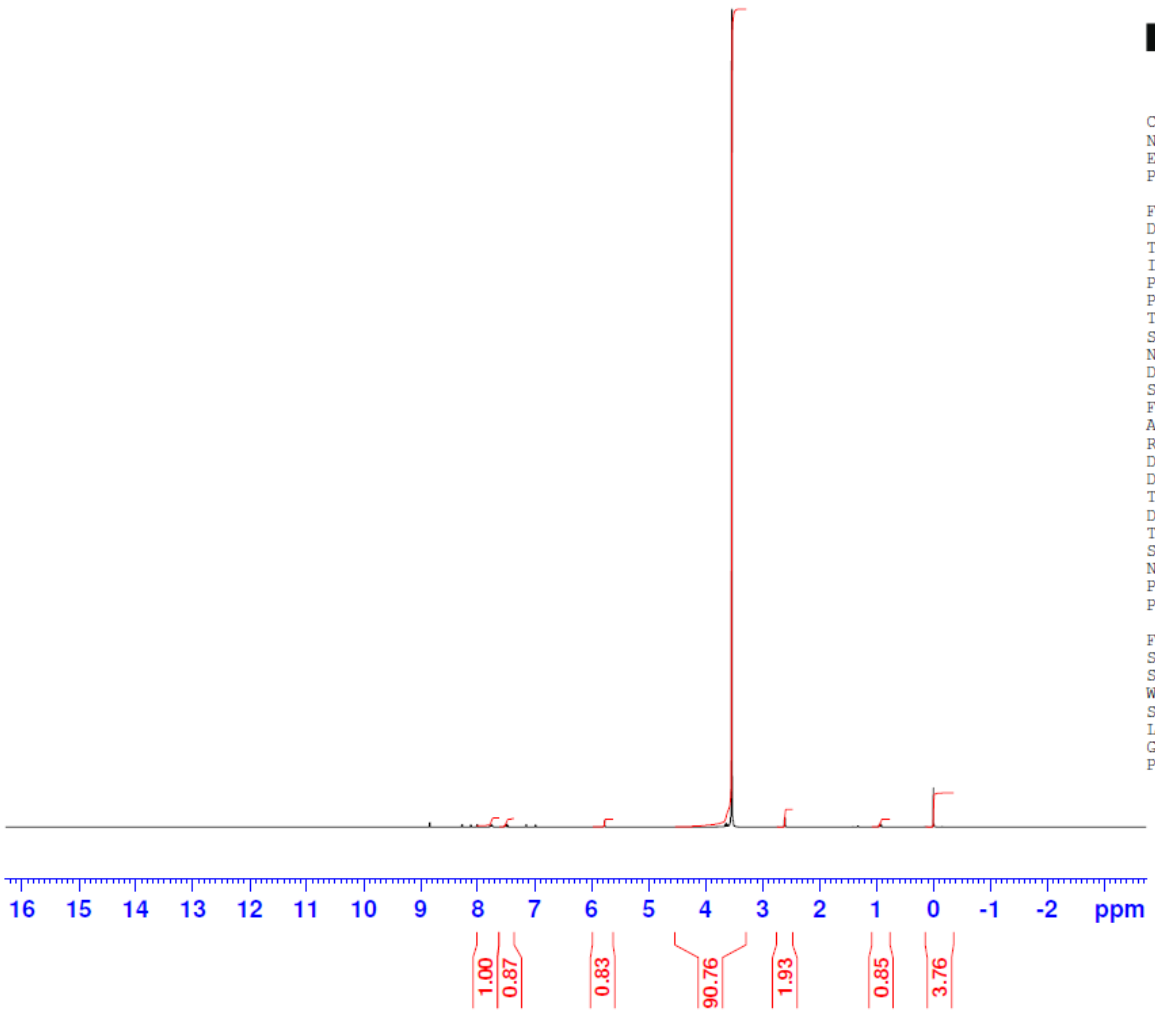


```
Current Data Parameters
NAME      silvestri02122019
EXPNO                     7
PROCNO                    1

F2 - Acquisition Parameters
Date_            20191202
Time                14.34 h
INSTRUM             spect
PROBHD   Z167430_0010 (
PULPROG              zg30
TD                  65536
SOLVENT              DMSO
NS                     16
DS                      2
SWH              8012.820 Hz
FIDRES           0.122266 Hz
AQ               4.0894465 sec
RG                  57.71
DW                62.400 usec
DE                10.00 usec
TE                290.8 K
D1            1.00000000 sec
TD0                     1
SFO1         400.1324708 MHz
NUC1                   1H
P1                 12.00 usec
PLW1          9.00000000 W

F2 - Processing parameters
SI                  65536
SF           400.1299594 MHz
WDW                    EM
SSB       0
LB                0.30 Hz
GB        0
PC                1.00
```

4.3.7

(2-Fluorophenyl)(1-(9-((2-(trimethylsilyl)ethoxy)methyl)-9*H*-purin-6-yl)-1*H*-pyrrol-3-yl)methanone

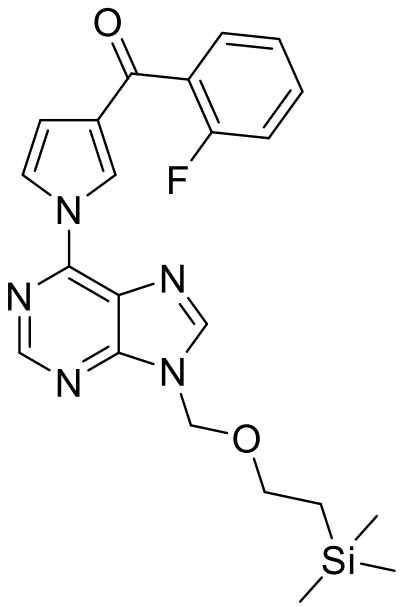

Code: RS6352

Chemical Formula: $C_{22}H_{24}FN_5O_2Si$

Molecular weight: 437.55

Appearance: Pale yellow oil

m.p.: NA

LogP: NA

R_f (7:3 CHex/EtOAc): 0.48

^{1}H NMR: (DMSO-d6, 400 MHz): δ 0.00 (s, 9H), 0.95 (t, *J* = 7.8 Hz, 2H), 3.70 (t, *J* = 7.8 Hz, 2H), 5.78 (s, 2H), 6.99-7.00 (m, 1H), 7.50 (t, *J* = 8.8 Hz, 2H), 8.04 (dd, *J* = 5.6 and 8.3 ,2H), 8.44-8.45 (m, 1H), 8.91 (s, 1H), 8.95 (d, *J* = 2.3, 2H) ppm

Elemental analysis (calculated): C, 60.39; H, 5.53; F, 4.34; N, 16.01; O, 7.31; Si, 6.42

5

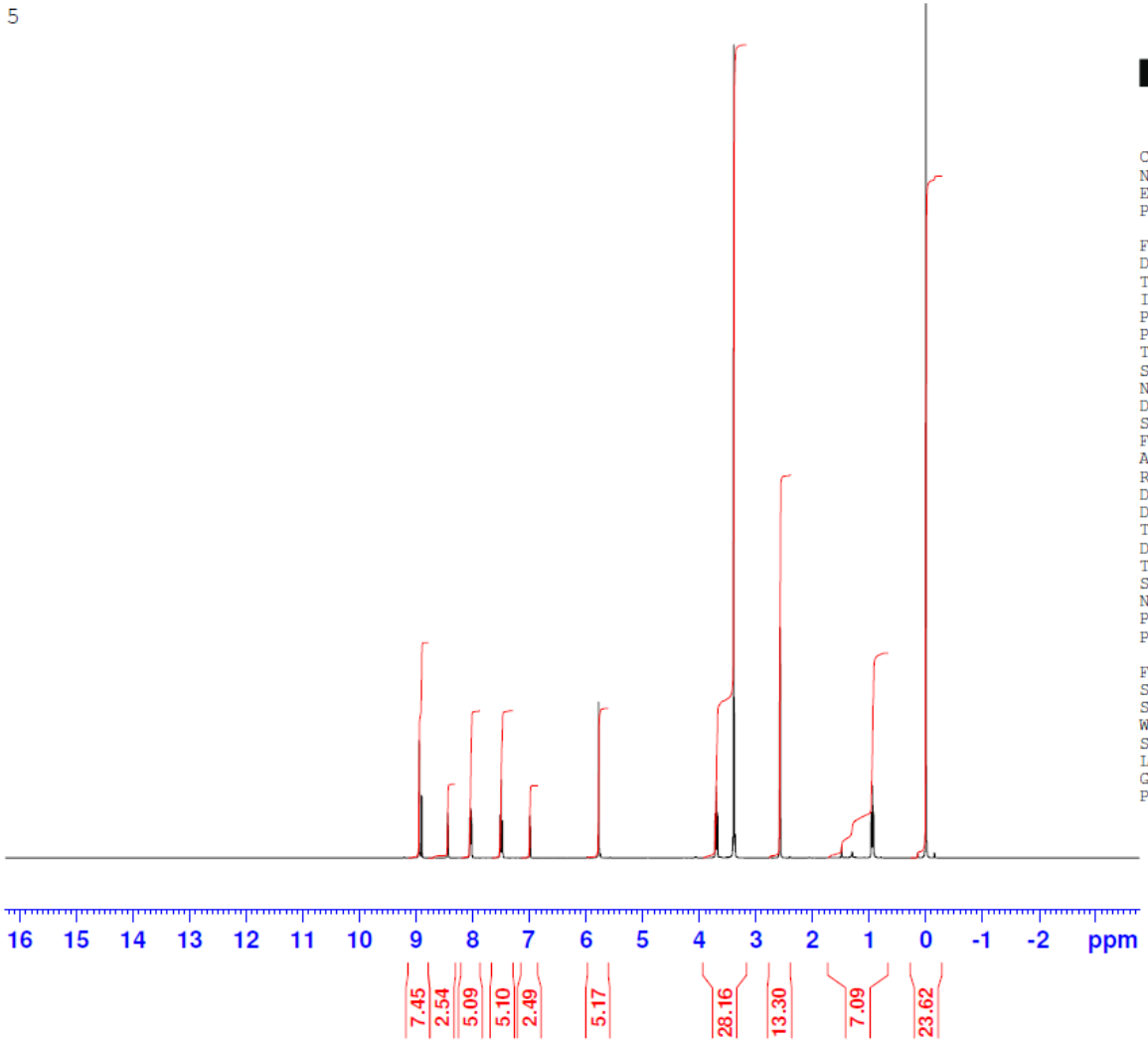

Current Data Parameters
NAME silvestri14112019
EXPNO 6
PROCNO 1

F2 - Acquisition Parameters
Date_ 20191114
Time 10.13 h
INSTRUM spect
PROBHD Z167430_0010 (
PULPROG zg30
TD 65536
SOLVENT DMSO
NS 16
DS 2
SWH 8012.820 Hz
FIDRES 0.122266 Hz
AQ 4.0894465 sec
RG 157.67
DW 62.400 usec
DE 10.00 usec
TE 298.1 K
D1 1.00000000 sec
TD0 1
SFO1 400.1324708 MHz
NUC1 1H
P1 12.00 usec
PLW1 9.00000000 W

F2 - Processing parameters
SI 65536
SF 400.1299726 MHz
WDW EM
SSB 0
LB 0.30 Hz
GB 0
PC 1.00

4.3.8

(1-(6-(Bis((2-(trimethylsilyl)ethoxy)methyl)amino)pyrimidin-4-yl)-1*H*-pyrrol-3-yl)(2-fluorophenyl)methanone

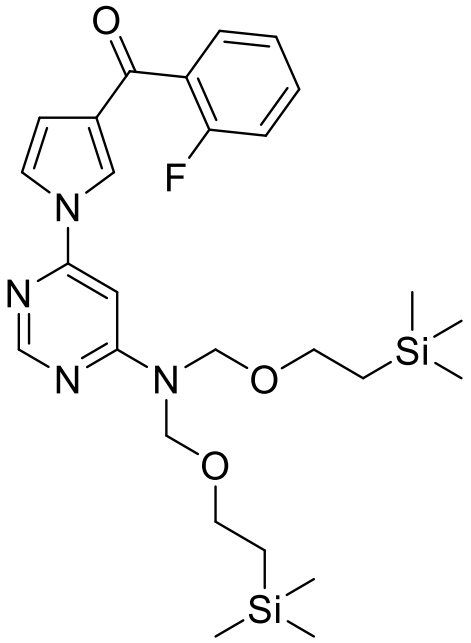

Code: RS6385

Chemical Formula: $C_{27}H_{39}FN_4O_3Si_2$

Molecular weight: 542.80

Appearance: Yellow oil

m.p.: NA

LogP: NA

R_f (7:3 CHex/EtOAc): 0.45

^{1}H NMR: (DMSO-d6, 400 MHz): δ 0.00 (s, 18H), 0.92 (t, *J* = 7.9 Hz, 4H), 3.61 (t, *J* = 7.9 Hz, 4H), 5.14 (s, 4H), 6.83-6.84 (m, 1H), 7.17 (s, 1H), 7.43 (t, *J* = 10.0 Hz, 2H), 7.65-7.72 (m, 2H), 7.94-7.96 (m, 1H), 8.19 (s, 1H), 8.61 (s, 1H) ppm

Elemental analysis (calculated): C, 59.74; H, 7.24; F, 3.50; N, 10.32; O, 8.84; Si, 10.35

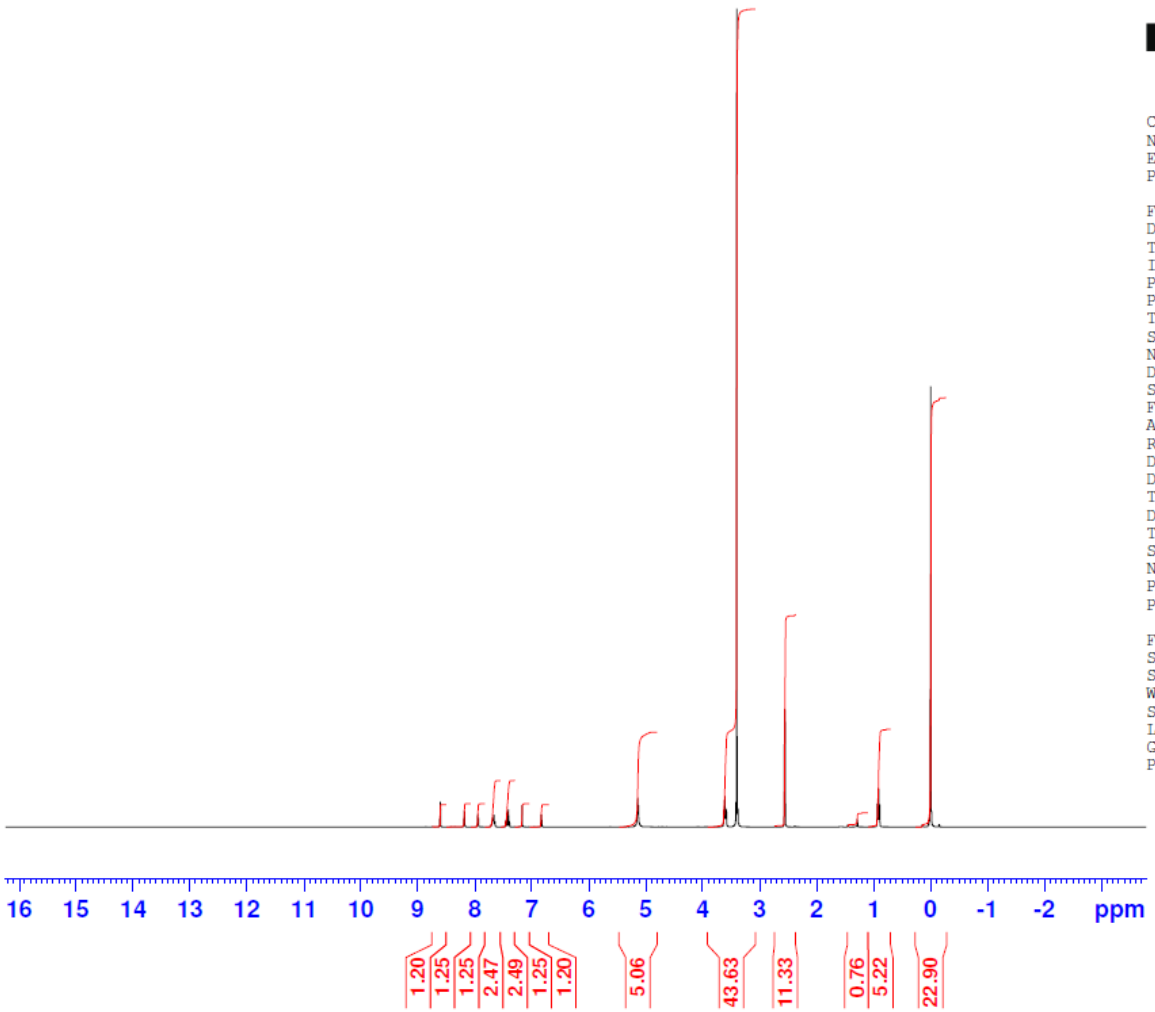


```
Current Data Parameters
NAME      silvestri16122019
EXPNO                    3
PROCNO                   1

F2 - Acquisition Parameters
Date_           20191216
Time              15.04 h
INSTRUM             spect
PROBHD   Z167430_0010 (
PULPROG             zg30
TD                 65536
SOLVENT             DMSO
NS                    16
DS                     2
SWH             8012.820 Hz
FIDRES          0.122266 Hz
AQ              4.0894465 sec
RG                   143
DW                62.400 usec
DE                10.00 usec
TE                 290.2 K
D1           1.00000000 sec
TD0                    1
SFO1         400.1324708 MHz
NUC1                  1H
P1                12.00 usec
PLW1          9.00000000 W

F2 - Processing parameters
SI                 65536
SF           400.1299790 MHz
WDW                   EM
SSB       0
LB                0.30 Hz
GB        0
PC                1.00
```

4.3.9

(1-(7*H*-pyrrolo[2,3-*d*]pyrimidin-4-yl)-1*H*-pyrrol-3-yl)(2-fluorophenyl)methanone

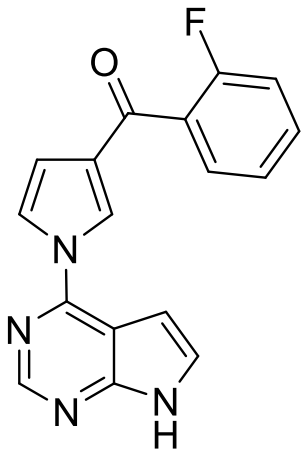

Code: RS6362

Chemical Formula: $C_{17}H_{11}FN_4O$

Molecular weight: 306.30

Appearance: White powder

m.p.: 257–260˚C

LogP: 2.86

R_f (3:7 CHex/EtOAc): 0.41

^{1}H NMR- (DMSO-d6, 400 MHz): δ 6.60 (d, *J* = 3.7 Hz, 1H), 6.96-6.98 (m, 1H), 7.60-7.62 (m, 1H), 7.67-7.73 (m, 3H), 7.90 (d, *J* = 3.7 Hz, 1H), 8.48 (dd, *J* = 2.1 and 3.3 ,1H), 8.63 (t, *J* = 1.6 Hz, 1H), 8.8 (s, 1H), 13.42 (S, 1H) ppm.

Elemental analysis (calculated): C, 66.66; H, 3.62; F, 6.20; N, 18.29; O, 5.22

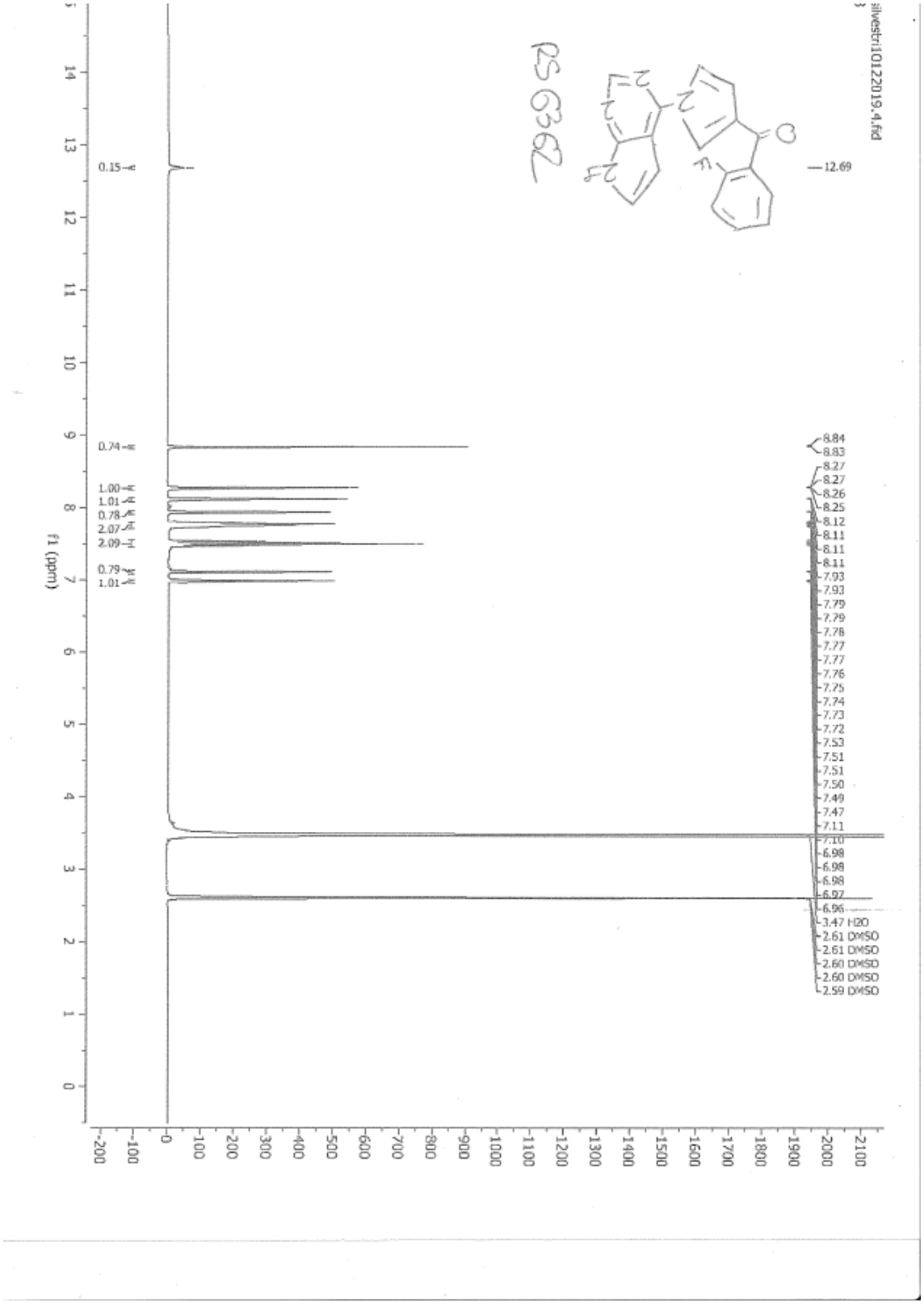
silvestri10122019_4.fid
RS 6362
12.69
0.15
0.74
1.00
1.01
0.78
2.07
2.09
0.79
1.01
8.84
8.83
8.27
8.27
8.26
8.25
8.12
8.11
8.11
8.11
7.93
7.93
7.79
7.79
7.78
7.77
7.77
7.76
7.75
7.74
7.73
7.72
7.53
7.51
7.51
7.50
7.49
7.47
7.11
6.98
6.98
6.98
6.97
6.96
3.47 H2O
2.61 DMSO
2.61 DMSO
2.60 DMSO
2.60 DMSO
2.59 DMSO
f1 (ppm)

4.3.10

(1-(9*H*-purin-6-yl)-1*H*-pyrrol-3-yl)(2-fluorophenyl)methanone

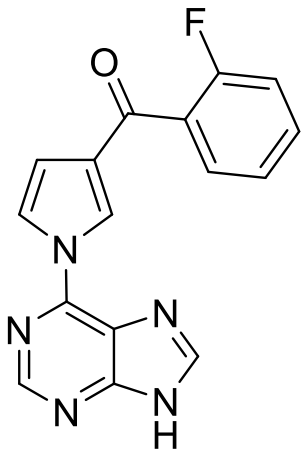

Code: RS6355

Chemical Formula: $C_{16}H_{10}FN_5O$

Molecular weight: 307.29

Appearance: White powder

m.p.: > 300˚C

LogP: 2.09

R_f (3:7 CHex/EtOAc): 0.3

^{1}H NMR: (DMSO-d6, 400 MHz): δ 6.96-6.97 (m, 1H), 7.48 (t, *J* = 8.7 Hz, 2H), 8.02 (dd, *J* = 5.6 and 8.5 Hz ,2H), 8.42-8.44 (m, 1H), 8.74 (s, 1H), 8.85 (s, 1H), 8.92 (s, 1H), 13.98 (s, 1H) ppm

Elemental analysis (calculated): C, 62.54; H, 3.28; F, 6.18; N, 22.79; O, 5.21

1

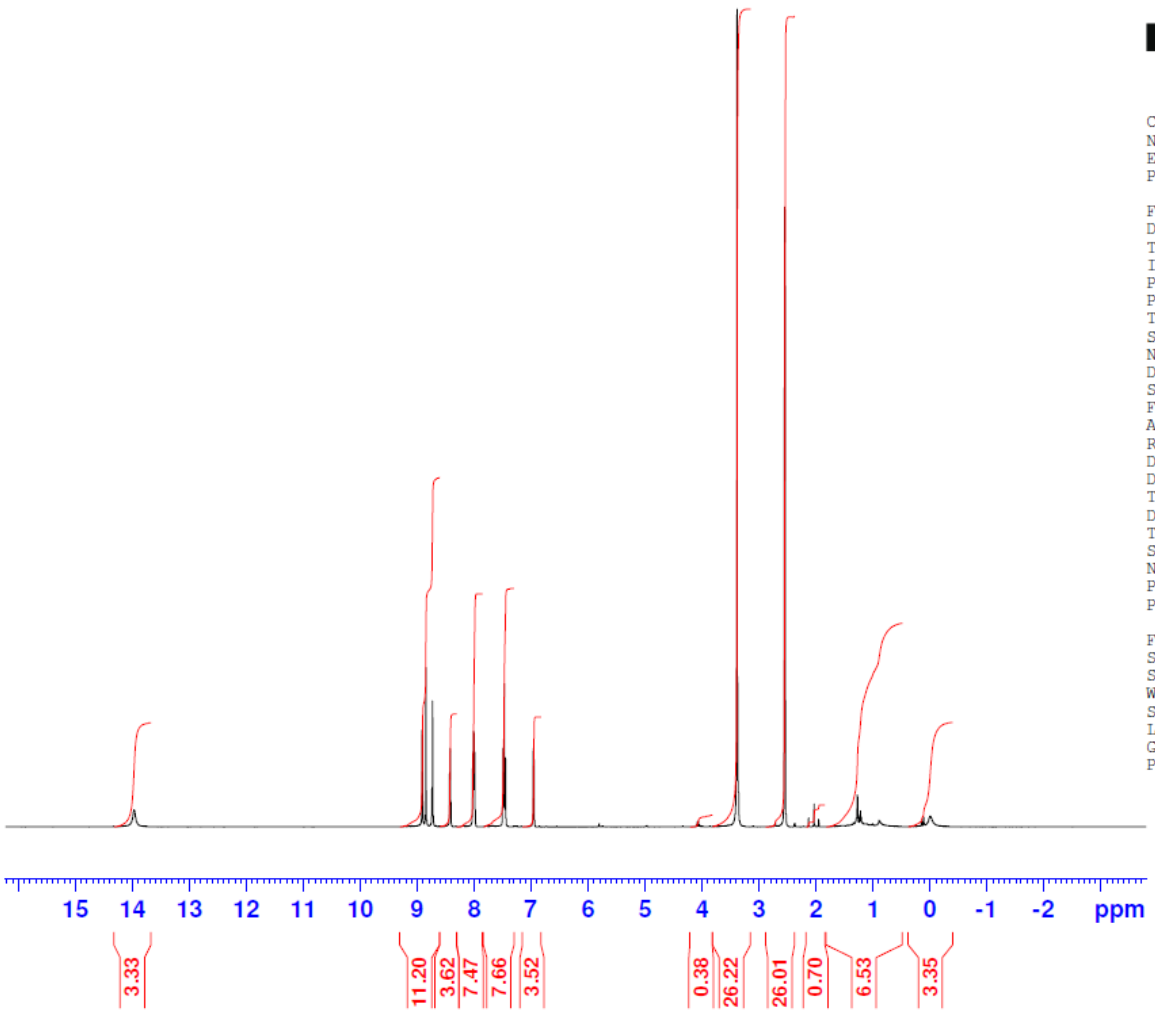

BRUKER

```
Current Data Parameters
NAME      silvestri18112019
EXPNO                     1
PROCNO                    1

F2 - Acquisition Parameters
Date_           20191119
Time              13.04 h
INSTRUM             spect
PROBHD   Z167430_0010 (
PULPROG             zg30
TD                 65536
SOLVENT             DMSO
NS                    32
DS                     2
SWH             8012.820 Hz
FIDRES          0.122266 Hz
AQ              4.0894465 sec
RG                   143
DW                62.400 usec
DE                10.00 usec
TE                290.7 K
D1           1.00000000 sec
TD0                    1
SFO1         400.1324708 MHz
NUC1                  1H
P1                12.00 usec
PLW1          9.00000000 W

F2 - Processing parameters
SI                 65536
SF           400.1299823 MHz
WDW                   EM
SSB       0
LB                0.30 Hz
GB        0
PC                1.00
```

4.3.11

(1-(6-Aminopyrimidin-4-yl)-1*H*-pyrrol-3-yl)(2-fluorophenyl)methanon

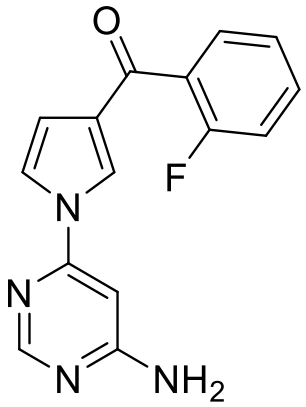

Code: RS6386

Chemical Formula: $C_{15}H_{11}FN_4O$

Molecular weight: 282.28

Appearance: White powder

m.p.: 245 °C

LogP: 2.48

R_f (3:7 CHex/EtOAc): 0.25

^{1}H NMR: (DMSO-d6, 400 MHz): δ 6.68 (s, 1H), 6.81-6.83 (m, 1H), 7.20 (s, broad signal, disappeared after treatment with D2O, 1H), 7.42 (q, *J* = 9.6 Hz, 2H), 7.64-7.71 (m, 2H), 7.74-7.76 (m, 1H), 7.98 (s, 1H), 8.35 (s, 1H) ppm

Elemental analysis (calculated): C, 63.83; H, 3.93; F, 6.73; N, 19.85; O, 5.67

2

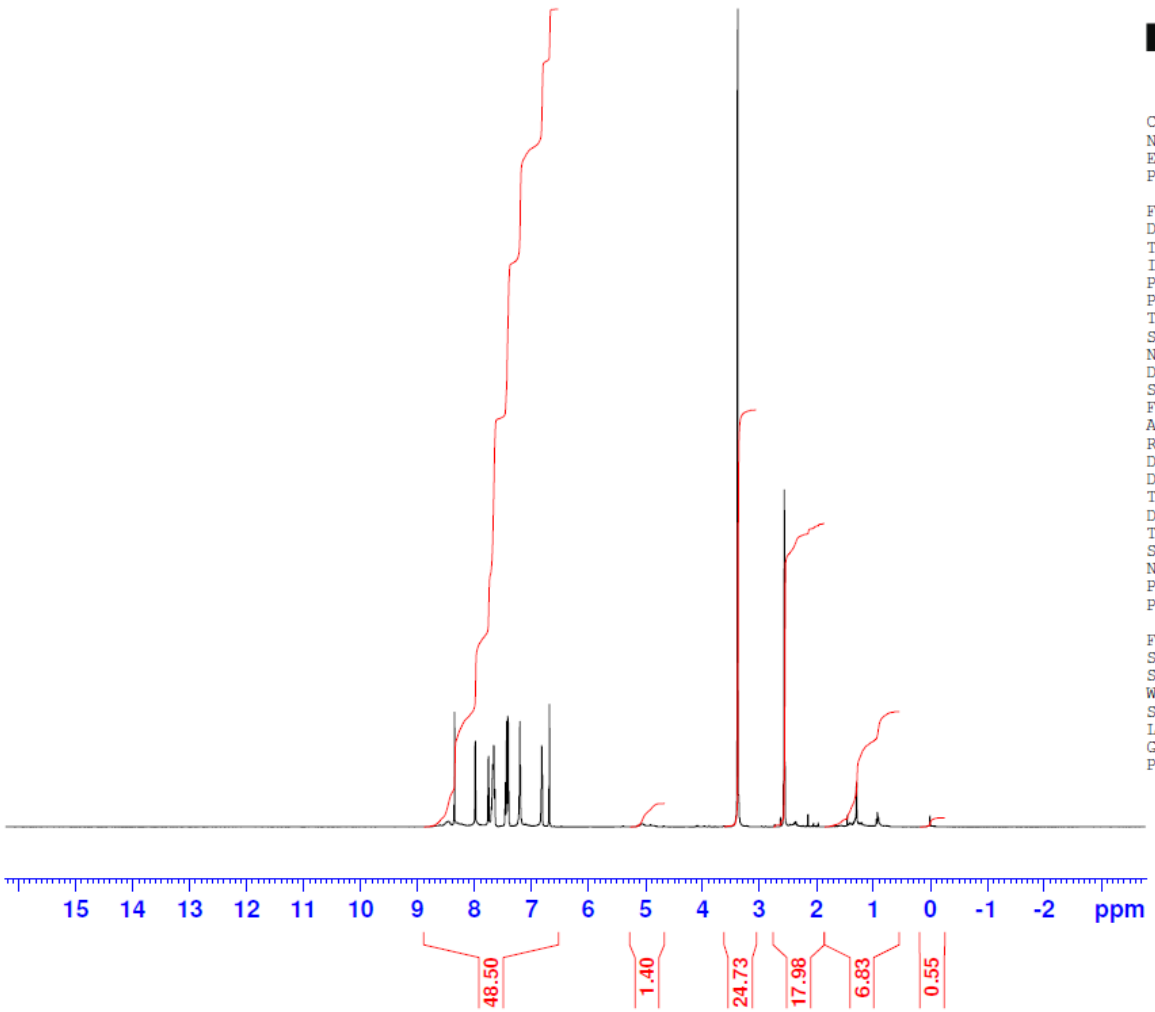


```
Current Data Parameters
NAME      silvestri17012020
EXPNO                    2
PROCNO                   1

F2 - Acquisition Parameters
Date_             20200117
Time                11.20 h
INSTRUM              spect
PROBHD   Z167430_0010 (
PULPROG              zg30
TD                  65536
SOLVENT              DMSO
NS                     16
DS                      2
SWH              8012.820 Hz
FIDRES           0.122266 Hz
AQ               4.0894465 sec
RG                  157.67
DW                62.400 usec
DE                10.00 usec
TE                298.0 K
D1            1.00000000 sec
TD0                     1
SFO1          400.1324708 MHz
NUC1                   1H
P1                12.00 usec
PLW1           9.00000000 W

F2 - Processing parameters
SI                   65536
SF            400.1299803 MHz
WDW                     EM
SSB       0
LB                 0.30 Hz
GB        0
PC                 1.00
```

4.4 Biological Assays

4.4.1 Tubulin assembly and colchicine binding assays

The assembly reaction mixtures will contain 0.8 M monosodium glutamate (pH 6.6 with HCl in a 2 M stock solution), 10 μM tubulin, 4% (v/v) DMSO, and varying concentrations of drug. Following a 15 min preincubation at 30 ˚C, samples will be chilled on ice, GTP to 0.4 mM will be added, and turbidity development will follow at 350 nm in a temperature-controlled recording spectrophotometer for 20 min at 30 ˚C. The extent of reaction will be measured. For the colchicine binding assay, reaction mixtures will contain 1.0 μM tubulin, 5.0 μM [^{3}H] colchicine, and 5.0 μM inhibitor and will be incubated for 10 min at 37 ˚C. As a tubulin assembly inhibitor, colchicine yields an IC50 of 3.2 ± 0.4 μM. For the tubulin assembly data described here, different tubulin preparations will be used. [Taken from 73]

4.4.2 Cell cultures

Cell lines will be obtained from American Type Culture Collection (ATCC), Rockville MD, unless otherwise specified. U343MG, U87MG and T98G cell lines will be obtained from the National Institute for Cancer Research of Genoa (Italy). All cell lines, except as indicated, will be grown in Dulbecco's modified Eagle's medium (DMEM) (RPMI-1640 medium for the SK-N-BE and SK-N-BE(2)-C cells) supplemented with 10% fetal bovine serum (FBS), 20 nM HEPES, 100 U/mL penicillin, 100 mg/mL streptomycin, and 1% L-glutamine; an additional specific component will be the addition of glucose (4.5 g/L for HT29 and HCT116 cells). Cell lines will be cultured at 37 ˚C in 5% CO_2/95% air in a humidified incubator. Treatments will be initiated 24 h after cell seeding using compounds diluted in 0.1% DMSO, the indicated reference compound, or 0.1% DMSO vehicle, for 24-72 h, as indicated. T98G and U87MG cells will be cultured in RPMI medium and minimum essential Eagle's medium, respectively, supplemented with 10% FBS, 2 nM L-glutamine, 100 U/mL penicillin, 100 mg/mL streptomycin and 1% non-essential amino acids at 37 ˚C in 5% CO_2. The U343MG cells will be cultured in minimum essential Eagle's medium with 2 nM L-glutamine and Earle's BSS adjusted to contain 1.5 mg/mL sodium bicarbonate and supplemented with 10% FBS, 100 U/mL penicillin 100 mg/mL streptomycin, 1% non-essential amino acids and 1.0 nM sodium pyruvate at 37 ˚C in 5% CO_2. KBM5, KU812, and LAMA84 cell lines expressing the

IM-sensitive wild type BCR/ABL will be derived from CML patients in blast crisis. These CML cell lines will be purchased from ATCC and cultured in RPMI-1640 (Life Technologies, Gaithersburg, MD) containing 10% FBS (Cambrex, Baltimore, MD), 100 units/mL penicillin, 100 µg/mL streptomycin, 2 nM L-glutamine (GibcoBRL, Paisley, UK) at 37 ˚C with 5% CO_2 atmosphere. KBM5-T3151 cells ectopically expressing the IM-resistant T3151 mutation of BCR-ABL will also be from ATCC and maintained in the presence of IM at 1.0 µM. PBMCs will be obtained after informed consent from 2 healthy donors and purified by standard Ficoll-Hypaque density gradient centrifugation (Amersham Biosciences, Uppsala, Sweden). IM will be kindly provided by Novartis (Basel, Switzerland) or synthesized by Dr Alfonso Zambon (University of Venezia, Italy). Stock solutions of IM at 1 or 10 nM in sterile water will be filtered and stored at -20 ˚C. [Taken from 73]

4.4.3 Cell Viability assay

Cell viability of KU812, LAMA84-S, LAMA84-R, KBM5-WT, KMB5-T3151, HT29, HCT116, SW480, SW620, T24, ES-2, SK-N-BE and SK-N-BE(2)-C cells will be determined using the MTT colometric assay. The cells will be seeded into 24-well plates to a density of 15 x 10^3/mL in each well. After 24 h of growth to allow attachment of cells to the wells, test compounds will be added at 20.320 nM. After 48 h of growth and removal of the culture medium, 500 µL/well of PBS containing 500 µM MTT will be added. Cell cultures will be further incubated at 37 ˚C for 2 h in the dark. The solutions will be then gently aspirated from each well, and the formazan crystals within the cells will be dissolved in propan-2-ol and 0.04 N HCl (200 µL). Optical densities will be read at 550 nm using a Multiskan Spectrum Thermo Electron Corporation reader. The results will be expressed as % relative to vehicle-treated control (0.1% DMSO), and IC_{50} values will be calculated by nonlinear regression analysis (GraphPad Prism statistics software). Experiments will be performed in triplicate. After compound incubation, the MTS reagent will be added, and the absorbance at 590 nm will be measured by a microplate reader (Wallac, Victor 2, 1420 Multilabel Counter, PerkinElmer). The percentage of proliferating cells after compound exposure will be calculated with respect to control cells (100%). [Taken from 73]

4.4.4 Results

The final compounds (codes RS6362, RS6355 and RS6386) were sent to Dr. Ernest Hamel, Screening Technologies Branch, Developmental Therapeutics Program, Division of Cancer Treatment and Diagnosis, Frederick National Laboratory for Cancer Research, National Cancer Institute, National Institutes of Health, Frederick, MD 21702, United States. Unfortunately, due to the restricted time, the results of the biological assays of my compounds won't be included in this thesis because they won't have been finished before this thesis publication.

5. CONCLUSIONS

Cancer has always been a major health problem and scientists have been developing novel drugs hoping to defeat this dreaded disease. Prof. Silvestri and his colleagues conduced to the effort and successfully synthetized 55 new ARAP (3-aroyl-1-arylpyrrole) derivatives, structurally related to colchicine and combretastatin, with potential tubulin inhibiting activity. After obtaining promising results from evaluating the final products on the MCF-7 cells, more ARAP derivatives have been designed and synthetized.

During my short Erasmus stay I worked in the laboratory of prof. Silvestri and contributed to the library of novel ARAP derivatives with 3 molecules. The 4 final products were attained after completing 5 complex reactions, each followed by a purifying procedure and an NMR identity check. The activity of the final products will be assessed on tubulin polymerization *in vitro*, the binding of [^{3}H]colchicine to tubulin and on the MCF-7 breast cancer cell growth.

6. ABSTRAKT (CZECH)

Univerzita Karlova

Farmaceutická fakulta v Hradci Králové

Katedra farmaceutické chemie a farmaceutické analýzy

Řešitel: Katharina Zenkerová

Vedoucí diplomové práce: doc. PharmDr. Jan Zitko, Ph.D.; Prof. Romano Silvestri

Název diplomové práce: Návrh a příprava nových derivátů 3-aroyl-1-arylpyrrolu jako potenciálních inhibitorů polymerizace tubulinu

Klíčová slova: protinádorové sloučeniny; pyrrol; inhibitory polymerizace tubulinu

Rakovina je celosvětově významným problémem a zůstává jednou z nejobtížněji léčitelných chorob. Jelikož procento lidí trpících rakovinou roste, je zapotřebí obrovské úsilí navrhnout a vyvinout lepší léčiva.

Mikrotubuly jsou klíčovou složkou cytoskeletu ve většině eukaryotických buněk a představují vhodný cíl pro protinádorová léčiva, v důsledku významné míry mitózy nádorových buněk. Protože rakovinné buňky obvykle vykazují vyšší míru proliferace než normální buňky, léčiva, která interferují s dynamickou rovnováhou mikrotubulů, také známá jako antimitotická léčiva, se stala plodným přístupem k vývoji protinádorových látek v klinickém použití. Ve skutečnosti, látky interferující s mikrotubuly mohou buď inhibovat tubulinovou polymerizaci nebo blokovat rozpad mikrotubulů, což způsobí zastavení buněčného dělení a následně buněčnou smrt.

V průběhu let bylo zjištěno, že řada sloučenin nesoucích ve své struktuře pyrrolové jádro je účinná jako inhibitory polymerizace tubulinu. V této souvislosti profesor Silvestri a spolupracovníci nedávno popsali deriváty 3-aroyl-1-arylpyrolu (ARAP) jako novou třídu silných inhibitorů tubulinu. Inspirována těmito slibnými výsledky, jsem založila svoji diplomovou práci na vývoji nových derivátů ARAP s cílem zlepšit inhibici jak tubulinové polymerizace, tak růstu nádorových buněk MCF-7, vazbou na kolchicinové vazebné místo. Byly syntetizovány tři deriváty ARAP, odlišně substituované v polohách 1 a 3 pyrrolového jádra. Syntetické schéma je založeno na pěti různých krocích.

Prvním krokem přípravy nových sloučenin ARAP byla Friedel-Craftova reakce mezi 1-(p-tolylsulfonyl) pyrrolem a příslušným benzoylchloridem v dichlormethanu, v přítomnosti bezvodého chloridu hlinitého při pokojové teplotě po dobu 20 min pod proudem argonu. Výsledný acylovaný meziprodukt byl poté hydrolyzován za použití NaOH 6 M, v ethanolu při 80 °C po dobu 4 hodin, čímž byla získána vhodná acylpyrolová sloučenina. Nakonec byl acylpyrolový meziprodukt rozpuštěn v dioxanu a nechal se zreagovat s vhodnou chráněnou purinovou bází (dříve syntetizovanou) za přítomnosti uhličitanu cesného, jodidu měďnatého a fenantrolinu. Reakce byla poté zahřívána při 110 °C přes noc, pod argonem, čímž byl získaný chráněný meziprodukt. Následné štěpení silylové ochranné skupiny kyselinou trifluoroctovou v dichlormethanu při pokojové teplotě, vedlo k získání požadované sloučeniny ARAP. Chráněná purinová báze byla syntetizována reakcí vhodné purinové báze s trimethylsilylchloridem v dichlormethanu při laboratorní teplotě přes noc.

Aktivita této nové malé knihovny derivátů 3-aroyl-1-arylpyrolu bude hodnocena na tubulinové polymeraci *in vitro*, vazbě [^{3}H] kolchicinu na tubulin a na růstu buněk rakoviny prsu MCF-7.

7. ABSTRACT (ENGLISH)

Charles University

Faculty of Pharmacy in Hradec Králové

Department of Pharmaceutical Chemistry and Pharmaceutical Analysis

Author: Katharina Zenkerová

Supervisors: Assoc. Prof. PharmD. Jan Zitko, Ph.D.; Prof. Romano Silvestri

Title of diploma thesis: Design and synthesis of novel 3-aroyl-1-arylpyrrole derivatives as potential tubulin polymerization inhibitors

Key word: anticancer agents; pyrrole; tubulin polymerization inhibitors

Cancer is a major burden of disease worldwide and it remains one of the most difficult illnesses to treat. Since the percentage of people suffering from cancer is increasing, an enormous effort to design and develop better medicaments is needed.

Microtubules are a key component of the cytoskeleton in most eukaryotic cells and they represent an attractive target for antitumor agents, due to the significant mitosis rate of tumor cells. Since cancer cells usually display higher proliferation rates than normal cells, drugs that interfere with microtubules dynamic equilibrium, also known as antimitotic agents, have become a fruitful approach to develop anticancer agents in clinical use. In fact, agents interfering with microtubules may either inhibit the tubulin polymerization or block microtubules to disassembly, both causing the arrest of cell division and the consequent cell death.

Over the years, a series of compounds, bearing a pyrrole nucleus in their structure, were found to be effective as inhibitors of tubulin assembly. In this context, professor Silvestri et al. have recently described 3-aroyl-1-arylpyrrole (ARAP) derivatives as a new class of potent inhibitors of tubulin. Encouraged by this promising result, the present thesis project is based on the development of new ARAP derivatives with the aim to improve the inhibition of both tubulin assembly and MCF-7 cancer cells growth, by binding the colchicine binding site. Three ARAP derivatives, differently substituted at positions 1 and 3 of the pyrrole nucleus, were synthesized. The synthetic scheme is based on five different steps.

The first step of the preparation of new ARAP compounds was the Friedel-Craft reaction between 1 (p-Tolylsulfonyl)pyrrole and the appropriate benzoylchloride in dichloromethane, in the presence of anhydrous aluminum chloride at room temperature for 20 min under Argon stream. The resulting acyl intermediate was then hydrolyzed using NaOH 6 M, in ethanol at 80 °C for 4 hours to obtain the appropriate acyl-pyrrole compound. Finally, the acyl-pyrrole intermediate was dissolved in dioxane and it was treated with the suitable protected purine base (previously synthesized) in the presence of cesium carbonate, copper iodide and phenanthroline. The reaction was then heated at 110 °C overnight under Argon to obtain the protected final compound. Subsequent cleavage of the silyl protecting group with trifluoroacetic acid in dichloromethane at room temperature led to the desired ARAP compound. The protected purine base was synthesized treating the suitable purine base with trimethylsilyl chloride in dichloromethane at room temperature overnight.

The activity of this novel small library of 3-aroyl-1-arylpyrrole derivatives will be evaluated on tubulin polymerization *in vitro*, the binding of [^{3}H]colchicine to tubulin and on the MCF-7 breast cancer cell growth.

8. REFERENCES

[1] LA REGINA, G.; BAI, R.; COLUCCIA, A.; FAMIGLINI, V.; PELLICCIA, S.; PASSACANTALLI, S.; MAZZOCCOLI, C.; RUGGIERI, V.; SISINNI, L.; BOLOGNESI, A.; RENSEN, W. M.; MIELE, A.; NALLI, M.; ALFONSI, R.; Di MARCOTULLIO, L.; GULINO, A.; BRANCALE, A.; NOVELLINO, E.; DONDIO, G.; VULTAGGIO, S.; VARASI, M.; MERCURIO, C.; HAMEL, E.; LAVIA, P.; SILVESTRI, R. New Pyrrole Derivatives with Potent Tubulin Polymerization Inhibiting Activity As Anticancer Agents Including Hedgehog-Dependent Cancer. *J. Med. Biochem.* **2014**, *57*, 6531−6552.

[2] *World Health Organization*: Cancer. Who.int [online]. Geneva: REBOUX, G., **2018** [cit. 2020-02-08]. Dostupné z: https://www.who.int/news-room/fact-sheets/detail/cancer.

[3] ARNST, K. E.; BANERJEE, S.; CHEN, H.; DENG, S.; HWANG, D.; LI, W.; MILLER, D. D. Current advances of tubulin inhibitors as dual acting small molecules for cancer therapy. *Med. Res. Rev.* **2019**, 39, 1398–1426.

[4] LU, Y.; CHEN, J.; XIAO, M.; LI, W..; MILLER, D. D. An Overview of Tubulin Inhibitors That Interact with the Colchicine Binding Site. *Pharm. Res.* **2012**, 29(11), 2943-2971.

[5] HUETHER, S. E.; MCCANCE, K. L.; Biology, Clinical Manifestations, and Treatment of Cancer. In: Valentina L. Brashers, Neal S. Rote (Ed.) *Understanding Pathophysiology*. 5th Ed., Elsevier, St. Louis **2012**, ISBN 978-0-323-07891-7

[6] *World Health Organization*: Cancer. Who.int [online]. Geneva: REBOUX, G. [cit. 2020-02-24]. Dostupné z: https://www.who.int/health-topics/cancer#tab=tab_1.

[7] GREENE, R. J.; HARRIS, N. D. *Pathology and Therapeutics for Pharmacists A basis for clinical pharmacy practice*. 3rd edition, Pharmaceutical Press, London **2008**. ISBN 978-0-85369-690-2

[8] LICHTENSTEIN, P.; HOLM, N. V.; VERKASALO, P. K.; ILIADOU, A.; KAPRIO, J.; KOSKENVUO, M.; PUKKALA, E.; SKYTTHE, A.; HEMMINKI, K. Environmental and Heritable Factors in the Causation of Cancer — Analyses of Cohorts of Twins from Sweden, Denmark, and Finland. *N. Engl. J. Med.*, **2000**; *343*:78-85.

[9] STŘÍTESKÝ, J. *Patologie*, EPAVA, Olomouc **2001**. ISBN 80-86297-06-3

[10] *Ústav zdravotnických informací a statistiky ČR*: Národní onkologický registr. Uzis.cz [online]. Prague: ÚZIS, **2019** [cit. 2020-03-19]. Dostupné z: https://www.uzis.cz/index.php?pg=registry-sber-dat--narodni-zdravotni-registry--narodni-onkologicky-registr#o-registru.

[11] *Česká onkologická společnost České lékařské společnosti J. E. Purkyně*: Cancer Epidemiology and cancer registries in the Czech Republic. Linkos.cz [online]. Prague: Linkos, **2017** [cit. 2020-03-19]. Dostupné z: https://www.linkos.cz/english-summary/national-cancer-control-programme/cancer-epidemiology-and-cancer-registries-in-the-czech-republic/.

[12] Zákon č. 372 / 2011 o zdravotních službách a podmínkách jejich poskytování (zákon o zdravotních službách), Ministerstvo vnitra, Sbírka zákonů 6. 11. **2011**, částka 131.

[13] Vyhláška č. 373 / 2016 o předávání údajů do Národního zdravotnického informačního systému, Ministerstvo vnitra, Sbírka zákonů 3. 11. **2016**, částka 149.

[14] Zákon č. 110 / 2019 o zpracování osobních údajů, Ministerstvo vnitra, Sbírka zákonů 12. 3. **2019**, částka 47.

[15] Nařízení Evropského Parlamentu a Rady (EU) 2016/679 o ochraně fyzických osob v souvislosti se zpracováním osobních údajů a o volném pohybu těchto údajů a o zrušení směrnice 95/46/ES (obecné nařízení o ochraně osobních údajů), Evropský Parlament a Rada (EU), Úřední věstník Evropské unie, 27. 4. **2016**, svazek 59

[16] *Epidemiologie zhoubných nádorů v České republice*: Incidence a mortalita - vývoj v čase. Svod.cz/ [online]. Brno: Svod, **2019** [cit. 2020-03-20]. Dostupné z: https://www.svod.cz/analyse.php?modul=incmor#.

[17] Vyhláška č. 70 / 2012 o preventivních prohlídkách, Ministerstvo vnitra, Sbírka zákonů 29. 2. **2012**, částka 27.

[18] ÚZIS ČR, Novotvary 2016 ČR, Ústav zdravotnických informací a statistiky ČR, Praha **2017**, 1-8.

[19] *International Agency for Research on Cancer*, Latest global cancer data: Cancer burden rises to 18.1 million new cases and 9.6 million cancer deaths in 2018, International Agency for Research on Cancer, Geneva **2018**, 1-3.

[20] *International Agency for Research on Cancer*: Global Cancer Observatory. Gco.iarc.fr/ [online]. Lyon: The Global Cancer Observatory, **2019** [cit. 2020-03-25].

Dostupné z: https://gco.iarc.fr/today/data/factsheets/cancers/39-All-cancers-fact-sheet.pdf.

[21] *International Agency for Research on Cancer*: Global Cancer Observatory. Gco.iarc.fr/ [online]. Lyon: The Global Cancer Observatory, **2019** [cit. 2020-03-25]. Dostupné z: https://gco.iarc.fr/today/online-analysis-map?v=2018&mode=population&mode_population=continents&population=900&populations=900&key=asr&sex=0&cancer=39&type=0&statistic=5&prevalence=0&population_group=0&ages_group%5B%5D=0&ages_group%5B%5D=17&nb_items=10&group_cancer=1&include_nmsc=1&include_nmsc_other=1&projection=natural-earth&color_palette=default&map_scale=quantile&map_nb_colors=5&continent=0&rotate=%255B10%252C0%255D.

[22] *International Agency for Research on Cancer*: Global Cancer Observatory. Gco.iarc.fr/ [online]. Lyon: The Global Cancer Observatory, **2019** [cit. 2020-03-25]. Dostupné z: https://gco.iarc.fr/today/online-analysis-map?v=2018&mode=population&mode_population=continents&population=900&populations=900&key=asr&sex=0&cancer=39&type=1&statistic=5&prevalence=0&population_group=0&ages_group%5B%5D=0&ages_group%5B%5D=17&nb_items=10&group_cancer=1&include_nmsc=1&include_nmsc_other=1&projection=natural-earth&color_palette=default&map_scale=quantile&map_nb_colors=5&continent=0&rotate=%255B10%252C0%255D.

[23] SLÁMA, O.; ŠEDO, J.; VYZULA, R.; VORLÍČEK, J. Bolest u pacientů s nádorovým onemocněním. In: Vlček Jiří; Vytřískalová Magda (Ed.) *Klinická farmacie II.* 1st Ed., Grada Publishing, Praha **2014**, ISBN 978-80-247-4532-9

[24] ZHANG, J. W.; WANG, J. Y.; CHEN, S. J.; CHEN, Z. Mechanisms of all-trans retinoic acid-induced differentiation of acute promyelocytic leukemia cells. *J. Biosci.* **2010**, *25(3)*, 275-84.

[25] ECKSCHLAGER, T.; PLCH, J.; STIBOROVA, M.; HRABETA, J. Histone Deacetylase Inhibitors as Anticancer Drugs. *Int. J. Mol. Sci.* **2017**, *18(7)*, 1414.

[26] RAMAGOPAL, U. A.; LIU, W.; GARRETT-THOMSON, S. C.; BONANNO, J. B.; YAN, Q.; SRINIVASAN, M.; WONG, S. C.; BELL, A.; MANKIKAR, S.; RANGAN, V. S.; DESHPANDE, S.; KORMAN, A. J.; ALMOA, S. C. Structural basis for cancer immunotherapy by the first-in-class checkpoint inhibitor ipilimumab. *Proc. Natl. Acad. Sci. U. S. A.* **2017**, *114(21)*, E4223–E4232.

[27] BUCHBINDER, E. I.; DESAI, A. CTLA-4 and PD-1 Pathways. *Am. J. Clin. Oncol.* **2016**, *39(1)*, 98–106.

[28] BOARDER, M.; DIXON, J.; NEWBY, D.; NAVTI, P.; ZETTERSTRÖM, T. Cancer chemotherapy. *Pharmacology for pharmacy and the health sciences- a patient-centred approach*. 2nd Ed., Oxford University Press, Oxford **2017**, ISBN 978-0-19-872883-2

[29] MARTÍNKOVÁ, J. Farmakoterapie nádorových onemocnění. *Farmakologie pro studenty zdravotnických oborů*. 2nd Ed., GRADA Publishing, Prague **2018**, ISBN 978-80-247-4157-4

[30] HOUSMAN, G.; BYLER, S.; HEERBOTH, S.; LAPINSKA, K.; LONGACRE, M.; SNYDER, N.; SARKAR, S. Drug Resistance in Cancer: An Overview. *Cancers*, **2014**, 6(3), 1769–1792.

[31] MANSOORI, B.; MOHAMMADI, A.; DAVUDIAN, S.; SHIRJANG, S.; BARADARAN, B. The Different Mechanisms of Cancer Drug Resistance: A Brief Review. *Adv. Pharm. Bull.*, **2017**, 7(3), 339–348.

[32] MOMPARLER, R. L. Optimization of cytarabine (ARA-C) therapy for acute myeloid leukemia. *Exp. Hematol. Oncol*., **2013**, 2, 20.

[33] UGHACHUKWU, P. O.; UNEKWE, P. C. Efflux Pump-Mediated Resistance in Chemotherapy. *Ann. Med. Health. Sci. Res.*, **2012**, 2(2), 191–198.

[34] MULCAHY LEVY, J. M.; TOWERS, C. G.; THORNBURN A. Targeting Autophagy in Cancer. *Nat. Rev. Cancer*, **2017**, 17(9), 528–542.

[35] PUCHALSKI, R. B.; FAHL, W. E. Expression of recombinant glutathione S-transferase pi, Ya, or Yb1 confers resistance to alkylating agents. *Proc. Natl. Acad. Sci. U. S. A.*, **1990**, 87(7), 2443-7.

[36] LI, G.; GUO, J.; SHEN, B. Q.; YADAV, D. B.; SLIWKOWSKI, M. X.; CROCKER, L. M.; LACAP, J. A.; PHILLIPS, G. D. L. Mechanisms of Acquired Resistance to Trastuzumab Emtansine in Breast Cancer Cells. *Mol. Cancer Ther.*, **2018**, 17(7), 1441-1453.

[37] HE, L.; LUO, L.; ZHU, H.; YANG, H.; ZHANG, Y.; WU, H.; SUN, H.; JIANG, F.; KATHERA, C. S.; LIU, L.; ZHUANG, Z.; CHEN, H.; PAN, F.; HU, Z.; ZHANG, J.; GUO, Z. FEN1 promotes tumor progression and confers cisplatin resistance in non-small-cell lung cancer. *Mol. Oncol.*, **2017**, 11(6), 640-654.

[38] CHEN, X.; ZHANG, Z.; GAN, H.; WANG, H.; LEE, J.; FANG, D.; KITANGE, G. J.; HE, L.; HU, Z.; PARNEY, I. F.; MEYER, F. B.; GIANNINI, C.; SARKARIA, J. N.; ZHANG, Z. A novel enhancer regulates MGMT expression and promotes temozolomide resistance in glioblastoma. *Nat. Commun.*, **2018**, 9, 2949.

[39] MATSUI, A.; IHARA, T.; SUDA, H.; MIKAMI, H.; SEMBA, K. Gene amplification: mechanisms and involvement in cancer. *Biomol. Concepts*, **2013**, 4(6), 567-82.

[40] OKUGAWA, Y.; GRADY, W. M.; GOEL, A. Epigenetic Alterations in Colorectal Cancer: Emerging Biomarkers. *Gastroenterology*, **2015**, 149(5), 1204-1225.

[41] ALMEIDA, L. O.; ABRAHAO, A. C.; ROSELLI-MURAI, L. K.; GIUDICE, F. S.; ZAGNI, C.; LEOPOLDINO, A. M.; SQUARIZE, C. H.; CASTILHO, R. M. NFκB mediates cisplatin resistance through histone modifications in head and neck squamous cell carcinoma (HNSCC). *FEBS Open Bio*, **2013**, 4, 96-104.

[42] WADE, R. H. Microtubules: an overview. *Methods Mol. Med.*, **2007**, 137, 1-16.

[43] HAIDER, K.; RAHAMAN, S.; YAR, M. S.; KAMAL, A. Tubulin inhibitors as novel anticancer agents: an overview on patents (2013-2018). *Expert Opin. Ther. Pat.*, **2019**, 29(8), 623-641.

[44] BROUHARD, G. J.; RICE, L. M. Microtubule Dynamics: an interplay of biochemistry and mechanics. *Nat. Rev. Mol. Cell Biol.*, **2018**, 19(7), 451–463.

[45] PETRY, S. Mechanisms of Mitotic Spindle Assembly. *Annu. Rev. Biochem.*, **2016**, 85, 659–683.

[46] BORISY, G. G.; TAYLOR, E. W. The mechanism of action of colchicine. Binding of colchincine-^{3}H to cellular protein. *J. Cell Biol.*, **1967**, 34(2), 525-33.

[47] YANG, C. H.; HORWITZ, S. B. Taxol®: The First Microtubule Stabilizing Agent. *Int. J. Mol. Sci.*, **2017**, 18(8), 1733.

[48] BRUNDEN, K. R.; LEE; V. M.; SMITH, A. B.; TROJANOWSKI, J. Q.; BALLATORE, C. Altered microtubule dynamics in neurodegenerative disease: Therapeutic potential of microtubule-stabilizing drugs. *Neurobiol. Dis.*, **2017**, 105, 328-335.

[49] GRADISHAR, W. J. Albumin-bound paclitaxel: a next-generation taxane. *Expert Opin. Pharmacother.*, **2006**, 7(8), 1041-53.

[50] BHARADWAJ, G.; NHAN, V.; YANG, S.; LI, X.; NARAYANAN, A.; MACARENCO, A. C.; SHI, Y.; YANG, D.; VIEIRA, L. S.; XIAO, W.; LI, Y.; LAM, K. S. Cholic acid-based novel micellar nanoplatform for delivering FDA-approved taxanes. *Nanomedicine (London, U. K.)*, **2017**, 12(10), 1153–1164.

[51] REICHENBACH, H.; HÖFLE, G. Discovery and Development of the Epothilones A Novel Class of Antineoplastic Drugs. *Drugs R&D*, **2008**, 9(1), 1–10.

[52] LI, J.; REN, J.; SUN, W. Systematic review of ixabepilone for treating metastatic breast cancer. *Breast Cancer*, **2017**, 24(2), 171-179.

[53] MCMEEKIN, S.; PATEL, R.; VERSCHRAEGEN, C.; CELANO, P.; BURKE, J.; PLAXE, S.; GHATAGE, P.; GIURESCU, M.; STREDDER, C.; WANG, Y.; SCHMELTER, T. Phase I/II study of sagopilone (ZK-EPO) plus carboplatin in women with recurrent platinum-sensitive ovarian cancer. *Br. J. Cancer*, **2012**, 106(1), 70-6.

[54] RUSTIN, G.; REED, N.; JAYSON, G. C.; LEDERMANN, J. A.; ADAMS, M.; PERREN, T.; POOLE, C.; LIND, M.; PERSIC, M.; ESSAPEN, S.; GORE, M.; CALVERT, H.; STREDDER, C.; WAGNER, A.; GIURESCU, M.; KAYE, S. A phase II trial evaluating two schedules of sagopilone (ZK-EPO), a novel epothilone, in patients with platinum-resistant ovarian cancer. *Ann. Oncol.*, **2011**, 22(11), 2411-6.

[55] MOOBERRY, S. L.; RANDALL-HLUBEK, D. A.; LEAL, R. M.; HEGDE, S. G.; HUBBARD, R. D.; ZHANG, L.; WENDER, P. A. Microtubule-stabilizing agents based on designed laulimalide analogues. *Proc. Natl. Acad. Sci. U. S. A.*, **2004**, 101(23), 8803-8808.

[56] LIU, J.; TOWLE, M. J.; CHENG, H.; SAXTON, P.; REARDON, C.; WU, J.; MURPHY, E. A.; KUZNETSOV, G.; JOHANNES, C. W.; TREMBLAY, M. R.; ZHAO, H.; PESANT, M.; FANG, F. G.; VERMELUEN, M. W.; GALLAGHER, B. M. Jr.; LITTLEFIELD, B. A. *In vitro* and *in vivo* anticancer activities of synthetic (-)-laulimalide, a marine natural product microtubule stabilizing agent. *Anticancer Res.*, **2007**, 27(3B), 1509-18.

[57] KLECKNER, I. R.; KAMEN, C.; GEWANDTER, J. S.; MOHILE, N. A.; HECKLER, C. E.; CULAKOVA, E.; FUNG, C.; JANELSINS, M. C.; ASARE, M.; LIN, P. J.; REDDY, P. S.; GIGUERE, J.; BERENBERG, J.; KESLER, S. R.; MUSTIAN, K. M. Effects of exercise during chemotherapy on chemotherapy-induced peripheral neuropathy: a multicenter, randomized controlled trial. *Support Care Cancer*, **2018**, 26(4), 1019-1028.

[58] BATES, D.; EASTMAN, A. Microtubule destabilising agents: far more than just antimitotic anticancer drugs. *Br. J. Clin. Pharmacol.*, **2017**, 83(2), 255-268.

[59] GRISSINGER, M. Death and Neurological Devastation From Intrathecal Vinca Alkaloids. *P.T.*, **2016**, 41(8), 464-465, 525.

[60] ZHANG, Y. S.; LI, J. D.; YAN, C. An update on vinpocetine: New discoveries and clinical implications. *Eur. J. Pharmacol.*, **2018**, 819, 30-34.

[61] KEGLEVICH, A.; DÁNYI, L.; RIEDER, A.; HORVÁTH, D.; SZIGETVÁRI, Á.; DÉKÁNY, M.; SZÁNTAY, C. Jr.; LATIF, A. D.; HUNYADI, A.; ZUPKÓ, I.; KEGLEVICH, P.; HAZAI, L. Synthesis and Cytotoxic Activity of New Vindoline Derivatives Coupled to Natural and Synthetic Pharmacophores. *Molecules*, **2020**, 25(4), 1010.

[62] KAUR, R.; KAUR, G.; GILL, R. K.; SONI, R.; BARIWAL, J. Recent developments in tubulin polymerization inhibitors: An overview. *Eur. J. Med. Chem.*, **2014**, 87, 89-124.

[63] MCLOUGHLIN, E. C.; O'BOYLE, N. M. Colchicine-Binding Site Inhibitors from Chemistry to Clinic: A Review. *Pharmaceuticals*, **2020**, 13(1), 8.

[64] BANERJEE, S.; HWANG, D.; LI, W.; MILLER, D. D. Current Advances of Tubulin Inhibitors in Nanoparticle Drug Delivery and Vascular Disruption/Angiogenesis. *Molecules*, **2016**, 21(11), 1468.

[65] MALDONADO, E. N.; PATNAIK, J.; MULLINS, M. R.; LEMASTERS, J. J. Free tubulin modulates mitochondrial membrane potential in cancer cells. *Cancer Res.*, **2010**, 70(24), 10192–10201.

[66] SHELDON, J. E.; DCONA, M. M.; LYONS, C. E.; HACKETT, J. C.; HARTMANN, M. C. T. Photoswitchable Anticancer Activity via trans-cis Isomerization of a Combretastatin A-4 Analog. *Org. Biomol. Chem.*, **2016**, 14(1), 40–49.

[67] WANG Q.; ARNST, K. E.; WANG, Y.; KUMAR, G.; MA, D.; WHITE, S. W.; MILLER, D. D.; LI, W.; LI, W. Structure-Guided Design, Synthesis, and Biological Evaluation of (2-(1H-Indol-3-yl)-1H-imidazol-4-yl)(3,4,5-trimethoxyphenyl) Methanone (ABI-231) Analogues Targeting the Colchicine Binding Site in Tubulin. *J. Med. Chem.*, **2019**, 62(14), 6734-6750.

[68] CHEN, H.; DENG, S.; WANG, Y.; ALBADARI, N.; KUMAR, G.; MA, D.; LI, W.; WHITE, S. W.; MILLER, D. D.; LI, W. Structure-Activity Relationship Study of Novel

6-Aryl-2-benzoyl-pyridines as Tubulin Polymerization Inhibitors with Potent Antiproliferative Properties. *J. Med. Chem.*, **2020**, 63(2), 827-846.

[69] MOONEY, C. J.; NAGAIAH, G.; FU, P.; WASMAN, J. K.; COONEY, M. M.; SAVVIDES, P. S.; BOKAR, J. A.; DOWLATI, A.; WANG, D.; AGARVALA, S. S.; FLICK, S. M.; HARTMAN, P. H.; ORTIZ, J. D.; LAVERTU, P. N.; REMICK, S. C. A phase II trial of fosbretabulin in advanced anaplastic thyroid carcinoma and correlation of baseline serum-soluble intracellular adhesion molecule-1 with outcome. *Thyroid*, **2009**, 19(3), 233-240.

[70] MONK, B. J.; SILL, M. W.; WALKER, J. L.; DARUS, C. J.; SUTTON, G.; TEWARI, K. S.; MARTIN, L. P.; SCHILDER, J. M.; COLEMAN, R. L.; BALKISSOON, J.; AGHAJANIAN, C. Randomized Phase II Evaluation of Bevacizumab Versus Bevacizumab Plus Fosbretabulin in Recurrent Ovarian, Tubal, or Peritoneal Carcinoma: An NRG Oncology/Gynecologic Oncology Group Study. *J. Clin. Oncol.*, **2016**, 34(19), 2279-86.

[71] COGLE, C. R.; COLLINS, B.; TURNER, D.; PETTIFORD, L. C.; BOSSÉ, R.; HAWKINS, K. E.; BEACHAMP, Z.; WISE, E.; CLINE, C.; MAY, W. S.; MOREB, J. S.; HSU, J.; HIEMENZ, J.; BROWN, R.; NORKIN, M.; WINGARD, J. R.; UCKUN, F. Safety, feasibility and preliminary efficacy of single agent combretastatin A1 diphosphate (OXi4503) in patients with relapsed or refractory acute myeloid leukemia or myelodysplastic syndromes. *Br. J. Haematol.*, **2020**, doi: 10.1111/bjh.16629.

[72] UCKUN, F. M.; COGLE, C. R.; LIN, T. L.; QAZI, S.; TRIEU, V. N.; SCHILLER, G.; WATTS, J. M. A Phase 1B Clinical Study of Combretastatin A1 Diphosphate (OXi4503) and Cytarabine (ARA-C) in Combination (OXA) for Patients with Relapsed or Refractory Acute Myeloid Leukemia. *Cancers*, **2019**, 12(1), 74.

[73] PUXEDDU, M.; SHEN, H.; BAI, R.; COLUCCIA, A.; NALLI, M.; MAZZOCCOLI, C.; DE POZZO, E.; CAVALLINI, C.; MARTINI, C.; ORLANDO, V.; BIAGIONI, S.; MAZZONI, C.; COLUCCIA, A.; HAMEL, E.; LIU, TE.; SILVESTRI, R.; LA REGINA, G. Structure-activity relationship studies and in vitro and in vivo anticancer activity of novel 3-aroyl-1,4-diarylpyrroles against solid tumors and hematological malignancies. *Eur. J. Med. Chem.*, **2020**, 1, 185.